



Norwegian University of
Science and Technology

Master's degree thesis

IP501909 MSc thesis - discipline oriented master

**Fatigue tool sensitivity analysis and design
curves**

Kateryna Tymofieienko

Number of pages including this page: 125

Aalesund, 02.06.2016

Supervisor: Karl Henning Halse and Juri Kuzjatkin

Mandatory statement

Each student is responsible for complying with rules and regulations that relate to examinations and to academic work in general. The purpose of the mandatory statement is to make students aware of their responsibility and the consequences of cheating. **Failure to complete the statement does not excuse from their responsibility.**

Please complete the mandatory statement by placing a mark in each box for statements 1-6 below.		
1.	I/we hereby declare that my/our paper/assignment is my/our own work, and that I/we have not used other sources or received other help than is mentioned in the paper/assignment.	<input checked="" type="checkbox"/>
2.	I/we hereby declare that this paper <ol style="list-style-type: none"> 1. Has not been used in any other exam at another department/university/university college 2. Is not referring to the work of others without acknowledgement 3. Is not referring to my/our previous work without acknowledgement 4. Has acknowledged all sources of literature in the text and in the list of references 5. Is not a copy, duplicate or transcript of other work 	Mark each box: 1. <input checked="" type="checkbox"/> 2. <input checked="" type="checkbox"/> 3. <input checked="" type="checkbox"/> 4. <input checked="" type="checkbox"/> 5. <input checked="" type="checkbox"/>
3.	I am/we are aware that any breach of the above will be considered as cheating, and may result in annulment of the examination and exclusion from all universities and university colleges in Norway for up to one year, according to the Act relating to Norwegian Universities and University Colleges, section 4-7 and 4-8 and Examination regulations .	<input checked="" type="checkbox"/>
4.	I am/we are aware that all papers/assignments may be checked for plagiarism by a software assisted plagiarism check	<input checked="" type="checkbox"/>
5.	I am/we are aware that NTNU will handle all cases of suspected cheating according to prevailing guidelines.	<input checked="" type="checkbox"/>
6.	I/we are aware of the NTNU's rules and regulation for using sources.	<input checked="" type="checkbox"/>

Publication agreement

ECTS credits: 30

Supervisor: Karl Henning Halse

Agreement on electronic publication of master thesis

Author(s) have copyright to the thesis, including the exclusive right to publish the document (The Copyright Act §2).

All theses fulfilling the requirements will be registered and published in Brage HiÅ, with the approval of the author(s).

Theses with a confidentiality agreement will not be published.

I/we hereby give Aalesund University College the right to, free of charge, make the thesis available for electronic publication: yes no

Is there an [agreement of confidentiality](#)? yes no

(A supplementary confidentiality agreement must be filled in and included in this document)

- If yes: Can the thesis be online published when the period of confidentiality is expired? yes no

This master's thesis has been completed and approved as part of a master's degree programme at Aalesund University College. The thesis is the student's own independent work according to section 6 of Regulations concerning requirements for master's degrees of December 1st, 2005.

Date: 25.05.2015



**MASTER THESIS 2016
FOR
STUD.TECHN. KATERYNA TYMOFIEIENKO**

FATIGUE TOOL SENSITIVITY ANALYSIS AND DESIGN CURVES

One of the main requirements for high speed vessels is light weight which is absolutely feasible due to use of aluminum as a primary material for hull structures. However, operations at high speeds cause high levels of dynamic wave induced loads, which are at some point can become critical for aluminium due to its reduced material properties comparing to steel. That is why design of aluminium vessels is a very challenging task and requires accuracy in prediction of fatigue lifetime.

Damen has already been engaged into the fatigue analysis of aluminium hulls for more than 15 years. During these years several developments have taken place (within and outside Damen) on the analysis procedure and questions have been raised about prediction accuracy and influence of input parameters. Therefore, an internal research project was initiated to investigate accuracy of fatigue lifetime prediction of ship structures, conducting sensitivity analysis. Next to that standard fatigue design curves were developed.

- Prestudy:
 - Literature review
 - Structural analysis on fatigue critical details
 - Preparation of required initial data for calculations
- Analysis:
 - Sensitivity analysis for one of the high speed crafts designed in Damen
 - Development of fatigue design curves for the range of vessels designed in Damen
- Discussion:
 - Influence of different parameters on fatigue lifetime of details on vessels
 - Accuracy of results and occurred uncertainty with respect to fatigue lifetime calculation
- Conclusions and recommendations for future work.

The work scope may prove to be larger than initially anticipated. Subject to approval from the supervisor, topics may be deleted from the list above or reduce in extent.

The thesis shall be written as a research report with summary, conclusion, literature references, table of contents, etc. During preparation of the text, the candidate should make efforts to create a well-arranged and well-written report. To ease the evaluation of the thesis, it is important to cross-reference text, tables and figures. For evaluation of the work a thorough discussion of results is needed. Discussion of research method, validation and generalization of results is also appreciated.

In addition to the thesis, a research paper for publication shall be prepared.

Three weeks after start of the thesis work, a pre-study has to be delivered. The pre-study has to include:

- Research method to be used
- Literature and sources to be studied
- A list of work tasks to be performed
- An A3 sheet illustrating the work to be handed in.

A template and instructions for thesis documents and A3-poster are available on the Fronter website under MSc-thesis. Please follow the instructions closely, and ask your supervisor or program coordinator if needed.

The thesis shall be submitted in electronic version according to standard procedures. Instructions are found on the college website and on Fronter. In addition one paper copy of the full thesis with a CD including all relevant documents and files shall be submitted to your supervisor.

Supervision at NTNU Aalesund: Karl Henning Halse
Contact at: Norwegian University of Science and Technology (Alesund)

Delivery: 3, June 2016

Signature candidate:  _____

Abstract

The paper looks at fatigue tool sensitivity analysis and design curves for aluminum high speed crafts. Spectral fatigue method developed by Det Norske Veritas was used to achieve the objective. As only limited initial data was available, preliminary fatigue analysis was relevant to conduct in order to receive a minimum required section modulus of a hull section. This parameter impacts fatigue lifetime and was used as a comparative value in current study.

To summarize, the results showed behavior of the minimum required section modulus influenced by different parameters; in addition, several findings were made during the study. All of them are described in Results and Discussion sections. Finally, this thesis contains several recommendations that may facilitate better design results.

Preface

This report is the result of thesis work as a master student in Ship Design at the Norwegian University of Science and Technology (NTNU in Alesund).

The master thesis project was offered by Research and Development Department of Damen Shipyards Gorinchem (Netherlands). The final proposal was agreed with NTNU. Moreover, a workplace was offered at the Research and Development Department at Damen Shipyards Gorinchem in order to investigate fatigue tool sensitivity analysis and generate design curves. The project was carried out in close collaboration with R&D Department at Damen Shipyards and NTNU.

I am very thankful to my supervisor in NTNU, namely Karl Henning Halse and all the people who were helpful during the time of my master thesis at Damen Shipyard in Gorinchem.



Gorinchem, May 10th 2016

Kateryna Tymofieienko

Table of contents

List of figures	xi
List of tables	xii
Terminology	xv
1 INTRODUCTION	1
1.1 Project background and problem statement.....	1
1.2 Objectives	1
1.3 Structure of the report.....	2
2 BACKGROUND AND THEORETICAL BASIS	3
2.1 General remarks.....	3
2.2 Basic knowledge about fatigue and its mechanism	3
2.3 General causes and common locations of crack initiation	5
2.4 Loads on structure. Stochastic process	6
2.5 Long term distribution	11
2.6 S-N curve	13
2.7 Cumulative damage. Miner-Palmgren's Rule	14
2.8 Design check format	15
3 METHODS	17
3.1 Applied theories.....	17
3.2 Overview and procedure for fatigue analysis	18
3.3 Method Description	20
3.3.1 Octopus Seaway.....	20
3.3.2 Alufastship.....	21
3.4 Case description of sensitivity analysis	27
3.5 Case description of fatigue design curves	28
3.6 Analysis parameters.....	29
3.6.1 Operational profile.....	31

3.6.2	Operating area.....	32
3.6.3	Engine power and speeds.....	32
4	RESULTS.....	34
4.1	Sensitivity analysis	34
4.2	Fatigue design curves	46
5	DISCUSSION	61
5.1	Sensitivity analysis	61
5.2	Fatigue design curves	64
6	CONCLUSION.....	69
6.1	Conclusion of the thesis.....	69
6.2	Suggestions for future study	71

APPENDIX A: STANDARD WAVE SCATTER DIAGRAMS

APPENDIX B: REPORT FROM ALUFASTSHIP (SPA 3007, STANDARD OPERATION PROFILE)

APPENDIX C: STANDARD FORMAT OF BENDING MOMENTS FOR ALUFASTSHIP

APPENDIX D: CATALOGUE OF DETAILS

APPENDIX E: FATIGUE DESIGN CURVES

APPENDIX F: COMPARISON OF DOMINATING WAVE LENGTH AND VESSEL LENGTH IN TWO AREAS

APPENDIX G: 3D FATIGUE CURVE

APPENDIX H: THE FATIGUE DESIGN CURVE WITH ALUMINUM AND HYBRID CONSTRUCTION MATERIALS

APPENDIX I: EFFECT OF WAVE PERIODS ON A RESPONSE SPECTRUM IN HEAVE

APPENDIX J: THE RESEARCH VERTICAL BENDING MOMENTS FOR FCS3307

APPENDIX K: THE RESEARCH PAPER

List of figures

Figure 1.1.1– An aluminum high speed supply vessel (Damen, 2016) 1

Figure 2.2.1– Multiple fatigue cracks (Berge, 1985) 4

Figure 2.3.1– Summary of common damages and main influencing factors (Lyngstad, 2002) 6

Figure 2.4.1– The time history of stochastic process (Fines, 1985)..... 6

Figure 2.4.2– Energy spectrum to the corresponded stochastic process (Fines, 1985)..... 8

Figure 2.4.3– Rayleigh and Rice distributions (Fines, 1985)..... 8

Figure 2.4.4– Time history for irregular waves (Fines, 1985) 9

Figure 2.4.5– Jonswap and Bretschneider (PM) wave spectrum on a frequency scale (Journee & Massie, 2001) 10

Figure 2.4.6– The excitation spectrum $S_x(\omega)$, the transfer function $T(\omega)$ and the response spectrum $S_y(\omega)$, (Lotsberg, A.Almer-Næss, & Veritec, 1985)..... 11

Figure 2.5.1– Diagram with the number of waves that exceeds a given wave height in one year (left figure) and the diagram of long term distribution of wave heights (right figure) (Lotsberg et al., 1985) 12

Figure 2.5.2– The long-term distribution of stress ranges divided into blocks (Lotsberg et al., 1985)..... 12

Figure 2.6.1– S-N curves for low-carbon steel and aluminum, (Roylance, 2001)..... 13

Figure 2.7.1– The block tress history (n_i – number of cycles in one block, $S_{r,i}$ – constant stress range within n_i cycles), (Berge, 1985) 14

Figure 3.1.1– Fatigue calculation procedure (DNV approach) 18

Figure 3.2.1– Structure for fatigue and required section modulus assessment 19

Figure 3.3.1– Input data screen 22

Figure 3.3.2– Wave energy spectrum..... 24

Figure 3.3.3 – Moment interval series (for 1 detail location in 3 speeds)..... 25

Figure 3.3.4– The distribution of stress levels 26

Figure 3.3.5– Cumulative stress spectrum 27

Figure 3.4.1– General layout SPa 3007 with locations for the sensitivity analysis 28

Figure 4.1.1– Minimum required section modulus for frame 5 35

Figure 4.1.2– Minimum required section modulus for frame 11 36

Figure 4.1.3– Minimum required section modulus for frame 11 with original operational profile but different year period 38

Figure 4.1.4– Comparison of results with different service conditions and intended service periods for frame 11 in the N-Arabian Sea for 2.5m significant wave height	40
Figure 4.1.5– Results of variable first and third service conditions, constant second service conditions for the N-Arabian Sea.....	41
Figure 4.1.6– Results of variable first and third service conditions, constant second service conditions for DNV-3.....	41
Figure 4.1.7– Results of minimum required section modulus for the N-Arabian Sea.....	43
Figure 4.1.8– Results of minimum required section modulus at the N-Arabian Sea.....	44
Figure 4.1.9– Results of minimum required section modulus at DNV-3	44
Figure 4.1.10– Results of Z for final comparison	45
Figure 4.2.1– Fatigue design curve for FCS at DNV-3 with variable operational profile and constant service conditions.....	48
Figure 4.2.2– Fatigue design curve for FCS at Gulf of Mexico with variable operational profile and constant service conditions	50
Figure 4.2.3– Fatigue design curve for SPa at DNV-3 with variable operational profile and constant service conditions.....	52
Figure 4.2.4– Fatigue design curve for SPa at the Gulf of Mexico with variable operational profile and constant service conditions	54
Figure 4.2.5 – Fatigue design curve for FCS at DNV-3 with different engine power.....	55
Figure 4.2.6– Fatigue design curve for SPa at DNV-3 with different engine power.....	57
Figure 4.2.7– 3D fatigue curve (lower surface – Z at 20kn; upper surface – Z at 26kn).....	58
Figure 4.2.8– Results of Z for FCS with constant speed.....	59
Figure 4.2.9– Results of Z for FCS with constant speed and displacement.....	60
Figure 5.1.1– Bending moment distribution along the length of vessel	61
Figure 5.1.2– Comparison of dominating wave length and vessel length in two areas	63
Figure 5.2.1– Directional distribution based on DNV report 97-0152	65
Figure 5.2.2– Behavior of bending moments along the vessel length at 8 and 28kn.....	67
Figure 5.2.3– Vertical motions at the bow,(Journee & Massie, 2001)	68

List of tables

Table 3.4.1– Variable operational profile for the sensitivity analysis	28
Table 3.5.1– Actual section modulus of already built vessels	29
Table 3.5.2– Variable operational profile for the fatigue design curves.....	29

Table 3.6.1– General particulars of Fast Crew Suppliers	30
Table 3.6.2– General particulars of Stan Patrol	30
Table 3.6.3– Standard operational profile	31
Table 3.6.4– Engine data and new achieved speeds for FCS.....	32
Table 3.6.5– Engine data and new achieved speeds for SPa.....	33
Table 4.1.1– Minimum required section modulus for frame 5	34
Table 4.1.2– Minimum required section modulus for frame 11	35
Table 4.1.3– Minimum required section modulus for frame 15	37
Table 4.1.4– Numerical results of minimum required section modulus for frame 11 with original operational profile but different year period.....	38
Table 4.1.5– Modified input parameters for a new test	38
Table 4.1.6– Results of minimum required section modulus for N-Arabian Sea and DNV-3	39
Table 4.1.7– Results of variable first and third service conditions, constant second service conditions for N-Arabian Sea and DNV-3	40
Table 4.1.8– Results of variable second service condition, constant first and third service conditions for N-Arabian Sea and DNV-3	42
Table 4.1.9– Results of minimum required section modulus for N-Arabian Sea and DNV-3	42
Table 4.1.10– Results of minimum required section modulus for N-Arabian Sea and DNV-3	43
Table 4.1.11– Results of Z for final evaluation.....	45
Table 4.2.1– Sailing periods used in fatigue design curves	46
Table 4.2.2– Results of minimum required section modulus for FCS at DNV-3 for fatigue design curves	47
Table 4.2.3– Results of minimum required section modulus for FCS at Gulf of Mexico for fatigue design curves	49
Table 4.2.4– Sailing periods used in fatigue design curves for Spa.....	51
Table 4.2.5– Results of Z for SPa at DNV-3 for fatigue design curves.....	51
Table 4.2.6– Results of minimum required section modulus for SPa at Gulf of Mexico for fatigue design curves	53
Table 4.2.7– Results of Z for variable engine power	55
Table 4.2.8– Increase of Z in percentage	56
Table 4.2.9– Increase of speed in percentage.....	56
Table 4.2.10– Results of Z for variable engine power	57
Table 4.2.11– Results of Z for the third type of fatigue 3D curves	58

Table 4.2.12– Results of Z for FCS with constant speed.....	59
Table 4.2.13– Results of Z for mentioned conditions	60
Table 5.1.1– Scatter diagram for North Sea.....	62
Table 5.1.2– Scatter diagram for N-Arabian Sea	62
Table 5.2.1– Largest bending moments for specified speeds	66

Terminology

Latin symbols

B	Breadth of a vessel [m];
D	Damage;
H_s	Significant wave height [m];
I	Initial moment of inertia [m ⁴];
I_s	Cross section moment of inertia of detail [m ⁴];
$M_b \text{ max}$	Maximum achieved bending moment [kNm/m];
N	Number of cycles;
σ	Response spectrum;
T_p	Peak period [s];
V_s	Vessel speed [kn];
y	Location of neutral axis [m];
Z or Z_{req}	Minimum required section modulus [m ³];
Z_{actual}	Actual section modulus [m ³].

Greek symbols

Δ	Displacement [t];
ΔM_b	Bending moment intervals [kNm/m];
$\Delta \sigma$	Stress range [MPa];
$\Delta \sigma_R$	Allowable stress for the structure [MPa];
ω	Wave frequency [r/s].

Abbreviations

CE	Central Engineering;
DNV	Det Norske Veritas;
D&P	Design and Proposal;
FAT	Stress level of the S-N curve at 2 million stress cycles;
FCS	Fast Crew Suppliers;
FEM	Finite Element Method;
GA	General arrangement;
JONSWAP	Joint North Sea Wave Program;
LOA	Length over all [m];
MCR	Maximum continuous rating;
PFA	Preliminary fatigue analysis;
PM	Pierson-Moskowitz spectrum;
RAO	Response Amplitude Operator;
SCF	Stress Concentration Factor;
SPa	Stan Patrol;
S-N	Stress range - Number of stress cycles until failure (S-N curve);
WOSR	Wide Operating Speed Range.

1 Introduction

1.1 Project background and problem statement

Recent decade showed a growing demand for high speed crafts with low operational costs. One of the main requirements for high speed vessels is light weight which is absolutely feasible due to use of aluminum as a primary material for hull structures. Rough estimation of an aluminum hull shows that it is approximately equal to one-third of the weight of an ordinary steel construction. However, such sensitive structure is exposed to higher operational stress levels and thus to reduced structural redundancy. Moreover, operations at high speeds cause a higher level of dynamic wave induced loads as compared with slow going vessels. Therefore, the fatigue strength of aluminum vessels is also approximately one-third of the construction steel. Furthermore, fatigue cracks in vessel structures normally have a self-limiting nature. That is why the fatigue design of many structures in the vessel that are very critical to dynamic loads is a very challenging task and requires accuracy in prediction of fatigue lifetime.

Damen has already been engaged into the fatigue analysis of aluminum hulls for more than 15 years. During these years several developments have taken place (within and outside Damen) on the analysis procedure and questions have been raised about prediction accuracy and influence of input parameters. Therefore, an internal research project was initiated to investigate these aspects.



Figure 1.1.1– An aluminum high speed supply vessel (Damen, 2016)

1.2 Objectives

The first objective of this thesis was to conduct the sensitivity analysis for one of the high speed crafts designed in Damen (Stan Patrol 3007) in order to indicate which parameters have the most significant impact on fatigue lifetime. In addition, current analysis should add to understanding which vessel details are mostly prone to fatigue failure.

The second objective was to develop fatigue design curves for the range of vessels designed in Damen in order to help engineers at the design stage to make a proper selection regarding the main particulars of the vessel for a specific operational profile or for an individual customer's requirement. The specific objective was to assess the accuracy of the fatigue lifetime prediction based on the results of these curves. Finally, the fatigue curves were established in order to indicate any trend between input parameters and the parameter that reflects fatigue lifetime (a minimum required section modulus) in order to develop standard fatigue curves.

1.3 Structure of the report

The structure of the report contains a short introduction to present the master thesis project and it is given above.

The next part is dedicated to the background and theoretical basics of the fatigue issue (section 2). This section is divided into 8 subsections in the chronological order: general information, basic knowledge, failure mechanism, general causes and common location of cracks. This is followed by a description of the stochastic process, loads on structure, long term distribution, S-N curve, Palmgren-Miner fatigue damage hypothesis and design check format.

Section 3 is divided into two main subsections. The first subsection contains a description of DNV approach with applied theories while the second one familiarises with stepwise explanations of the calculation procedure. The methodology section ends with a case description of the conducted analysis and an overview of all initial data required for calculations.

Section 4 presents the achieved results. Firstly, the outcomes of sensitivity analysis complemented by intermediate discussions and conclusions are given. Secondly, based on the results in subsection 4.1 and the intermediate conclusions, the fatigue design curves have been established. Three different types of curves were designed and intermediate discussion with a conclusion follows after each type.

The most important and controversial results are discussed in section 5 which is similar to the structure of section 4. These two sections contain the main findings of this thesis.

Section 6 presents final conclusions and recommendations with respect to future work. A detailed literature review is presented after section 6.

2 Background and Theoretical basis

2.1 General remarks

In general, all structures are designed to their mission; they should meet certain safety requirements and be efficient. In order to match these demands effectively, the structure should contain bracings or other members. In case of a local design, material plate thickness should be determined in a proper way to meet strength, fabrication and inspection criteria. The failure modes which refer to the strength criteria are the following: rupture by overloading, fatigue failure of individual structural components or total failure of the system (Moan, 1985). The fatigue damage has less severe consequences than other reasons but economical losses are more significant.

The most susceptible to fatigue failure are light weight structures where aluminum is used as the construction material for the hull of high speed crafts. Most of high speed crafts designed by DNV regulations are made of aluminum and should withstand the same loads as a craft made of steel (Lyngstad, 2002). However, aluminum alloys are more prone to fatigue damages than the steel ones due to no fatigue limit, i.e. the stresses below which the fatigue failure will never occur (Allday, 1993). Furthermore, high speed operation causes a higher level of dynamic wave induced load as compared with conventional ships. Fatigue cracks are of self-restraint nature. The quality of detailed design will result either in success or failure in structural terms. The need for fatigue analysis of aluminum fast craft therefore is of high priority from both safety and maintenance reasons (Hall, Violette, & CHung, 1998).

2.2 Basic knowledge about fatigue and its mechanism

The process of accumulative damage due to repetitive loading application of structure at stresses well below yield stress is defined as a fatigue. The important feature of the fatigue is that the applied loads do not cause immediate failure of the structure. Instead, over a number of cyclic loads, the accumulative damage reaches the critical level that causes fatigue failure. The time of crack initiation directly depends on the severity of the stress concentration, frequency and magnitude of the load.

The fatigue process consists of several steps starting with the initial state of the material and finishing with the final destruction. Engineers identify three main phases:

- Initiation or crack nucleation;
- Crack growth;

- Final failure.

The fatigue initiation originates with a cumulative plastic strain. The development of plastic strain is referred to dislocation mobility especially at the surface rather than in the bulk of the material. The initial crack is associated with changes of the material only at a microscopic level. The defects arising in the lattice structure accumulate and result in progressive fatigue damage.

There is no clear description of the transition from stage 1 (fatigue initiation) to stage 2 (fatigue propagation). At the crack growth stage, the size of cracks is transformed to subgrain. Along with its growth, the crack changes in its form as well as the growth direction tends to the perpendicular to the largest applied stress. The driving force will be the maximum principal stress at this stage (Berge, 1985). In addition, the environment and corrosion adversely affect the crack growth due to the nature of the environment (sea water properties such as conductivity, salinity, pH, temperature, etc.), magnitude and frequency of applied loads (such as wave, wind, etc.) (Capanoglu, 1993).

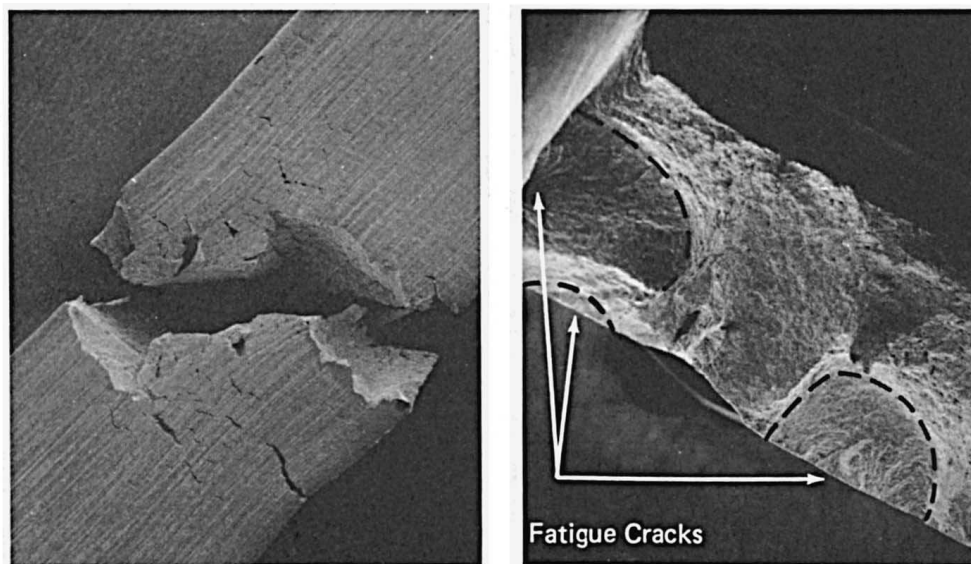


Figure 2.2.1– Multiple fatigue cracks (Berge, 1985)

After certain fluctuating loads, a rapid increase in growth rate appears and tends to infinity. In case this trend continues for some time, the final failure is inevitable at a certain stage of the crack growth. This finally results in brittle, ductile fracture or plastic collapse, depending on the strength of the material, loading rate, plate thickness and constraints. The final failure means the end of fatigue life (defined by S-N tests) and correspondingly fatigue life assessment (Berge, 1985).

2.3 General causes and common locations of crack initiation

Generally, the fatigue initiation occurs at locations with high ratio of dynamic to static load. A good example of this is high load application with low frequency (fast craft claims into head seas, catamaran wracks in quartering seas) or low load application with high frequency (vibrations by propellers and engine). Secondly, at the locations where a structure is welded, even accurate welding leads to lowering fatigue strength due to heating of the structure. In addition, fatigue cracks occur at places of stress concentration, such as holes, changes of section, discontinuous welded structures with different plate thickness etc. (Allday, 1993). Each of the above mentioned reasons is a primary source of crack initiation. Therefore, the emphasis should be given to the detailed design of the hull due to structural and watertight integrity reasons (Hall et al., 1998). Moreover, attention should be paid to make smooth geometrical transitions and locate weld joints outside of the highest stress concentration areas.

DNV rules for classification single out areas that are normally critical and should be considered during a fatigue strength assessment, namely:

- On bottom (in longitudinal direction) due to global bending moment and sea pressure;
- Areas with low stress concentration at still water and high stress concentration in waves;
- Stiffener transition through web frames or bulkheads in critical sections;
- Cross structure in a twin hull or a multihull craft, particularly in the transition between cross structure and pontoon;
- Details in the midship area with large stress concentrations such as tripping brackets etc.;
- Engine foundations and water jet area, low stress range and high number of cycles;
- Pillar connections;
- Cross bracing connections;
- At discontinuities;
- Termination of primary and secondary members, (DNV, 2012), (DNV, 1997).

Most common damages and their reasons of high speed crafts are as follows:


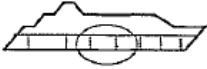
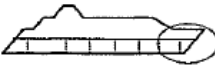

Aft ship	Hull general	Fore ship	Superstructure
			
Damages	Damages	Damages	Damages
- Cracks - Corrosion	- Cracks - Corrosion - Buckling	- Cracks - Corrosion - Buckling	- Cracks - Loosening of windows
Loads / factors	Loads / factors	Loads / factors	Loads / factors
- Vibrations - Cyclic loads - Galvanic currents	- Cyclic bending - Cyclic sea loads - Humid environment	- Cyclic sea loads - Slamming loads - Contact - Humid environment	- Global Deflections

Figure 2.3.1– Summary of common damages and main influencing factors (Lyngstad, 2002)

In addition, other reasons such as bad workmanship or unexpected sources of fatigue loading may promote the emergence of cracks and predominantly dynamic loads promote the fatigue cracks growth.

2.4 Loads on structure. Stochastic process

The crafts experience thousands of loads during the lifetime. All environmental loads that are caused by wave, wind, current, ice, snow, earthquake, etc., are different in magnitude and direction. They cause stress variations in the hull and lead to fatigue damage. In order to describe waves and the associated structural response the theory of stochastic (non-deterministic) process is used (Fines, 1985).

The basic principle of the stochastic process is considered using its time history (Newland, 1975), (Bendat & Piersol, 1971), (Langen & Sigbjørnsson, 1979).

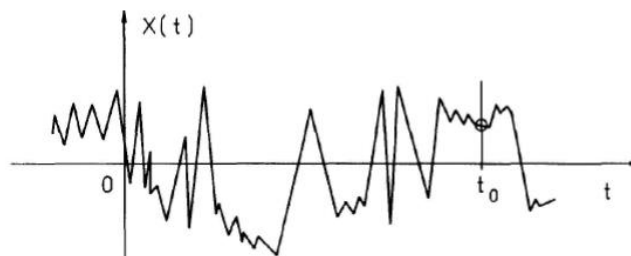


Figure 2.4.1– The time history of stochastic process (Fines, 1985)

The value of stochastic process $x(t)$ at time t is plotted as ordinate. The values of x at certain time are unpredictable, but it is possible to estimate the probability with some limits. Since it is not possible to describe the process as a function of time, the process will be

described by its statistical properties (mean value, standard deviation, etc.). This process can be stationary because mentioned statistical properties do not vary in time. Also, some processes are considered as stationary within the time interval, for example, the sea surface elevation with time intervals of three to six hours.

The probability density function of x is defined as:

$$p(x) \cdot dx = \text{prob}(x \leq x(t) \leq (x + dx)) \quad (\text{Eq. 2.4.1})$$

The cumulative distribution is defined as:

$$P(x) = \int_{-\infty}^x p(x) \cdot dx \quad (\text{Eq. 2.4.2})$$

The expected value of the process is defined as:

$$E(x) = \int_{-\infty}^{\infty} x \cdot p(x) \cdot dx \quad (\text{Eq. 2.4.3})$$

where the expected value is equal to mean value. In some cases the mean value of process is zero, like in the case of the sea surface variation about the mean water level

The autocorrelation function is given by:

$$R_x(\tau) = E[x(t) \cdot x(t + \tau)] \quad (\text{Eq. 2.4.4})$$

where τ – time interval.

In case the mean value of the process is equal to zero and $\tau = 0$, then the autocorrelation function for selected time interval is equal to variance of the process:

$$R_x(0) = E[\{x(t)\}^2] = \sigma_x^2 \quad (\text{Eq. 2.4.5})$$

where σ_x – standard deviation of the process.

The relation of energy spectrum and autocorrelation is following:

$$S_x(\omega) = \frac{1}{\pi} \cdot \int_{-\infty}^{\infty} R_x(\tau) \cdot e^{-i\omega\tau} \cdot d\tau \quad (\text{Eq. 2.4.6})$$

where ω – angular frequency.

The stationary stochastic process may contain infinitely harmonic components, each with individual frequency. The energy spectrum that shows how the energy is distributed at frequencies is presented in the figure below. The energy at any chosen $\Delta\omega$ corresponds to sinusoidal wave with amplitude a_l .

The moments of energy spectrum are given by:

$$m_n = \int_0^{\infty} \omega^n \cdot S_x(\omega) \cdot d\omega \quad (\text{Eq. 2.4.7})$$

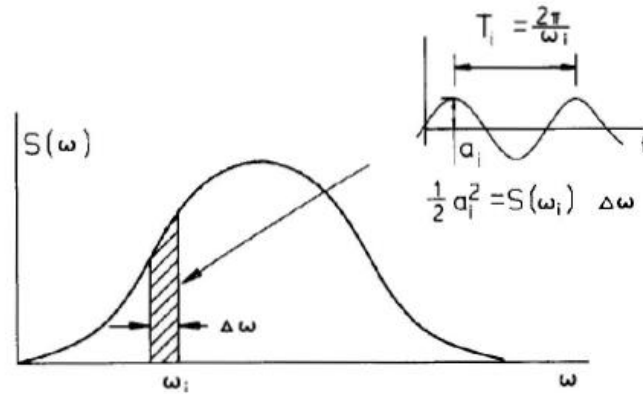


Figure 2.4.2– Energy spectrum to the corresponded stochastic process (Fines, 1985)

The total energy of the process is described by zero order moment. The zero order moment is found as:

$$m_0 = \sigma_x^2 \quad (\text{Eq. 2.4.8})$$

The spectral width parameter is found as:

$$\varepsilon = \left(1 - \frac{m_2^2}{m_0 \cdot m_4} \right)^{1/2} \quad (\text{Eq. 2.4.9})$$

This value can vary between zero and one. In case the spectral width parameter is near 0, the time history is irregular; the energy spectrum is narrow and follows Rayleigh distribution. In case the value is near 1, the time history is smoother and more regular; the energy spectrum is extensive and follows Rice distribution.

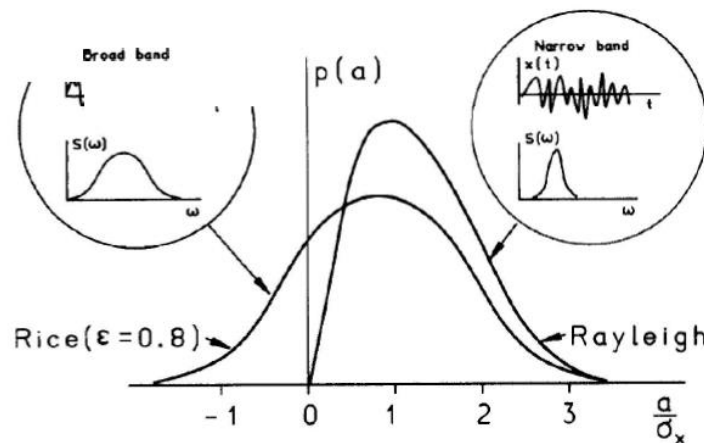


Figure 2.4.3– Rayleigh and Rice distributions (Fines, 1985)

A real sea is represented by irregular waves. Then, wave periods are considered as zero upward crossing periods and wave heights are considered as the difference between the

wave crest level and the wave through level within wave periods. It is assumed that the sea is stationary and the statistical properties of the sea state are constant.

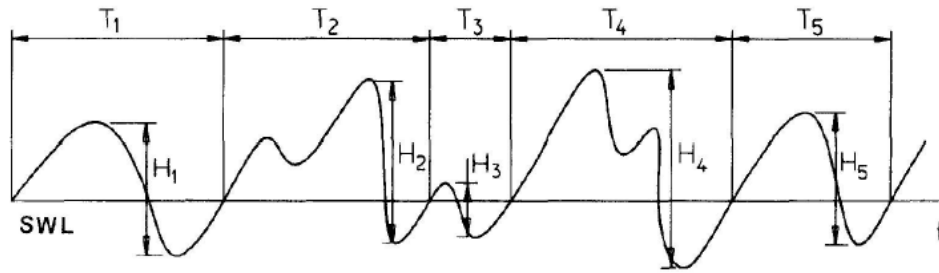


Figure 2.4.4– Time history for irregular waves (Fines, 1985)

Weather buoys make records of waves approximately every four hours at each sea area all over the world and during all seasons. All data are further sorted, processed and represented in matrix diagrams of each $H_s - T_z$ combination. This is a Wave Scatter Diagram, as shown in Appendix A. The probability of different sea state can be obtained from Scatter diagrams. One particular short term sea state may be designed using one of the standard wave spectra. Two most common wave spectra are the Pierson-Moskowitz (PM) spectrum and JONSWAP spectrum. JONSWAP spectrum is defined as:

$$S(\omega) = \alpha \cdot g^2 \cdot \omega^{-5} \cdot \exp\left[-\frac{5}{4} \cdot \left(\frac{\omega}{\omega_p}\right)^{-4}\right] \cdot \gamma \cdot \exp\left[-\frac{\left(\frac{\omega}{\omega_p} - 1\right)^2}{2\omega^2}\right] \quad (\text{Eq. 2.4.10})$$

where α , ω_p , γ – functions of the significant wave height and the zero upcrossing period;

ω_p – peak angular frequency, maximum value of the wave spectrum.

The PM spectrum is relevant for describing areas with ocean swell (in case there are no limitations in the growth of waves), while JONSWAP spectrum is applicable for describing areas with short-crested, steep wind waves (in that case there are limitations in the growth of waves depending on the generation area) (Fines, 1985). The main difference between these two spectra is a way of the wave energy distribution. In JONSWAP spectra most of the energy is located at a small wave frequency range. In PM spectra the wave energy is scattered over all frequencies; this results in structural damages over the whole range of wave frequencies. The figure below shows that the JONSWAP spectrum has one definite energy peak at a small range of frequencies compared to a wide scattered energy distribution of the Bretschneider (comparable to Pierson-Moskovitz) wave spectrum.

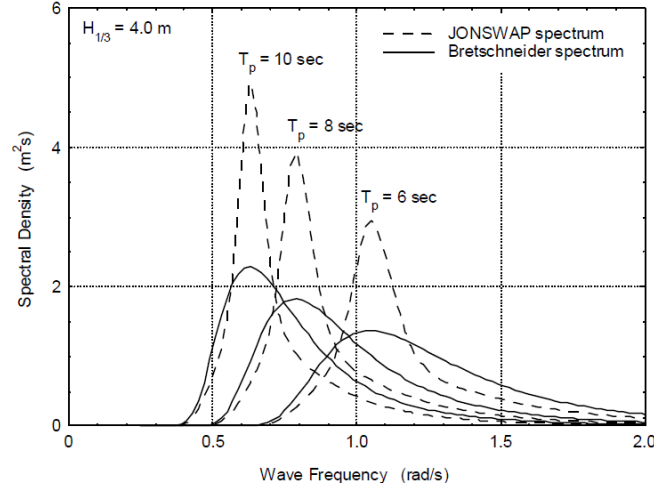


Figure 2.4.5– Jonswap and Bretschneider (PM) wave spectrum on a frequency scale (Journee & Massie, 2001)

It was already mentioned above, that for irregular wave the Rayleigh distribution is used. The wave height also follows Rayleigh distribution. Then, the probability density function is:

$$p(H) = \frac{H}{4m_0} \cdot \exp\left[-\frac{H^2}{8m_0}\right] \quad (\text{Eq. 2.4.11})$$

Cumulative distribution function of wave heights is following:

$$P(H) = 1 - \exp\left[-\left(\frac{H}{2\sqrt{2m_0}}\right)^2\right] \quad (\text{Eq. 2.4.12})$$

Significant wave height:

$$H_s = 4\sqrt{m_0} \quad (\text{Eq. 2.4.13})$$

Zero crossing period:

$$T_z \cong T_{02} = 2\pi \cdot \sqrt{\frac{m_0}{m_2}} \quad (\text{Eq. 2.4.14})$$

The most probable highest of N successive peaks is defined as:

$$H_{\max} = 2\sigma \cdot \sqrt{2 \ln N} = H_s \cdot \sqrt{\frac{1}{2} \ln N} \quad (\text{Eq. 2.4.15})$$

Returning to linear system, it is possible to notice that there is a relationship between the excitation $x(t)$ (input) and the response $y(t)$ (output), which may be described by a linear differential equation with constant coefficients. So, the wave loading on a structure can be considered as such a system where excitation will be the ocean wave forces and the response will be the stress on structure. In addition, as before the stationary stochastic process consists

of infinitely harmonic components each with individual frequency. In this case, such component of the excitation is described as:

$$x_{\omega}(t) = x_0 \cdot e^{i\omega t} \quad (\text{Eq. 2.4.16})$$

Then, the component of the response for the same frequency is defined as:

$$y_{\omega}(t) = T(\omega) \cdot x_0 \cdot e^{i\omega t} \quad (\text{Eq. 2.4.17})$$

where $T(\omega)$ is the transfer function.

From the equation above, it may be concluded that the excitation and the response has proportional relation.

The energy spectrum is proportional to the square amplitude of the harmonic component at the same frequencies. From the equation above it is clear that amplitude of input and output processes has relation through the transfer function. Therefore, the response energy spectrum can be defined as:

$$S_y(\omega) = |T(\omega)|^2 \cdot S_x(\omega) \quad (\text{Eq. 2.4.18})$$

The relation between excitation process and the response process through transfer function is shown in figure below.

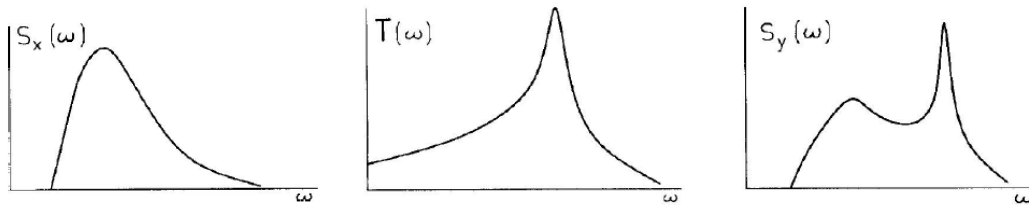


Figure 2.4.6– The excitation spectrum $S_x(\omega)$, the transfer function $T(\omega)$ and the response spectrum $S_y(\omega)$, (Lotsberg, A.Almer-Næss, & Veritec, 1985)

2.5 Long term distribution

From the observation it is also possible to estimate the cumulative distribution of long term significant wave heights. In order to find the number of waves that exceeds a given wave height in one year, the equation below can be used and the results are plotted in Figure 2.5.1.

$$N = \exp \left[- \left(\frac{H}{C \cdot H_c} \right)^D \right] \cdot N_0 \quad (\text{Eq. 2.5.1})$$

where N_0 is the total number of waves in one year.

In order to obtain the long-term distribution of individual wave height the approximation $D=1$ can be specified to equation $H_c = \frac{H_{100}}{(\ln N_{100})}$ (where, H_{100} is most

probable largest wave during 100 years; N_{100} – total number of waves during 100 years) can be implemented to equation Eq. 2.5.1.

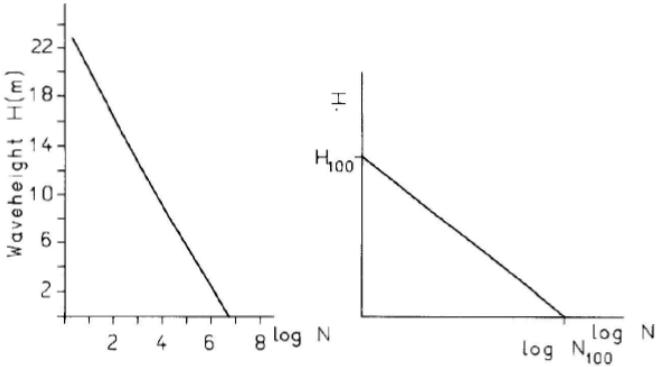


Figure 2.5.1– Diagram with the number of waves that exceeds a given wave height in one year (left figure) and the diagram of long term distribution of wave heights (right figure) (Lotsberg et al., 1985)

Then, the long term stress range distribution can be achieved from the wave height distribution. The relation between the wave height and the response of structure is described below.

The wave height is:

$$H = H_{100} \cdot \left(1 - \frac{\log N}{\log N_{100}} \right) \tag{Eq. 2.5.2}$$

The relation between wave height and the stress range is following:

$$\Delta\sigma = C \cdot H^\kappa \tag{Eq. 2.5.3}$$

The long term stress range distribution then can be found by:

$$\Delta\sigma = \Delta\sigma_{100} \cdot \left(1 - \frac{\log N}{\log N_{100}} \right)^\kappa \tag{Eq. 2.5.4}$$

where $\Delta\sigma_{100}$ is the stress range summoned by 100 year wave (Fines, 1985).

In case of the variable amplitude loading the long-term distribution of stress ranges is divided by blocks with constant stress range.

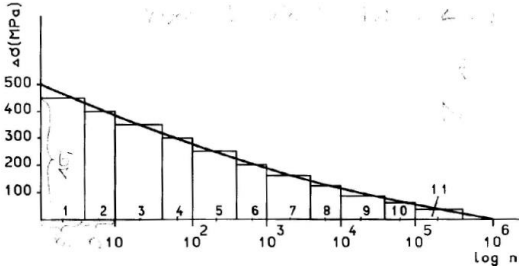


Figure 2.5.2– The long-term distribution of stress ranges divided into blocks (Lotsberg et al., 1985)

2.6 S-N curve

S-N curve is a plot representing the relation of fatigue life versus constant cyclic stress amplitude S. The stress parameter σ , strain ϵ or load P is normally plotted as ordinate while the number of loading cycles N until the specimen undergoes final disruption is normally plotted as an abscissa. Numbers of cycles are usually plotted in a logarithmic scale but it can also be linear. Millions of cycles can be applied to cause failure especially when the loading level is considerably low (Roylance, 2001).

The basic design S-N curve is given as:

$$\log N = \log \bar{a} - m \cdot \log \Delta\sigma \tag{Eq. 2.6.1}$$

where N is a predicted number of cycles to failure;

$\log \bar{a}$ – the intercept of curve with $\log N$ axis;

m – negative inverse slope;

$\Delta\sigma$ – stress range (DNV, 1997).

S-N curves are usually created based on constant amplitude loading, so parameters of stress and fatigue life are easy to define. When applied loading is variable, data are plotted on SN formats. All S-N curves are different due to material, environmental conditions, etc. An example of such diagram for steel and aluminum structures is shown below.

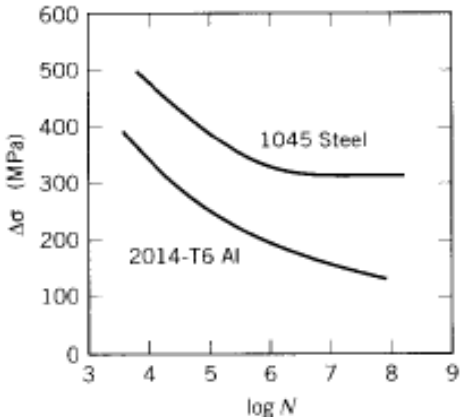


Figure 2.6.1– S-N curves for low-carbon steel and aluminum, (Roylance, 2001)

In some materials, such as ferrous alloys, S-N curve begins to flatten out and this means that σ_e failure will never occur below certain endurance limit. However, aluminum is a material with no existed fatigue limit. So, engineers should evaluate the construction lifetime carefully and balance between increasing fatigue strength and lowering structure weight (Roylance, 2001).

2.7 Cumulative damage. Miner-Palmgren's Rule

Fatigue design of a structure is based on SN data with constant amplitudes. However, marine structures undergo a load history with stochastic nature.

The development of fatigue damage under the repeated fluctuating loads is generally termed as the cumulative damage. There are various theories to calculate cumulative damage using S-N curves. However, Miner summation is widely used to calculate all fatigue designs of structures or vessels due to accuracy of results and ease of use.

The basic rule of Miner summation is that the damage on the structure per load cycle is constant at a particular stress range and is defined as:

$$D = \frac{1}{N} \tag{Eq. 2.7.1}$$

where N – constant amplitude endurance at a given stress range.

In case of constant amplitude test, this results in failure criteria, which is:

$$D_f \geq 1 \tag{Eq. 2.7.2}$$

During the fatigue history several numbers of cycles at several stress ranges are summed and the fatigue lifetime is calculated by the Miner-Palmgren formula which still contains the failure criterion, (Eq. 2.7.2) :

$$D = \sum_{i=1}^k \frac{n_i}{N_i}, \tag{Eq. 2.7.3}$$

where k – number of stress blocks;

n_i – number of stress cycles in stress block i with constant stress range $\Delta\sigma_i$;

N_i – number of cycles to failure at constant stress range $\Delta\sigma_i$.

There is a relation between the Miner summation and the fracture mechanics approach to crack growth and this is shown by the block stress history.

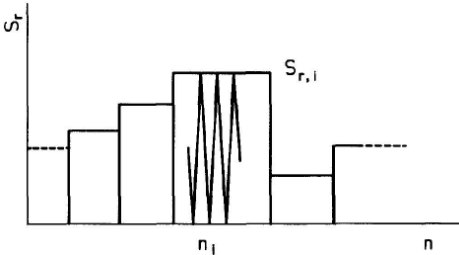


Figure 2.7.1– The block stress history (n_i – number of cycles in one block, $S_{r,i}$ – constant stress range within n_i cycles), (Berge, 1985)

The fatigue calculations are based on both Miner's rule and on the Paris-Erdogan law. Assume the Paris crack growth law:

$$\frac{da}{dN} = C \cdot (\Delta K)^m \quad (\text{Eq. 2.7.4})$$

where C , m – fitting (material) parameters; C depend on m value and is dimensional parameter;

$\frac{da}{dN}$ – the fatigue crack propagation rate. da – the crack length, defined as difference between initial crack length and failure crack length; N – number of cycles before to failure; ΔK – alternating stress intensity.

The number of cycles in each block is defined as:

$$n_i = \frac{1}{C \cdot (S_{r,i})^m} \int_{a_i}^{a_{i+1}} \frac{da}{[(\pi a)^{0.5} \cdot F]^m} \quad (\text{Eq. 2.7.5})$$

The fatigue life at a stress range $S_{r,i}$ with constant amplitude is defined as:

$$\frac{n_i}{N_i} = \frac{\int_{a_i}^{a_{i+1}} \frac{da}{[(\pi a)^{0.5} \cdot F]^m}}{\int_{a_0}^{a_f} \frac{da}{[(\pi a)^{0.5} \cdot F]^m}} \quad (\text{Eq. 2.7.6})$$

The damage sum with all blocks is defined as (Berge, 1985):

$$D = \sum_{i=1}^k \frac{n_i}{N_i} = \frac{\sum_{i=1}^k \int_{a_i}^{a_{i+1}} \frac{da}{[(\pi a)^{0.5} \cdot F]^m}}{\int_{a_0}^{a_f} \frac{da}{[(\pi a)^{0.5} \cdot F]^m}} \quad (\text{Eq. 2.7.7})$$

2.8 Design check format

The design check should be done and there are a lot of various formats. The simplest and the most common way to check the design is the allowable cumulative damage format:

$$D = \sum_{i=1}^k \frac{n_i}{N_i} \leq \eta \quad (\text{Eq. 2.8.1})$$

where η – acceptable cumulative damage ratio, given in the design codes, see Reference (Veritas, 1977),(API_RP_2A, 1982).

In most codes it is estimated that damage ratios cannot exceed unity. When allowable damage ratio is found, the degree of redundancy can be considered. In different codes the allowable damage ratio is also different, for example, according to API RP 2A the damage should be less than 0.5 (API_RP_2A, 1982), while the new proposal from the Department of Energy's Guidance Notes offers damage below 1 (D.En., 1983). Based on the importance of the structure and access for incapacitation, there are stricter requirements for the damage, for example, in DNV rules for very important details that cannot be inspected, the damage cannot exceed 0.1 (Veritas, 1977). In case damage D is larger than 1 , the design is not acceptable and should be modified.

3 Methods

3.1 Applied theories

The fatigue design is usually performed by the methods based on S-N data (fatigue tests) and estimation of cumulative damage. Moreover, a fundamental requirement for fatigue calculation is the long term stress distribution which may be computed by various methods. The Classification Note highlights two methods for the long term stress range calculation: the Postulated form and the Spectral method. In this project the second method is selected as it allows calculating the long term stress from the assumed wave climate. The spectral method implies simultaneous appearance of different load effect areas retained during calculations. Thus, this method indicates a significant reduction of uncertainties as compared with other methods (DNV, 2010).

In general, this method is based on the theory of stochastic process for response calculation which was explained in subsection 2.4. For a specific sea state, the spectrum of the stress response is defined as a combination of the wave spectrum with the transfer function, which expresses the relation between heading and frequency (Eq. 2.4.18). The transfer function may be defined by the time history approach, as explained in subsection 2.4 (Fines, 1985). The long term stress distribution may be defined through a short term Rayleigh distribution for a particular sea state, as explained in subsection 2.4. In determination of the long term conditions, it is not necessary to define the completely worst case but rather worst "normal operational case" that vessel experiences as expected loads during its lifetime (Segers, 2004). When the long term stresses are defined, the fatigue damage for one-slope S-N curve may be calculated (DNV, 2010).

The main steps of calculation procedure are described in Figure 3.1.1 and the equation procedure will be explained in next subsection. In this method the ship response is linearly modelled and it is sufficient for fatigue assessment. Since the ship response is described by the superposition of the response of all regular wave components, the response in irregular waves is described as a combination of all responses in regular waves and leads to frequency domain analysis. The summation over all contributing dynamic loads gives the resulting stress.

The spectral method contains several assumptions for fatigue damage calculation, which are as follows:

- Waves are described by scatter diagram;
- Rayleigh distribution is relevant for stresses with short term condition;
- A cycle count corresponds to the zero crossing period of a short term response;
- Cumulative summation from each sea state in the wave scatter diagram is linear (Segers, 2004).

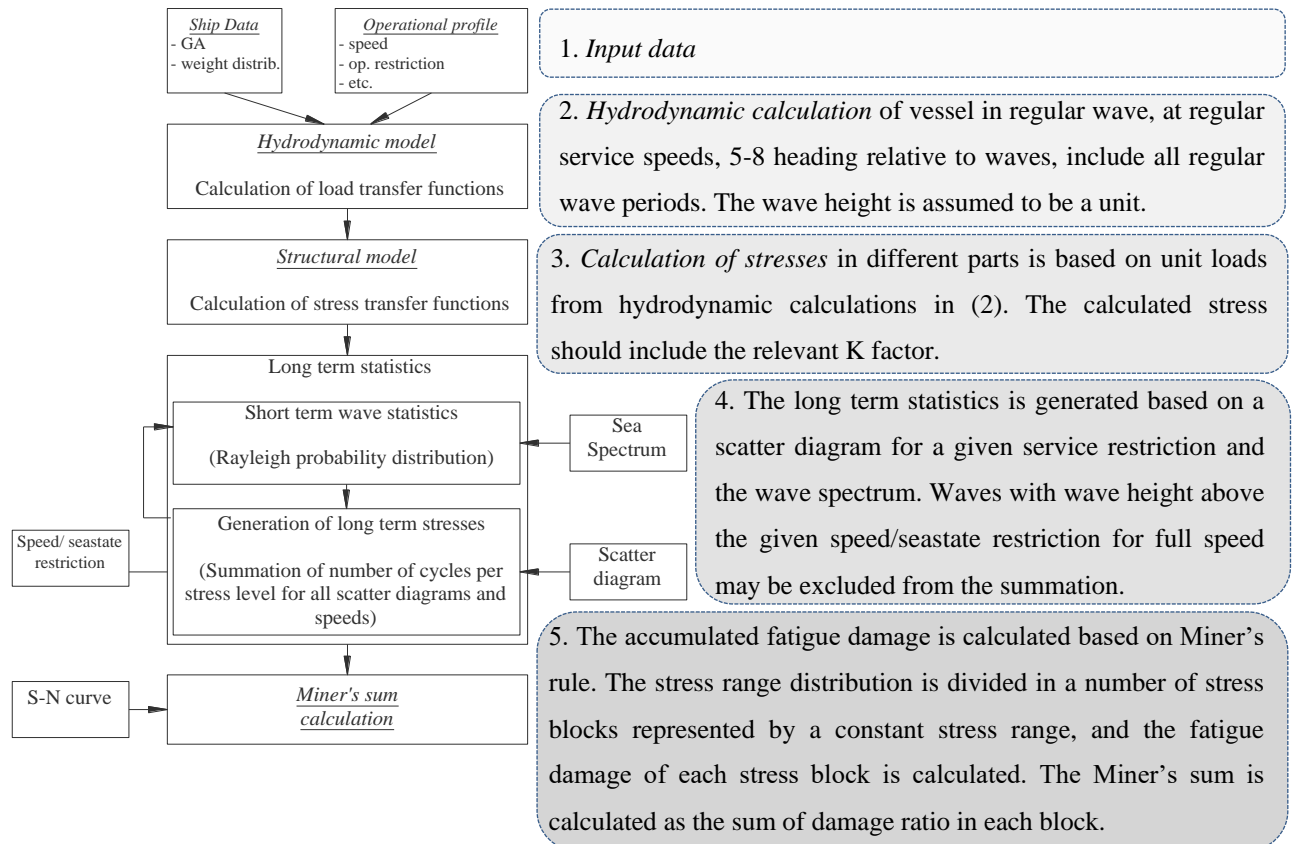


Figure 3.1.1– Fatigue calculation procedure (DNV approach)

3.2 Overview and procedure for fatigue analysis

This section describes the workflow of fatigue analysis, carried out for global hull cyclic loads due to waves. In general, at the design stage only limited initial data is available, so preliminary fatigue analysis (PFA) is relevant to conduct. The main target of this analysis is to calculate the minimum required section modulus at the particular cross sections of the vessel. The achieved values are most probably restricting the scantlings of the structure in the midship of the vessel, which will be calculated at a later stage at the Central Engineering (CE) department. The PFA will most often result in global changes to the scantlings of the structure.

For fatigue investigation, there are some equal steps that should be taken in order to acquire the desired answers, such as the required section modulus (Hydra & Jorinus, 2010).

The produce is based on DNV recommendation for fatigue (see Figure 3.1.1) and may be divided in following steps:

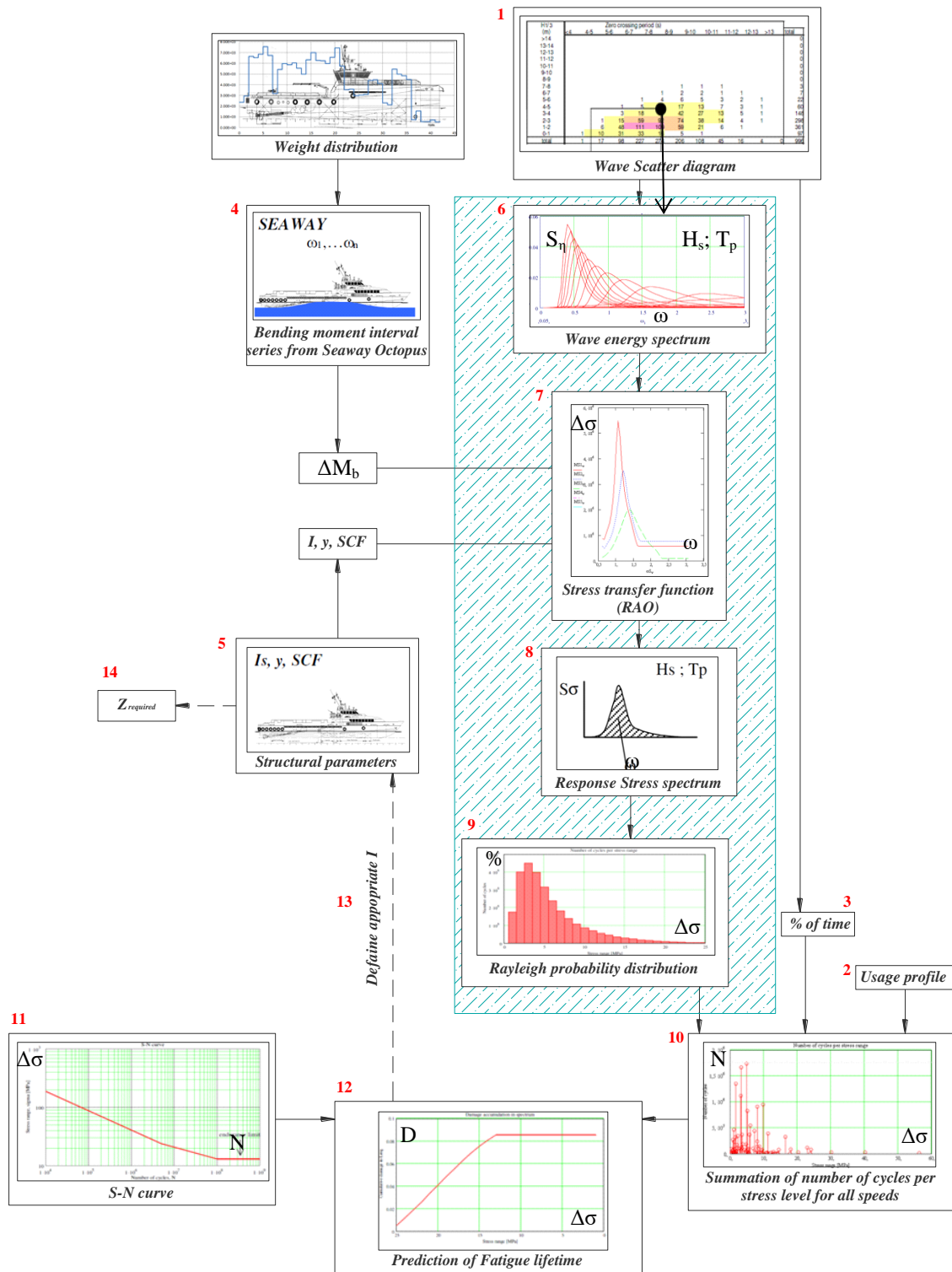




Figure 3.2.1– Structure for fatigue and required section modulus assessment

- | | | |
|---|--|---|
| <ol style="list-style-type: none"> 1) Define wave scatter diagram 2) Define of Usage profile (operating speeds and amount of active hours per year) 3) Time spent for particular speed in combination with wave height and wave period 4) Bending moments RAO from the program “Octopus Seaway” 5) Structural parameters: initial moment of inertia, location of neutral axis and stress concentration factor |  | <p style="text-align: center;">Input parameters
for
fatigue calculation</p> |
| <ol style="list-style-type: none"> 6) Generation of wave energy spectrum 7) Generation of stress transfer function 8) Generation of stress spectrum 9) Rayleigh probability distribution 10) Summation of number of cycles per stress level for all scatter diagrams and speeds 11) S-N curve 12) Calculation of cumulative damage / prediction of fatigue life 13) Define the appropriate moment of inertia 14) Calculate actual section modulus and compare with minimum required value. |  | <p style="text-align: center;">Fatigue
calculation
procedure</p> |

The calculation is conducted in 2 programs: Seaway Octopus and Alufastship. An overview of all required initial data for PFA is given in section 3.6 and Appendix B.

3.3 Method Description

3.3.1 Octopus Seaway

Based on general arrangement, several locations of expected fatigue critical details are selected for the analysis. The marked locations are preferred to investigate based on experience that particular cross sections are dealing with the combination of high loads, local stress concentrations, large transitions in stiffness of hull girder (Hydra & Jorinus, 2010) and other causes mentioned in subsection 2.3. Then, the bending moments at these locations are necessary to obtain.

These bending moments are acquired in the strip theory program “Octopus Seaway” using the weight distribution as a load on vessel. This program allows measurement of the hull girder bending moments due to encountered waves with 6 degrees of freedom (Journee, 2001). The accuracy of the results primarily depends on hull shape. For example, slender hulls tend to have more accurate results and thus, this program is acceptable to use.

Besides the marked locations (cross sections) which are decided to analyze, other required input parameters for bending moments calculation are as follows:

- Hull shape and designed lines (provided by D&P or engineering);
- Weight distribution (provided by D&P or engineering), corresponding displacement (50% loading condition) and draft;
- Operating speeds (provided by D&P);
- Wave directions (For hydrodynamic load calculations the wave direction is 180 degree (head seas)).

The desired bending moments RAO are produced in regular waves for each location, speed and wave frequency, relative to $1m$ significant wave height. Basically, the output from “Seaway” is the transfer function ($T(\omega)$), see Figure 2.4.6. Next, obtained results are presented digitally in the format as shown in Appendix C, and are used as one of the input parameters for fatigue calculation program “Alufastship” (step 4 in Figure 3.2.1), which combines the loading data of vessel, wave scatter diagram and applicable S-N curve for each location on vessel (Hydra & Jorinus, 2010), (Hydra, 2013).

3.3.2 Alufastship

In order to obtain the required section modulus for each vessel at several locations, the Alufastship program is used. This application allows making a fatigue prediction at the design stage of vessel by calculating the occurring stress levels and number of cycles from the input parameters.

Based on achieved bending moments the expected weak locations are selected and entered in Alufastship application as input parameters (enter both x and z coordinates of each detail). Then, for each detail the FAT class and material are applied. The catalogue of details is described in Appendix D. For preliminary fatigue analysis the first FAT class (fatigue detail No.6) is selected based on Germanisher Lloyd rules as this type of joint is the most encountered in the hull bottom and deck of high speed crafts of Damen. Since aluminum is a construction material for the hull, the detail category is then $\Delta\sigma_R = 18 MPa$, which means that

allowable stress for the structure and initial crack will occur after 2×10^6 load cycles. The slope exponent of S-N curve is $m = 3$ (for welded joints). The selected detail class is relative to a minimum acceptable quality level in Damen.

The first part of the analysis may be launched now. For marked locations the operational area, speeds (should be corresponded with obtained bending moments RAO) and limiting wave height are entered, see figure below.

Number of locations:

Limiting wave heights
Number of different WSD's (max: 5)

Input wave scatter diagram

- Standard WSD (acc. Global wave statistics)
- Manual input WSD

Calculation of limitation of WSD's

- Limitation of WSD influences other WSD's
- Limitation of WSD does NOT influence other WSD's

Export data

Save input

IMPORTANT!!
Speeds should be entered from highest (Speed 1) to lowest (Speed 5) speed.

Select Wave scatter diagram

- Northsea
- Gulf of Mexico
- N-Brazil
- S-Brazil
- Nigeria
- Angola
- Red Sea
- Persian Gulf
- N-Arabian Sea
- Bengal Sea
- N-Chinese Sea
- S-Chinese Sea
- W-Pacific Sea
- W-Mediterranean Sea
- E-Mediterranean Sea
- DNV-3

Limiting wave heights - Set 1
Vessel speed Knots

Wave period Tz [s]	0,5	1,5	2,5	3,5	4,5	5,5	6,5	7,5	8,5	9,5	10,5	11,5	12,5	13,5
Limiting Wave height [m]	3	3	3	3	3	3	3	3	3	3	3	3	3	3

Limiting wave heights - Set 2
Vessel speed Knots

Wave period Tz [s]	0,5	1,5	2,5	3,5	4,5	5,5	6,5	7,5	8,5	9,5	10,5	11,5	12,5	13,5
Limiting Wave height [m]	3	3	3	3	3	3	3	3	3	3	3	3	3	3

Limiting wave heights - Set 3
Vessel speed Knots

Wave period Tz [s]	0,5	1,5	2,5	3,5	4,5	5,5	6,5	7,5	8,5	9,5	10,5	11,5	12,5	13,5
Limiting Wave height [m]	3	3	3	3	3	3	3	3	3	3	3	3	3	3

Figure 3.3.1– Input data screen

Due to the application of limited height of waves, all waves with height above selected, for example $H_s = 3m$, are removed from the Scatter diagram. Since several speeds are applied, the waves sailed at high speed are also removed from the Scatter diagram. This results in reduction of the occurring loads and stress level. When waves are normalized to 1000 waves, the Scatter diagram is ready to be used in Alufastship application for fatigue calculation, see step 1 in Figure 3.2.1 Moreover, the result of the first part of the analysis is also transfer function (RAO) for each detail location, based on (Eq. 3.3.2) and this is step 7 in Figure 3.2.1.

Having obtained the data, the second part of the analysis may be take place. The stepwise process is given below:

- a) Enter the operational profile (step 2 in Figure 3.2.1). This includes the operational lifetime, operating hours per year and sailing directions which are relative to wave directions. A directional distribution reduction parameter $D_{dr} = 0.5$ (DNV, 1997) is included here in order to account all wave directions instead of one (head sea), see (DNV, 1996).
- b) Check/enter corresponding ship details for global stress range and enter structural parameters, such as initial moment of inertia and stress concentration factor (step 5 in Figure 3.2.1). The fatigue lifetime of a detail primary depends on the hot spot stress range (the total actual stress at the root of a notch) (DNV, 1997), (Biot, Marino, & Susmel, 2005). This stress is influenced by weld shape irregularities (unavoidable notches, discontinuous, significant influence of axial and angular misalignment, etc.). Due to high localization of stress and difficulty to quantify values, no systematic stress analysis is conducted. Instead, the hot spot stress is defined as nominal stress multiplied by stress concentration factor which includes all geometrical influences. Different equations are used to calculate this factor based on the geometry of joint and load condition (Gibstein & T.Moe, 1985). The SCF in the preliminary analysis is estimated 1.15 due to butt welds corresponding to FAT class 6, based on Germanisher Lloyd (GL, 2007). However, in detailed fatigue analysis the SCF should be individual for each detail.
- c) Enter Sea-Speed conditions which means estimating the percentage of time spent at each marked speed (step 3 in Figure 3.2.1).
- d) Check the safety factor. This factor γ allows to secure the occurrence that the failure does not happen very frequently due to natural uncertainties, for example, extreme environmental loads occur only once in 100 years. However, in some cases, such as environmental loads with annual occurrence, this factor could be equal to 1.2. For preliminary fatigue analysis this factor is equal to 1 due to assumption that for the ordinary ultimate strength check the safety factor is higher (Moan, 1985).

When all initial data is prepared and entered to Alufastship application, the spectral analysis in the program may be launched. The formulas described below are actual equations used in Alufastship code. As it was mentioned above the spectral analysis consists of 5 steps that are described by equation procedure in details below:

6. Wave energy spectrum

Based on the applied theory of spectral analysis described in subsection 2.1, first of all it is necessary to calculate the mechanical response of vessel in all regular seas for all wave heights and wave periods. The wave energy distribution is defined as a function of wave frequency and is set by wave spectrum S_η , corresponding to (Eq. 2.4.10). The wave energy spectrum for one scatter diagram and one wave height is described by the equation below:

$$S(\omega) = 487 \cdot \frac{H_s^2}{T_p^4 \cdot \omega^5} \cdot \exp \left[-1950 \cdot \frac{\omega^{-4}}{T_p^4} \right] \cdot (1 - 0.287 \ln(\gamma)) \cdot \gamma \cdot \frac{\exp \left(\left(\frac{\omega - \frac{2\pi}{T_p}}{2s^2 \left(\frac{2\pi}{T_p} \right)^2} \right)^2 \right)}{2s^2 \left(\frac{2\pi}{T_p} \right)^2 - 1} \quad (\text{Eq. 3.3.1})$$

where H_s is a significant wave height;

T_p – peak period, which defined as $T_p = 1.407 \cdot T_z$ and $\gamma = 1$ (γ – peak enhancement factor) for PM spectrum; and as $T_p = 1.285 \cdot T_z$ and $\gamma = 3.3$ for JONSWAP spectrum;

ω – wave frequency;

$s = 0.09$ if $\omega > 2\pi/T_p$ and $s = 0.07$ if $\omega < 2\pi/T_p$; (Dijkstra, 2004).

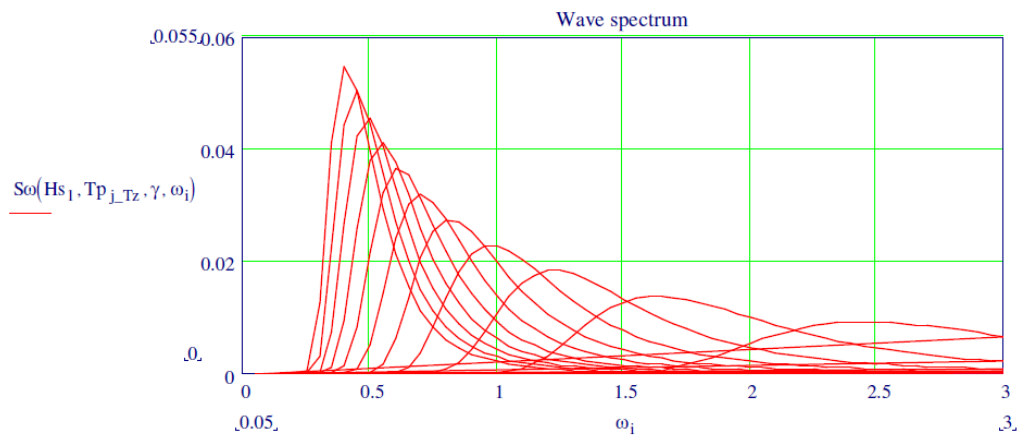


Figure 3.3.2– Wave energy spectrum

7. Transfer function (RAO)

In the program “Seaway Octopus” the bending moments (RAO) are calculated in regular waves, for each detail location (in x -axis), in several speeds, 1 heading and $1m$ significant wave height. Each combination of load case, heading and wave height gives the stress transfer function for a given detail location in several speeds. However, for fatigue calculation the stress transfer function should be represented by stresses at each detail location

(in z -axis) against the wave frequency. Thus, the stress transfer function is defined by the following equation:

$$\sigma(\omega) = \frac{SCF \cdot M_b(\omega) \cdot (|h_{na} - h_{dt}|)}{I_s} \quad (\text{Eq. 3.3.2})$$

where SCF – stress concentration factor;

$M_b(\omega)$ – bending moment transfer function;

h_{na} – location of neutral axis in z -axis;

h_{dt} – location of detail in z -axis ;

I_s – cross section moment of inertia of detail,

(Segers, 2004).

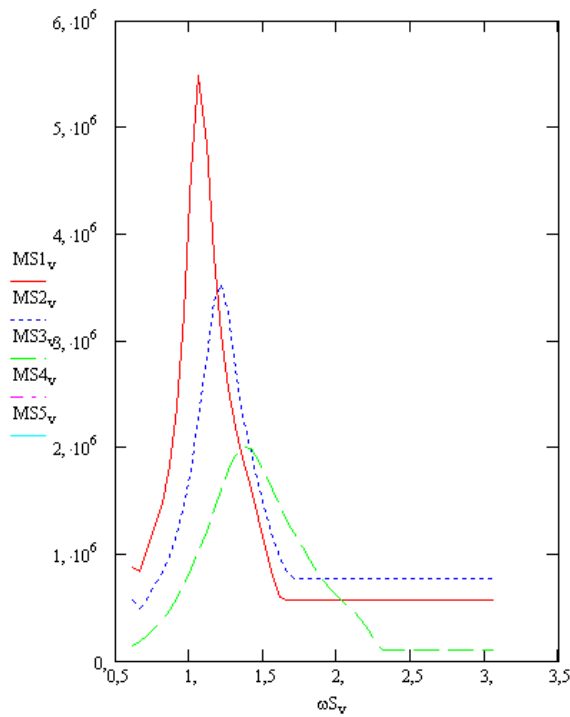
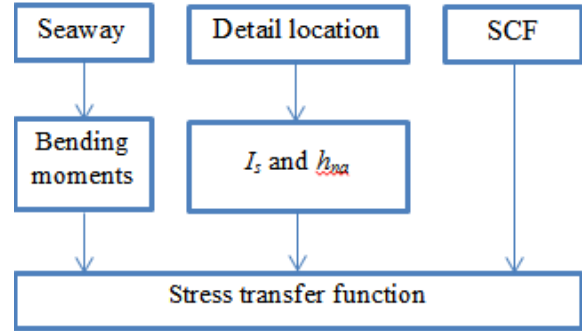


Figure 3.3.3 – Moment interval series (for 1 detail location in 3 speeds)

8. Stress spectrum

Based on the theory described in subsection 2.4 and (Eq. 2.4.18), the response stress spectrum may be obtained by the following formula:

$$S_{\sigma}(H_s, T_p, \gamma, \omega) = S_{\omega}(H_s, T_p, \gamma, \omega) \cdot \sigma(\omega)^2 \quad (\text{Eq. 3.3.3})$$

The summation of stress spectrum for each wave frequency interval is calculated by:

$$M_{\sigma}(H_s, T_p, \gamma, \omega) = \left(\sum_i^n S_{\sigma}(H_s, T_p, \gamma, \omega) \right) \cdot \Delta\omega \quad (\text{Eq. 3.3.4})$$

(Segers, 2004).

9. Rayleigh distribution

In Alufastship it is assumed that the wave height is distributed according to Rayleigh, also see theory in subsection 2.4. The distribution of stress levels is defined as an occurring stress between the upper and lower stress levels and looks as follows:

$$\text{prob}(H_s, T_p, \gamma, \omega, \sigma_l, \sigma_h) = \exp\left(-\frac{\left(\frac{\sigma_l}{2}\right)^2}{-2M_{\sigma}(H_s, T_p, \gamma, \omega)}\right) - \exp\left(-\frac{\left(\frac{\sigma_h}{2}\right)^2}{-2M_{\sigma}(H_s, T_p, \gamma, \omega)}\right) \quad (\text{Eq. 3.3.5})$$

where σ_l – lower stress level and σ_h – upper stress level, (Segers, 2004).

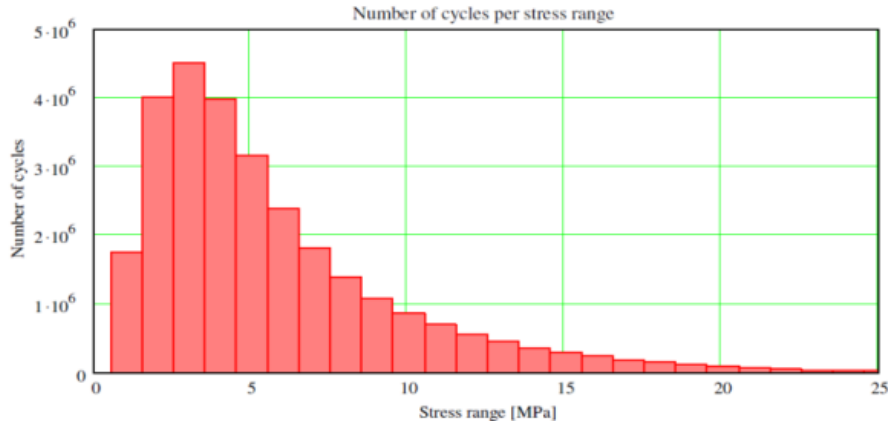


Figure 3.3.4– The distribution of stress levels

10. Summation of number of cycles per stress level

The combination of wave speeds, wave lengths and vessel speeds gives the encounter frequency, as follows:

$$\omega_e = \frac{c + V_s}{\lambda} \quad (\text{Eq. 3.3.6})$$

where c – wave speed;

λ – wave length;

V_s – ship speed.

Then, the original number of cycles per combination of wave height and wave period can be obtained by the equation:

$$N_{sc} = \frac{c \cdot V_s \cdot \omega_e \cdot n_{wcd_sp}}{N_{tot}} \quad (\text{Eq. 3.3.7})$$

where n_{wcd_sp} – number of cycles in combination of the wave scatter diagram and speed;

N_{tot} – total number of cycles.

The total number of cycles per stress level can be obtained by multiplying (Eq. 3.3.7) with (Eq. 3.3.5).

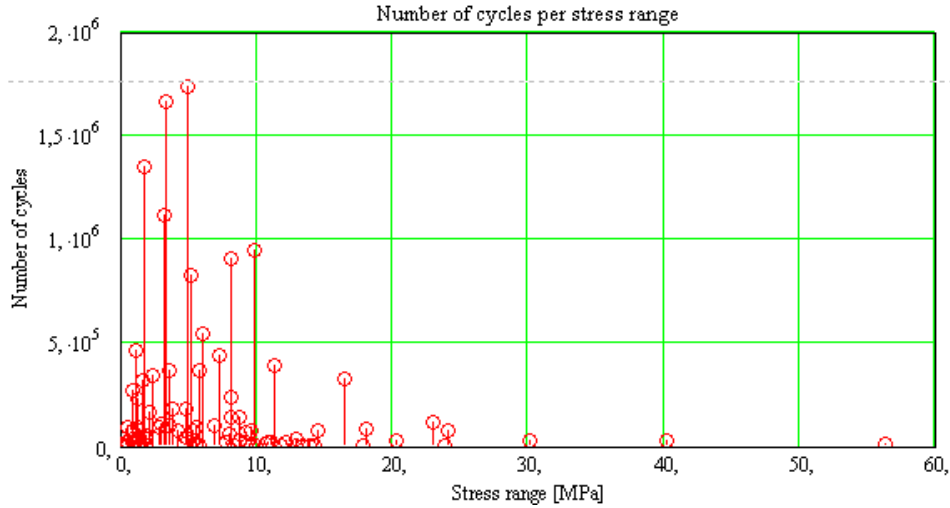


Figure 3.3.5– Cumulative stress spectrum

Next, the total number of cycles per stress level is calculated for all speeds and then is summed up. Finally, fatigue damage can be calculated by Miner's rule (see Eq. 2.7.3), while appropriate moment of inertia may be determined by several iterations and, in conclusion, the required section modulus is calculated by (see step 14 in Figure 3.2.1):

$$z = \frac{I_s}{h_{na} - h_{dt}} \quad (\text{Eq. 3.3.8})$$

The example of calculation (report from Alufastship) is shown in Appendix B.

3.4 Case description of sensitivity analysis

The achieved value of the required section modulus is very sensitive to different input parameters and there are still many uncertainties with fatigue life predictions and accuracy of the results. Thus, the sensitivity analysis will give the insight of how variable parameters influence fatigue lifetime and which of them affects the most.

As a test vessel for this analysis the Stan Patrol 3007 was selected, see subsection 3.6 and as analyzed locations three frames were defined (see Figure 3.4.1).

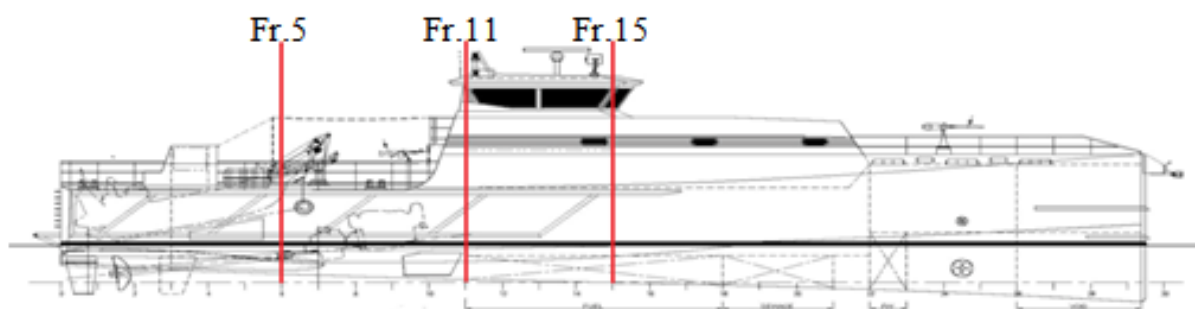


Figure 3.4.1– General layout SPa 3007 with locations for the sensitivity analysis

Frame 5 was selected due to presence of the slipway; at frame 11 a transition from hull to the superstructure took place and at this location the highest calculated bending moment was identified. Frame 15 contains a superstructure and it was selected to get an idea of the section modulus sufficiency.

As for input parameters, the standard operational profile (see Table 3.6.3) was followed but several input parameters were variable (see Table 3.4.1). Analysis was carried out in 14 operational areas (see subsection 3.6.3).

Table 3.4.1– Variable operational profile for the sensitivity analysis

Service conditions (% of time)	100% MCR 50% MCR 10% MCR	3% 75% 22%	5% 70% 25%	5% 75% 20%	5% 80% 15%	10% 75% 15%	10% 80% 10%	15% 75% 10%	15% 80% 5%	20% 75% 5%
Wave height constraint (H_s , [m])	2.5; 3; 3.5; 4 m									
Intended service period	20 and 25 years									
Sailing hours per year	2000 h/y									

3.5 Case description of fatigue design curves

Based on the results of sensitivity analysis, several most influenced variable parameters have been selected, as multi-axis of fatigue design curves. Moreover, one of the axes is the length of vessel which means that preliminary fatigue analysis has been conducted for the range of vessels FCS (Fast Crew Suppliers) and SPa (Stan Patrol) (see section 3.6.1). The fatigue design curves were expected to show the behavior of required section modulus influenced by different parameters (see Table 3.5.2), and combination of them. For example, one of fatigue design curves shows how variable engine power for each vessel influences

minimum required section modulus. The fatigue design curves include points of actual section modulus of already built aluminum vessels. Vessels larger 40 meters are made of hybrid material, which means steel hull and aluminum superstructure.

Table 3.5.1– Actual section modulus of already built vessels

<i>Type of vessel</i>	<i>Fast Crew Supplier</i>			<i>Stan Patrol</i>		
	<i>3307</i>	<i>4008</i>	<i>5009</i>	<i>3007</i>	<i>4207</i>	<i>5009</i>
$Z_{actual}, [m^3]$	0.18	0.19	0.23	0.22	0.13	0.26

The main target of creating fatigue design curves was to help engineers at the design stage to make a proper selection regarding main particles of vessel for specific operational profile or individual customer requirement. In addition, such curves can help to identify any dependency between input parameters and minimum required section modulus. For example, for this purpose the third type of fatigue design curves, namely 3D-fatigue curve, was created.

As regards the operation areas, only DNV-3 and the Gulf of Mexico were selected due to several reasons. Generally, all high speed crafts in Damen are designed based on the standard operational profile as a requirement (see Table 3.6.3), where DNV-3 is the required operation sea. In order to compare the results and to investigate the influence of sea on required section modulus, another operational area (Gulf of Mexico) with different wave behavior was selected.

Table 3.5.2– Variable operational profile for the fatigue design curves

Type of vessel	Fast Crew Supplier	Stan Patrol
Wave height constraint ($H_s, [m]$)	1; 2.5; 3; 3.5; 4 m	
Total sailing hours	45 000 – 125 000 hours	40 000 – 125 000 hours


3.6 Analysis parameters




For fatigue analysis 11 high speed crafts have been investigated. General information for each vessel is described below and detailed information can be found at the official website of the company (<http://products.damen.com/en>, April 2016).

Table 3.6.1– General particulars of Fast Crew Suppliers

FCS	Design	LOA, [m]	B, [m]	Δ , [t]	Speeds, [kn]	Analyzed frame #
1905		19.7	8.2	41.5	32kn, 22kn, 11.5kn	6
2610		25.75	10	79	25kn, 18kn, 7kn	10
3307		33.32	7	135	21.5kn, 17.5kn, 8kn	14
4008		41.2	8	168	24.7kn, 17.5kn, 8kn	16
4207		42.2	7	186	24kn, 18kn, 8kn	20
5209		52.25	9	339	25.5kn, 19.8kn, 11.1kn	20

Table 3.6.2– General particulars of Stan Patrol

SPa	Design	LOA, [m]	B, [m]	Δ , [t]	Speeds, [kn]	Analyzed frame #
3307		30.93	7	94	30kn, 20kn, 9kn	11

3808		38.9	8	229	20kn, 15kn, 10 kn	16
4207		42.8	7	186	28kn, 16kn, 11kn	18
4708		47.6	8	250	30kn, 17kn, 12kn	20
5009		50.02	9	285	30kn, 18kn, 12kn	24

The cell “analyzed frame” means the selected frame for the analysis with largest hull girder bending moment. All vessels are assumed to be made of aluminum.

3.6.1 Operational profile

Based on the expected utilization of vessels by clients, a standard operational profile was created. Basically, it depends on the total amount of sailing hours per year and loading conditions.

Table 3.6.3– Standard operational profile

Type of vessel	Fast Crew Supplier	Stan Patrol
Weight distribution	50% of loading conditions	
Speed	According to the engine power. 3 speeds	
Service conditions	100% MCR – 50% of time 50% MCR – 20% of time 10% MCR – 30% of time	100% MCR – 5% of time 25% MCR – 75% of time Idle engine speed – 20% of time

Wave height constraint (H_s , [m])	2.5	3.5
WSD	DNV-3	
Intended service period	15 years	20 years
Sailing hours per year	5000h/y	2000 h/y

3.6.2 Operating area

Vessels should be able to operate worldwide; this means that vessels should withstand a certain quantity of repeating waves with a given wave frequency and height. In Damen most customers require these vessels to operate in the following 15 seas, which were used as the operation areas in this project, in addition to DNV-3.

- North Sea;
- Gulf of Mexico;
- North Brazil;
- South Brazil;
- Nigeria;
- Angola;
- Red Sea;
- Persian Gulf;
- North Arabian Sea;
- Bengal Sea;
- North Chinese Sea;
- South Chinese Sea;
- West Pacific Sea;
- West Mediterranean Sea;
- East Mediterranean Sea.

The corresponded standard wave scatter diagrams can be found in Appendix A.

3.6.3 Engine power and speeds

For sensitivity analysis and fatigue design curves alternate engines were selected in order to investigate how speeds influence on minimum required section modulus. Based on a power prediction chart, new speeds were identified and are listed below for each vessel. The detailed information can be also found at the official website of the company (<http://products.damen.com/en>, April 2016).

Table 3.6.4– Engine data and new achieved speeds for FCS

Vessel	Engine	Speeds for service conditions		
FCS 1905	No alternate engine	–		
FCS 2610	No alternate engine	–		
FCS 3307	2× CAT 32 D-rating WOSR 2× 1193 bkW @ 2100-2300 rpm	27.9kn	19.6kn	11kn
FCS 4008	4× MTU16V2000 M93	35kn	28kn	12kn

	4× 1790 bkW @ 2320-2450 rpm			
FCS 4207	4× MTU 16V 4000 M73L 4× 2880kW @ 2050-2350 rpm	35kn	27kn	13kn
FCS 5209	4× CAT 3516C-rating 4× 2350 bkW @ 1600-1800 rpm	35kn	26kn	15kn

Table 3.6.5– Engine data and new achieved speeds for SPa

Vessel	Engine, [kW]	Speeds for service conditions, [kn]		
SPa 3007	2× CAT C32 TTA D-rating WORS 2× 1193 bkW @ 2000-2300 rpm	27.5kn	14kn	12kn
	4× MTU 16V2000 M94 1DS 4× 1939bkW @ 2250-2450 rpm	32.5kn	16.2kn	11kn
FCS 3808	4× Caterpillar C32 A-rating 4× 746bkW @ 1600-1800 rpm	18kn	12.5kn	8.5kn
	4× MTU 16V2000 M84 4× 1630 bkW @ 2180-2450 rpm	28kn	15.9kn	12kn
FCS 4207	4× Caterpillar C32 4× 1081 kW @ 2100 - 2300 rpm	24.5kn	15kn	9kn
	4× Caterpillar 3516C 4× 2350 kW @ 1600 - 1800 rpm	33kn	19kn	14.5kn
FCS 4708	4× Caterpillar 3512C 4× 1678 kW @ 1600 -1800 rpm	26.5kn	15.5kn	11kn
	4× Caterpillar 3516C 4× 2350 kW @ 1600 - 1800 rpm	33.5kn	20.6kn	14kn
FCS 5009	4× Caterpillar C32 4× 1081 bkW @ 2250-2450 rpm	26kn	16kn	10.5kn
	4× Caterpillar 3516C 4× 2350 bkW @ 1600-1800 rpm	35.5kn	20.5kn	13kn

4 Results

The results are presented below. Firstly, the issue of sensitivity analysis is discussed. Secondly, several fatigue design curves with variable operational profile but constant service conditions for FCS and SPa are represented. Thirdly, diagrams with constant operational profile but variable service conditions are presented for both types of the vessels. The difference between the curves consists in selected input parameters for the axis. Finally, 3D curve for FCS and analysis of impact due to length, displacement and speed of vessels on the minimum required section modulus are discussed.

4.1 Sensitivity analysis

As it was discussed above, the sensitivity analysis is made for SPa 3007 for three locations frames 5, 11 and 15. The study was conducted on the basis of standard operational profiles but for 16 operational areas and four types of wave height. The required section modulus (Z) is a comparative value in the analysis that reflects the fatigue lifetime. Table 4.1.1-Table 4.1.3 and Figure 4.1.1-Figure 4.1.2 contain the results for given conditions.

Table 4.1.1– Minimum required section modulus for frame 5

No.	Operational area	$H_s=2.5m$	$H_s=3m$	$H_s=3.5m$	$H_s=4m$
		$Z_{req}, [m^3]$	$Z_{req}, [m^3]$	$Z_{req}, [m^3]$	$Z_{req}, [m^3]$
1	North Sea	0.18	0.19	0.2	0.21
2	Gulf of Mexico	0.27	0.29	0.3	0.31
3	N-Brazil	0.16	0.16	0.16	0.17
4	S-Brazil	0.12	0.13	0.13	0.14
5	Nigeria	0.24	0.25	0.25	0.25
6	Angola	0.13	0.14	0.14	0.14
7	Red Sea	0.3	0.33	0.34	0.35
8	Persian Gulf	0.29	0.32	0.34	0.36
9	N-Arabian Sea	0.3	0.33	0.35	0.37
10	Bengal Sea	0.15	0.16	0.16	0.17
11	N-Chinese Sea	0.23	0.25	0.26	0.27
12	S-Chinese Sea	0.27	0.3	0.31	0.32
13	W-Pacific Sea	0.17	0.18	0.19	0.19
14	W- Mediterranean Sea	0.28	0.3	0.32	0.34
15	E- Mediterranean Sea	0.21	0.23	0.24	0.25
16	DNV-3	0.18	0.19	0.19	0.19

Results for the frame 5 show that values of Z grow with increasing significant wave height, as seen in Figure 4.1.1. The growth rate is unique for each operational area and depends on dominating wave periods, wave length and operability of the vessel.

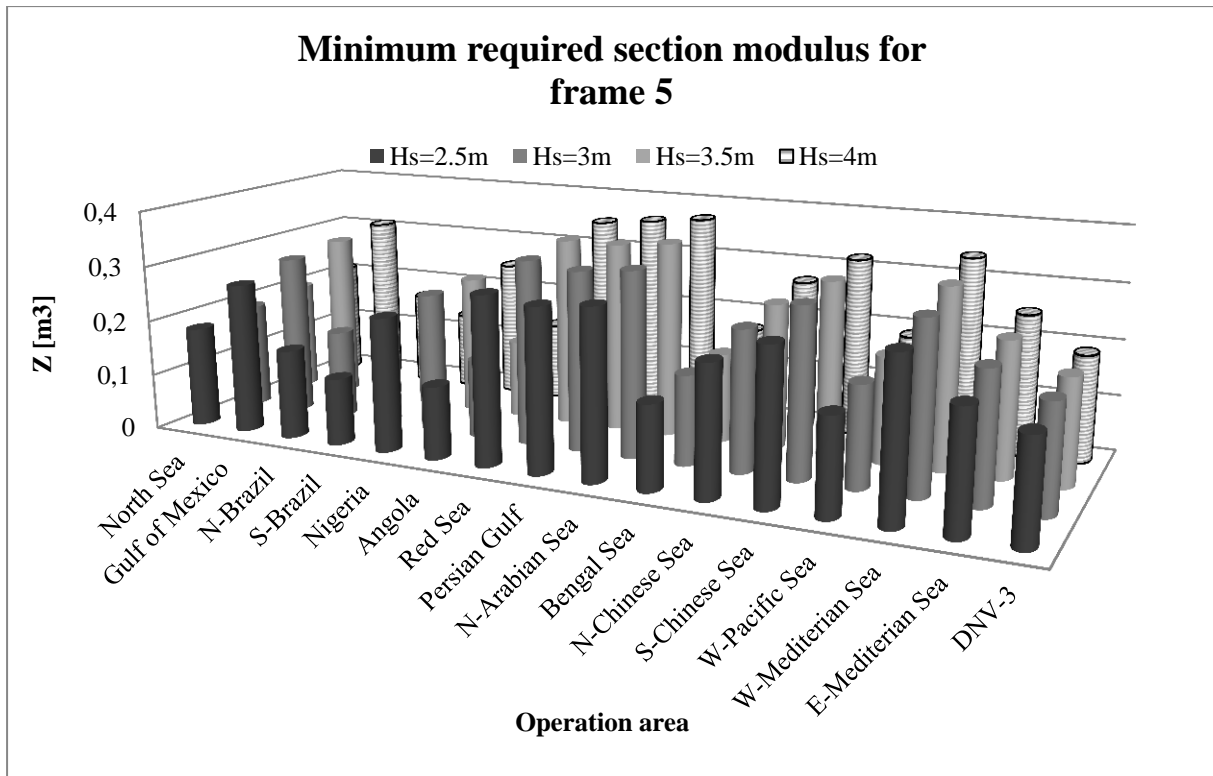


Figure 4.1.1– Minimum required section modulus for frame 5

As it is evident from Figure 4.1.1 the largest value of the required section modulus is for 4m wave height in the N-Arabian Sea (0.37 m^3), followed by less value for the Persian Gulf (0.36 m^3), the Red Sea (0.35 m^3) and the lowest value is for the S-Brazil Sea (0.14 m^3).

Table 4.1.2– Minimum required section modulus for frame 11

No.	Operational area	$H_s=2.5\text{m}$	$H_s=3\text{m}$	$H_s=3.5\text{m}$	$H_s=4\text{m}$
		$Z_{\text{req}}, [\text{m}^3]$	$Z_{\text{req}}, [\text{m}^3]$	$Z_{\text{req}}, [\text{m}^3]$	$Z_{\text{req}}, [\text{m}^3]$
1	North Sea	0.19	0.2	0.21	0.22
2	Gulf of Mexico	0.28	0.3	0.31	0.32
3	N-Brazil	0.17	0.17	0.18	0.18
4	S-Brazil	0.14	0.14	0.15	0.16
5	Nigeria	0.25	0.26	0.26	0.26
6	Angola	0.15	0.15	0.16	0.17
7	Red Sea	0.31	0.34	0.36	0.37
8	Persian Gulf	0.31	0.34	0.36	0.38
9	N-Arabian Sea	0.31	0.35	0.37	0.39
10	Bengal Sea	0.16	0.17	0.18	0.18
11	N-Chinese Sea	0.24	0.26	0.27	0.28
12	S-Chinese Sea	0.29	0.31	0.33	0.34
13	W-Pacific Sea	0.18	0.19	0.2	0.2
14	W- Mediterranean Sea	0.29	0.32	0.34	0.35
15	E- Mediterranean Sea	0.22	0.24	0.25	0.27
16	DNV-3	0.19	0.2	0.2	0.2

The results of minimum required section modulus for frame 11 show the same trend of dependency on the above mentioned parameters as for frame 5.

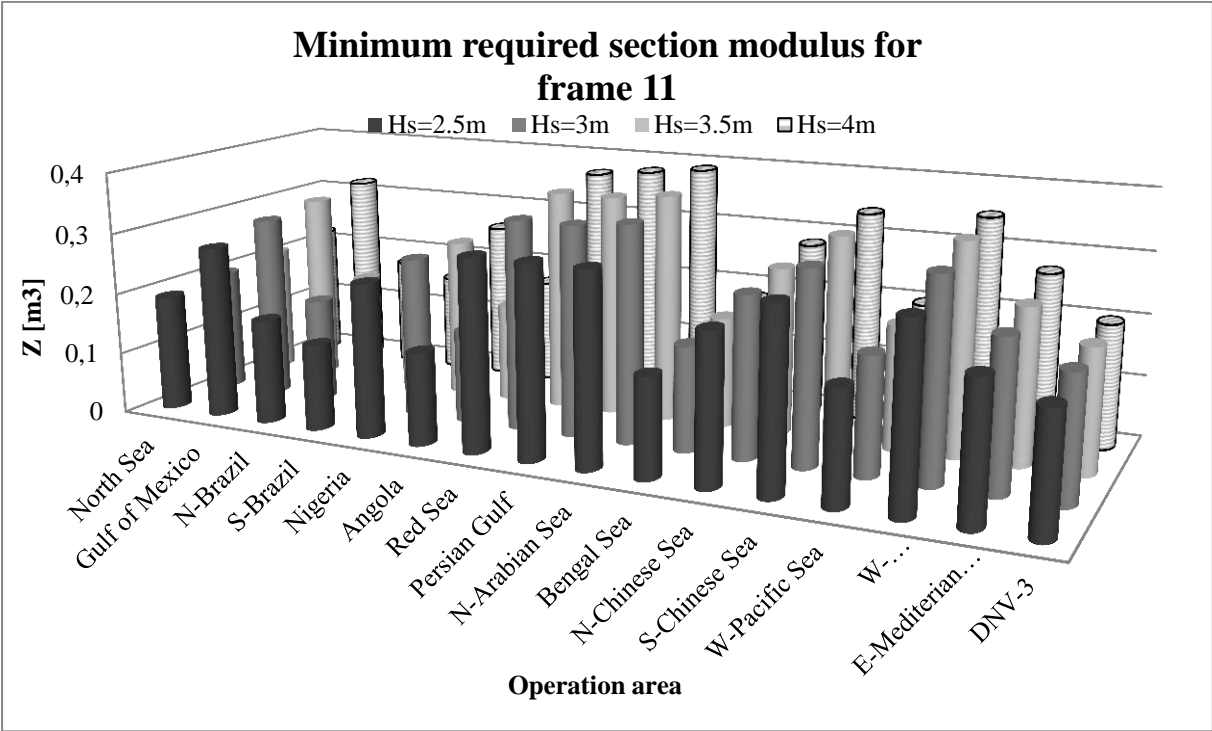


Figure 4.1.2– Minimum required section modulus for frame 11

The required section modulus still grows with increasing wave height, and severity of the sea areas is absolutely the same as for frame 5. The Northern part of the Arabian Sea still shows the highest result ($Z=0.39\text{m}^3$ for 4m wave height) while the Southern part of the Brazil Sea confirms the lowest value ($Z=0.16\text{m}^3$ for 4m wave height). In order to give an idea of severity of other operational areas, the following list may be useful (the severity level is given in the descending order).

- | | |
|--------------------------|--------------------------|
| 1. N-Arabian Sea; | 9. E- Mediterranean Sea; |
| 2. Persian Gulf; | 10. North Sea; |
| 3. Red Sea; | 11. DNV-3; |
| 4. W- Mediterranean Sea; | 12. W-Pacific Sea; |
| 5. S-Chinese Sea; | 13. N-Brazil; |
| 6. Gulf of Mexico; | 14. Bengal Sea; |
| 7. N-Chinese Sea; | 15. Angola; |
| 8. Nigeria; | 16. S-Brazil Sea. |

More detailed review of different severity of seas will be explained in section 5.

Table 4.1.3 shows results for frame 15 and the trend of dependency parameters is also preserved for this frame.

Table 4.1.3– Minimum required section modulus for frame 15

No.	Operational area	$H_s=2.5m$ $Z_{req}, [m^3]$	$H_s=3m$ $Z_{req}, [m^3]$	$H_s=3.5m$ $Z_{req}, [m^3]$	$H_s=4m$ $Z_{req}, [m^3]$
1	North Sea	0.16	0.17	0.18	0.19
2	Gulf of Mexico	0.24	0.26	0.27	0.27
3	N-Brazil	0.15	0.15	0.16	0.17
4	S-Brazil	0.13	0.13	0.15	0.15
5	Nigeria	0.21	0.22	0.22	0.22
6	Angola	0.13	0.14	0.15	0.16
7	Red Sea	0.27	0.29	0.31	0.32
8	Persian Gulf	0.26	0.29	0.31	0.32
9	N-Arabian Sea	0.27	0.29	0.32	0.33
10	Bengal Sea	0.14	0.15	0.16	0.16
11	N-Chinese Sea	0.21	0.22	0.23	0.24
12	S-Chinese Sea	0.24	0.27	0.28	0.29
13	W-Pacific Sea	0.16	0.17	0.17	0.18
14	W- Mediterranean Sea	0.25	0.27	0.29	0.3
15	E- Mediterranean Sea	0.19	0.2	0.22	0.23
16	DNV-3	0.16	0.17	0.17	0.18

Current tests show that results for frame 11 are the highest as compared with other frames. For example, the minimum required section modulus for 4m wave height in the North Sea is $0.22m^3$ while for frame 5 and 15 the value is $0.21m^3$ and $0.19m^3$ respectively. The explanation of this finding can be found in the Discussion section. So, based on the first test, it may be concluded that largest hull girder bending moment makes the frame weakest for fatigue for these types of vessels. That is why all subsequent tests on sensitivity analysis were carried out for only frame 11. Moreover, the results show that peak values were achieved for N-Arabian Sea, thus, Z for this operational area was considered in resulting tests together with DNV-3 as the standard operational area.

The ensuing test shows how time affects the minimum required section modulus. Two operational areas and two time periods, 20 years (original period) and 25 years (new assumed period) long, were analyzed and compared. The results are represented in the table below and plotted in Figure 4.1.3.

Table 4.1.4– Numerical results of minimum required section modulus for frame 11 with original operational profile but different year period

Operational area	20 years				25 years			
	$Z_{req}, [m^3]$ $H_s=2.5m$	$Z_{req}, [m^3]$ $H_s=3m$	$Z_{req}, [m^3]$ $H_s=3.5m$	$Z_{req}, [m^3]$ $H_s=4m$	$Z_{req}, [m^3]$ $H_s=2.5m$	$Z_{req}, [m^3]$ $H_s=3m$	$Z_{req}, [m^3]$ $H_s=3.5m$	$Z_{req}, [m^3]$ $H_s=4m$
N-Arabian Sea	0.31	0.35	0.37	0.39	0.33	0.37	0.4	0.42
DNV-3	0.19	0.2	0.2	0.2	0.2	0.21	0.21	0.21

As it is already evident from Figure 4.1.3, operation time only slightly influences fatigue: the increased time period within 5 years led to the increased required section modulus only within 0.1-0.2m3 for all wave heights.

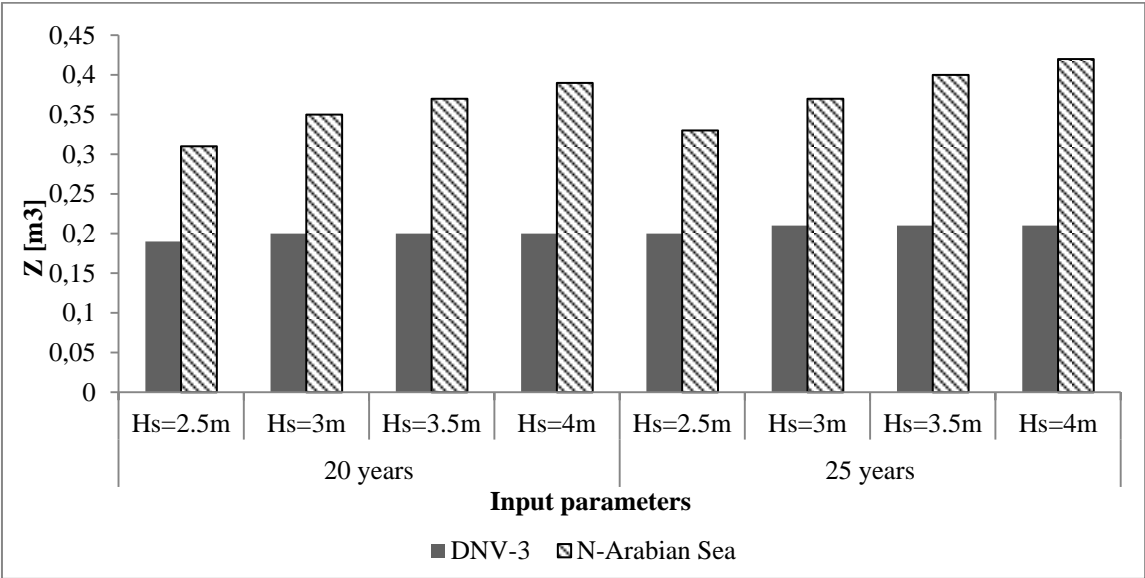


Figure 4.1.3– Minimum required section modulus for frame 11 with original operational profile but different year period

Then, one more test was conducted to consider a change in the time for service conditions which implies changes in the amount of time in percentage for each speed, as seen in the table below.

Table 4.1.5– Modified input parameters for a new test

Original operational profile	Modified operational profile
100% MCR, 5% of time	100% MCR, 10% of time
25% MCR, 75% of time	25% MCR, 80% of time
Idle engine speed, 20% of time	Idle engine speed, 10% of time

Next, the intended service period was expanded till 25 years. So, current test gives an picture of how a combination of new input parameters impacts the required section modulus and fatigue lifetime, correspondently. In addition, Table 4.1.6 reflects which input parameter is more important at this stage.

Table 4.1.6– Results of Z for N-Arabian Sea and DNV-3

N-Arabian Sea								
Intended service period, [years]	H _s = 2.5m		H _s = 3m		H _s = 3.5m		H _s = 4m	
	Original service conditions	Modified service conditions	Original service conditions	Modified service conditions	Original service conditions	Modified service conditions	Original service conditions	Modified service conditions
20	0.31	0.36	0.35	0.39	0.37	0.42	0.39	0.44
25	0.33	0.38	0.37	0.42	0.4	0.45	0.42	0.47
DNV-3								
Intended service period, [years]	H _s = 2.5m		H _s = 3m		H _s = 3.5m		H _s = 4m	
	Original service conditions	Modified service conditions	Original service conditions	Modified service conditions	Original service conditions	Modified service conditions	Original service conditions	Modified service conditions
20	0.19	0.21	0.2	0.22	0.2	0.22	0.2	0.22
25	0.2	0.22	0.21	0.24	0.21	0.24	0.21	0.24

As it is clear from the table, the significant increase of minimum required section modulus was due to the change of the amount of time spent in each service condition rather than the increased required fatigue lifetime till 25 years.

Results for the N-Arabian Sea and 2.5m limiting wave height are visualized, see Figure 4.1.4. It can be assumed that increased intended service period slightly impacts the minimum required section modulus (increased by only 0.02m³) but minor changes in the amount of time spent at speeds led to significant increase by 0.05m³. It was expected that combination of

modified input parameters would give peak values (increased by 0.07m^3). However, current test does not show which service condition out of three has the highest impact.

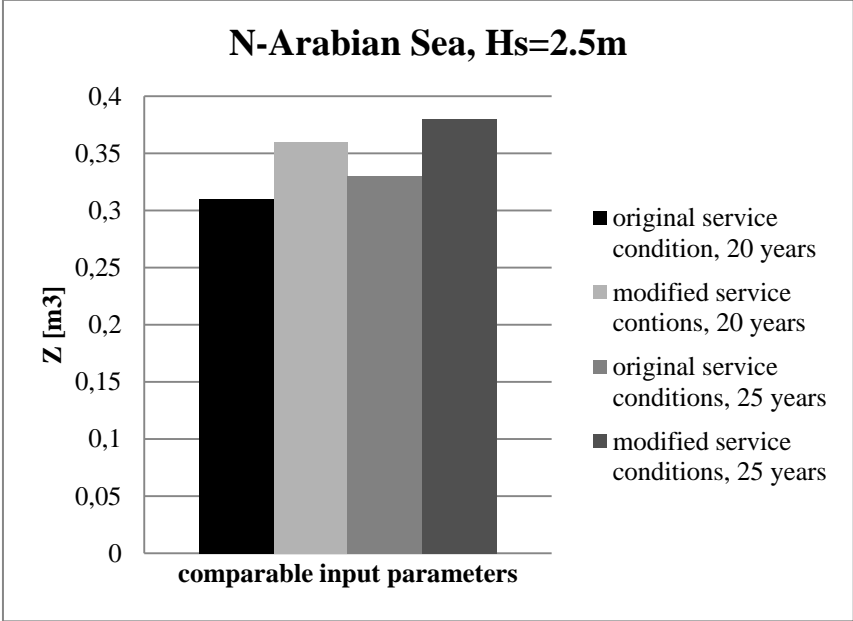


Figure 4.1.4– Comparison of results with different service conditions and intended service periods for frame 11 in the N-Arabian Sea for 2.5m significant wave height

A series of tests were carried out in order to understand the sensitivity of service conditions on fatigue lifetime. Firstly, it is assumed that the second service condition does not change (25% MCR) and attention was paid to the range of time, namely, from 3% to 20% spent at the first service condition (100% MCR). The table below represents the results.

Table 4.1.7– Results of variable first and third service conditions, constant second service conditions for the N-Arabian Sea and DNV-3

Service condition for 3 speeds, [% of time]	N-Arabian Sea				DNV-3			
	$Z_{req}, [m^3]$	$Z_{req}, [m^3]$	$Z_{req}, [m^3]$	$Z_{req}, [m^3]$	$Z_{req}, [m^3]$	$Z_{req}, [m^3]$	$Z_{req}, [m^3]$	$Z_{req}, [m^3]$
	$H_s=2.5m$	$H_s=3m$	$H_s=3.5m$	$H_s=4m$	$H_s=2.5m$	$H_s=3m$	$H_s=3.5m$	$H_s=4m$
3% 75% 22%	0.29	0.32	0.35	0.37	0.18	0.19	0.19	0.19
Original	0.31	0.35	0.37	0.39	0.19	0.2	0.2	0.2
10% 75% 15%	0.35	0.39	0.42	0.44	0.21	0.22	0.22	0.22
15% 75% 10%	0.39	0.43	0.46	0.48	0.22	0.24	0.24	0.24
20% 75% 5%	0.42	0.46	0.49	0.52	0.24	0.25	0.25	0.25

Available results indicate a dramatic growth of required section modulus with increasing time spent at the top speed. Values of Z in the N-Arabian Sea are more significant than for DNV-3; peak values at the last type of service conditions can be a good example, $0.42-0.52\text{m}^3$ in the N-Arabian Sea while $0.01-0.02\text{m}^3$ in DNV-3. This can be explained by different severity of operational area due to fatigue as the N-Arabian Sea is more severe than

DNV-3 in fatigue for such type of vessels, as seen in the Discussion section 5. The visualization of received results is represented in Figure 4.1.5 and Figure 4.1.6.

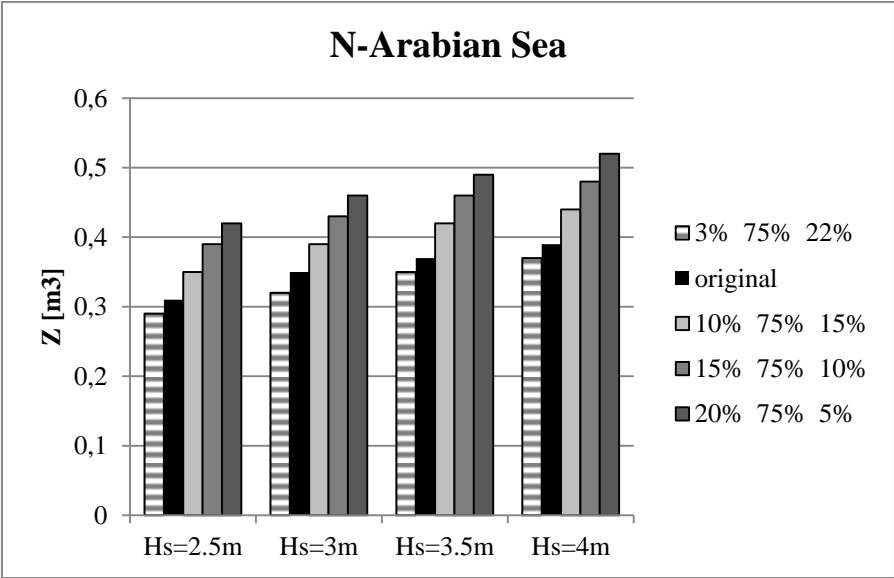


Figure 4.1.5– Results of variable first and third service conditions, constant second service conditions for the N-Arabian Sea

Figure 4.1.5 shows that 5% increase in time results in the growth of minimum required section modulus per 0.04m^3 for all four types of waves. A similar trend was found at DNV-3 operational area, as seen in Figure 4.1.6, but the growth of Z is slower and achieved values of Z are absolutely the same for a wave from 3 to 4 meters high. Small geometry, light weight of a vessel, light engine and low engine power lead to low speed, lower load and finally, slower growth of Z in current operational area.

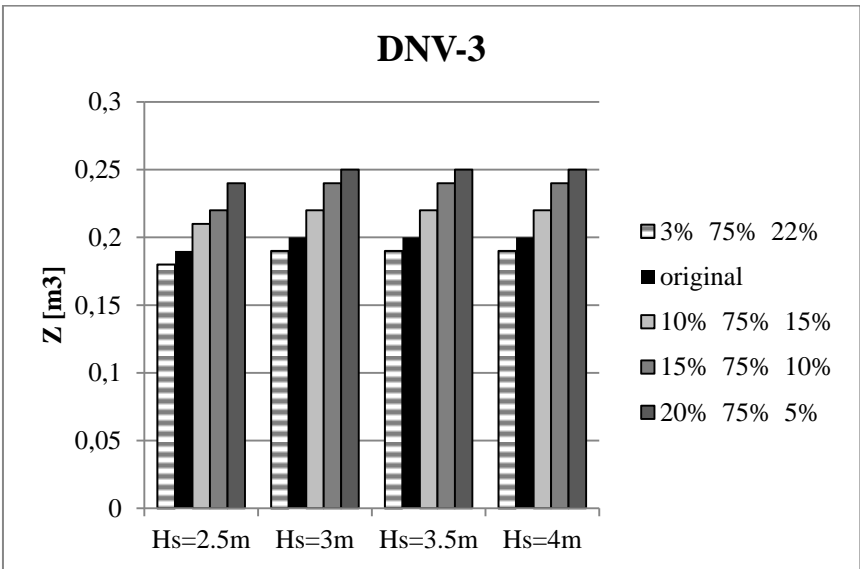


Figure 4.1.6– Results of variable first and third service conditions, constant second service conditions for DNV-3

A similar approach was applied to the vessel in the next test but now the first service condition is constant (100% MCR) and attention was paid to the range of time, namely, from 70% to 80% for the second service condition (25% MCR). Table 4.1.8 represents the results.

Table 4.1.8– Results of variable second service condition, constant first and third service conditions for the N-Arabian Sea and DNV-3

Service condition for 3 speeds, [% of time]	N-Arabian Sea				DNV-3			
	Z_{req} , [m ³]	Z_{req} , [m ³]	Z_{req} , [m ³]	Z_{req} , [m ³]	Z_{req} , [m ³]	Z_{req} , [m ³]	Z_{req} , [m ³]	Z_{req} , [m ³]
	$H_s=2.5m$	$H_s=3m$	$H_s=3.5m$	$H_s=4m$	$H_s=2.5m$	$H_s=3m$	$H_s=3.5m$	$H_s=4m$
5% 70% 25%	0.31	0.34	0.37	0.39	0.18	0.2	0.2	0.2
original	0.31	0.35	0.37	0.39	0.19	0.2	0.2	0.2
5% 80% 15%	0.31	0.35	0.37	0.4	0.19	0.2	0.2	0.2

In general, the influence of time spent at 25% MCR on the minimum required section modulus was small; this was expected due to slower speed of 20 knots, as compared with the top speed of 30 knots. Table 4.1.8 shows that 5% increase in time led to the growth of minimum required section modulus by 0.01m³ only for the original service condition that assumes 3m wave height in the N-Arabian Sea (0.35m³), original service condition for 2.5m wave height in DNV-3 (0.19m³) and the third type of service condition for 4m wave height in the N-Arabian Sea (0.4m³); the rest of the cases remained unchanged. Thus, it may be concluded that time spent at 25% MCR only slightly impacts the required section modulus and actual fatigue lifetime, correspondingly. This can be explained by low speed, 20 knots, which does not induce repetitive high loads on the vessel and cracks, correspondingly. In this project variable time at idle engine speed is out of consideration.

In order to indicate which input parameter, time at 30kn or time at 20kn influence on Z at most, one more test was carried out, see results in Table 4.1.9. Three cases are considered in this test, which are: 1. Original for comparison; 2. Service condition – 20% 75% 5%, intended service period is 20 years; 3. Service condition – 15% 80% 5%, intended service period is 20 years.

Table 4.1.9– Results of minimum required section modulus for the N-Arabian Sea and DNV-3

Service condition	N-Arabian Sea				DNV-3			
	Z_{req} , [m ³]	Z_{req} , [m ³]	Z_{req} , [m ³]	Z_{req} , [m ³]	Z_{req} , [m ³]	Z_{req} , [m ³]	Z_{req} , [m ³]	Z_{req} , [m ³]
	$H_s=2.5m$	$H_s=3m$	$H_s=3.5m$	$H_s=4m$	$H_s=2.5m$	$H_s=3m$	$H_s=3.5m$	$H_s=4m$
1	0.31	0.35	0.37	0.39	0.19	0.2	0.2	0.2
2	0.42	0.46	0.49	0.52	0.24	0.25	0.25	0.25
3	0.39	0.43	0.46	0.49	0.22	0.24	0.24	0.24

Figure 4.1.7 shows the results of Z for specified conditions and it is easy to see the significant difference between the original operational profiles and modified, namely increased by 0.1m^3 on the average. Second case shows the largest value (0.52m^3 for 4m limiting wave height), which is 0.25m^3 difference with the original. The increased operating time at 30 knots with the factor of 4 led to increased Z by 25%. Thus, it may be concluded that time spent at top speed impacts actual fatigue lifetime at most.

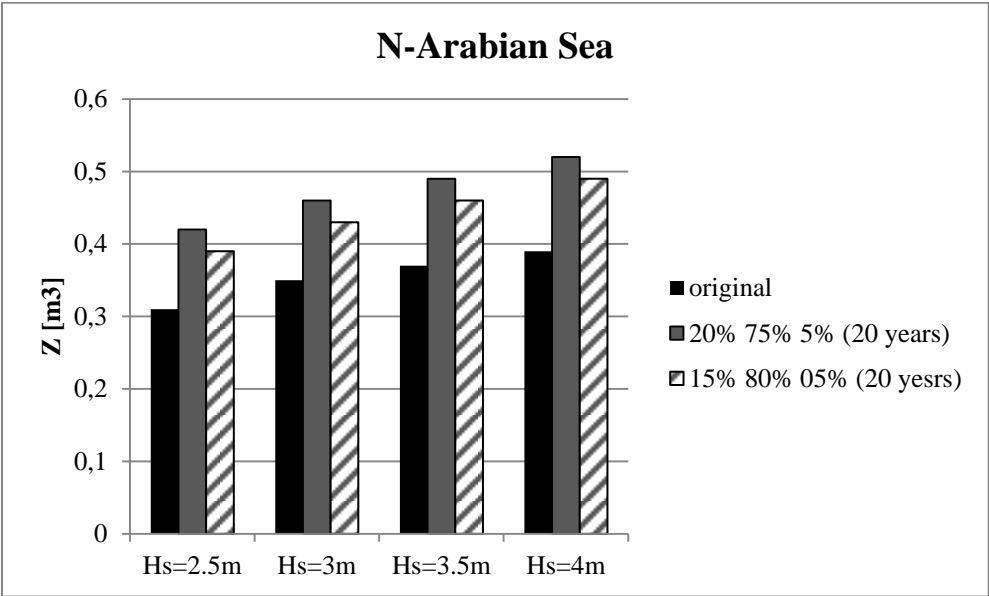


Figure 4.1.7– Results of minimum required section modulus for the N-Arabian Sea

Next comparison was made to understand how speeds influence the fatigue lifetime. Thus, after engine (CAT 32 TTA D-rating) was selected and based on a power prediction chart for that vessel, new speeds (27.5kn, 14kn, 12kn) were identified. Required data used in this case is given in subsection 3.4 and the results are shown in the table below.

Table 4.1.10– Results of Z for the N-Arabian Sea and DNV-3

Speeds	N-Arabian Sea				DNV-3			
	$Z_{req}, [m^3]$	$Z_{req}, [m^3]$	$Z_{req}, [m^3]$	$Z_{req}, [m^3]$	$Z_{req}, [m^3]$	$Z_{req}, [m^3]$	$Z_{req}, [m^3]$	$Z_{req}, [m^3]$
	$H_s=2.5m$	$H_s=3m$	$H_s=3.5m$	$H_s=4m$	$H_s=2.5m$	$H_s=3m$	$H_s=3.5m$	$H_s=4m$
original	0.31	0.35	0.37	0.39	0.19	0.2	0.2	0.2
new	0.21	0.23	0.25	0.26	0.12	0.13	0.13	0.13

In Figure 4.1.8 grey columns represent a required section modulus for each limiting wave height if a vessel operates at new speeds. This comparison of required section modulus shows that difference in speeds led to the difference in archived Z of 0.12m^3 on the average, which means approximately 34%.

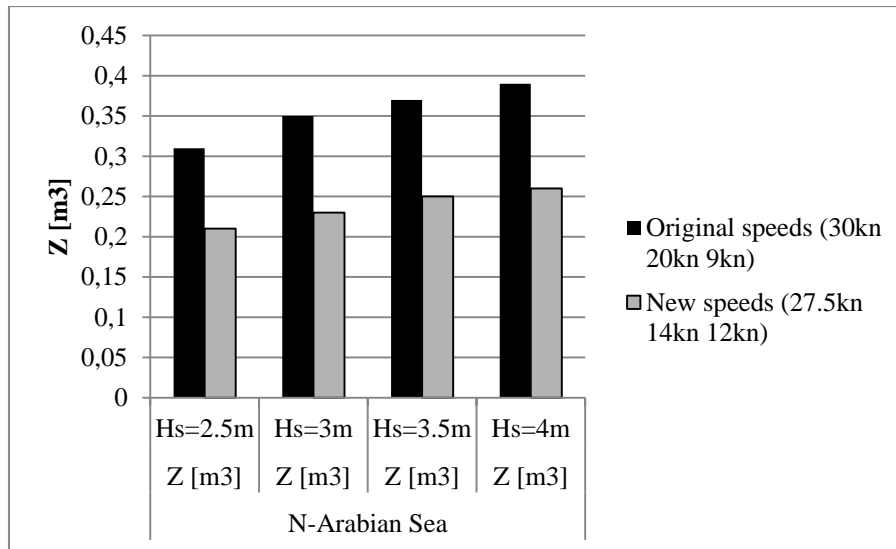


Figure 4.1.8– Results of minimum required section modulus at the N-Arabian Sea

The difference of archived Z at DNV-3 has approximately the same trend as for the N-Arabian Sea, 0.07m^3 (35%), as seen in Figure 4.1.9.

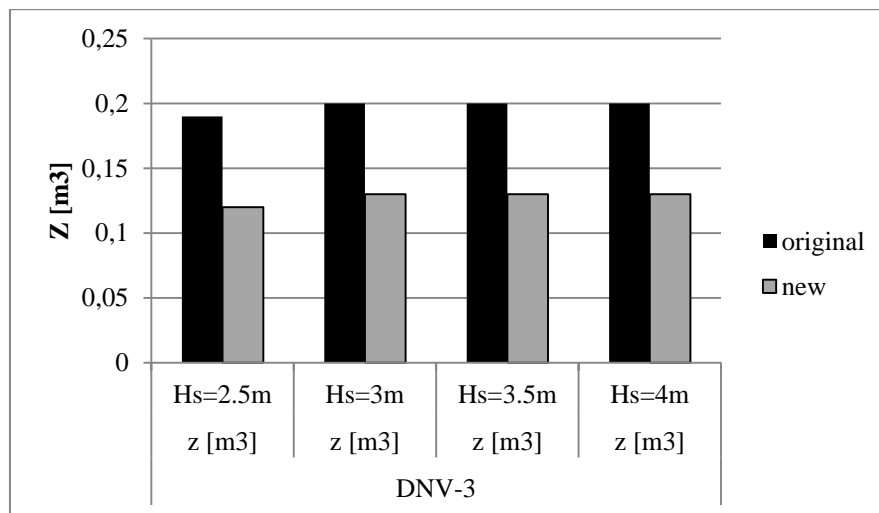


Figure 4.1.9– Results of minimum required section modulus at DNV-3

A number of experiments were carried out with different modified input parameters in the sensitivity study and intermediate discussions with conclusions were estimated. However, in order to finally evaluate which input parameter is the most significant, the following table has been compiled to represent the results of minimum required section modulus with original and modified input parameters in the N-Arabian Sea (as the most sensitive area). The test was carried out based on the standard operational profile ($H_s=3.5\text{m}$; 40000hours) whereas each input parameter was increased independently from others by a constant value, namely 25%. In addition to the parameters which were investigated in the sensitivity study, two more parameters were added, namely, the length of the vessel and its displacement.

Table 4.1.11– Results of Z for final evaluation

No.	Input parameter	Original value	New value	Z, [m ³]	Increased Z in %
1	Original	----	----	0,37	----
2	Intended service condition	20 [years]	25 [years]	0,4	8%
3	Time at top speed	5 [% of time]	6,25 [% of time]	0,39	5%
4	Time at average speed	75 [% of time]	93,75 [% of time]	0,38	3%
5	Top speed	30 [kn]	37,5 [kn]	0,43	14%
6	Average speed	20 [kn]	25 [kn]	0,43	14%
7	Vessel length	30 [m]	37,5 [m]	0,42	12%
8	Displacement	94 [t]	117,5 [t]	0,42	12%

This vivid example definitely shows that speed influences fatigue lifetime mostly. Next significant parameters (in the descending order) are the vessel length and displacement, but these two parameters were increased manually and such rough modification cannot provide accurate results. Less important parameters are intended service period and time spent at top speed. However, increased intended service period till 25 years is a rational upper limit for such vessels, but time spent at top speed can be increased by 4 times or even more and thus, this parameter and speed will influence the fatigue time most of all. Finally, time spent at an average speed and intended service period provide the least influence.

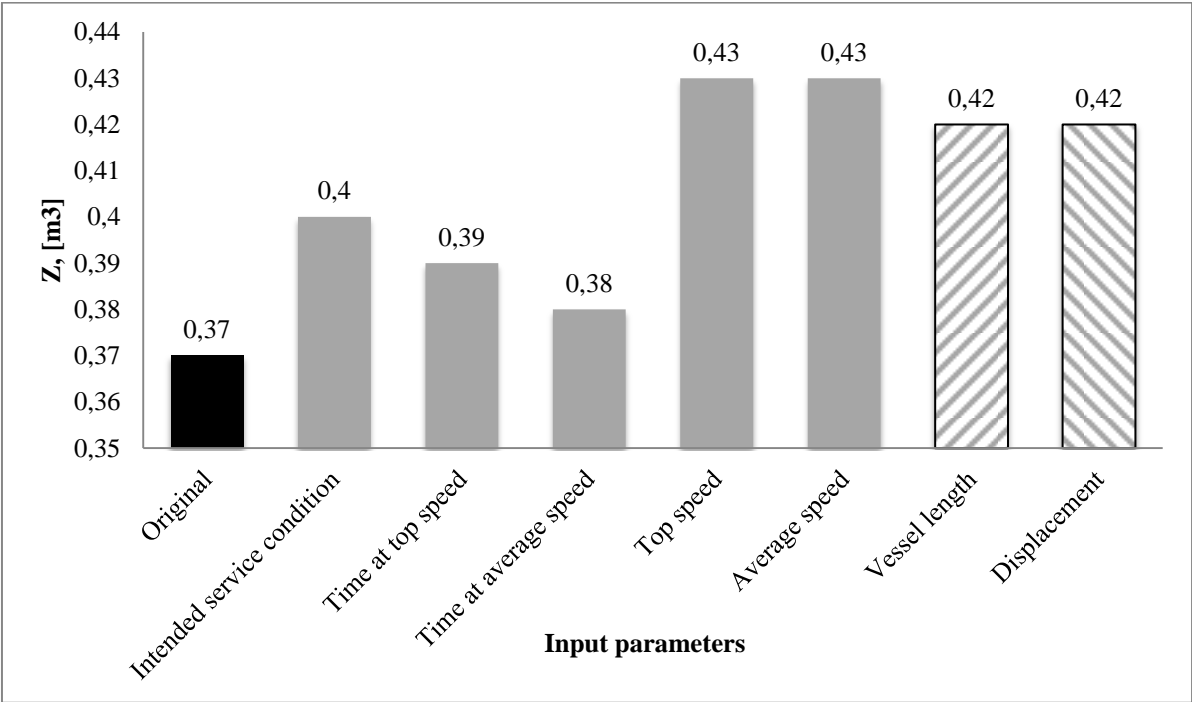


Figure 4.1.10– Results of Z for final comparison

The sensitivity analysis showed that the most prone vessel details to fatigue failure are the parts located at frames with the calculated largest hull girder bending moment. Thus,

fatigue design curves are made for the details located at these parts of the vessel. Moreover, current analysis showed that most influenced input parameters on fatigue lifetime of the vessel’s details are: an intended service period, speeds, time spent on top speeds and the operating area. In Damen standard service conditions are assumed as a requirement for product design and recommendations for captains. So, actual service conditions are unknown and are not provided to the company. Thus, for fatigue design curves this input parameter is assumed as constant and out of consideration.

4.2 Fatigue design curves

As was discussed above, the fatigue design curves are made for the range of Fast Crew Suppliers (6 vessels) and Stan Patrols (5 vessels). All curves show minimum required section modulus for selected length of vessel and required operational profile and actual Z for already built vessel.

Firstly, the design curves for FCS are represented. Tests for achieving Z at these curves were carried out based on the standard operational profile, as seen Table 3.6.3. However, the sailing period was extended for possible future modification of standard operational profile or unique customer order. Total intended service period covers required lifetime from 15 to 25 years and operating hours per year from 3000 to 5000 h/y. During small tests it was found that only total operating time in seconds influences required section modulus. It means that results of Z are the same for 15 years required lifetime, 5000 operating hours per years (75000 hours in total) and 25 years, 3000 h/y (also 75000 hours in total), for example. Thus, for easy understanding of service periods in curves, the total operation time is represented in hours. The table below shows decoding of selected total sailing hours in fatigue design curves.

Table 4.2.1– Sailing periods used in fatigue design curves

Required lifetime	15 years		20 years		25 years	
Operating hours per year, [h/y]	3000	5000	3000	5000	3000	5000
Total operation hours, [h]	45 000	75 000	60 000	100 000	75 000	125 000

In addition, required section moduli were achieved for several wave heights. Current analysis includes Z for 1m limiting wave height in order to understand the lower limit of Z from this point of view. Moreover, design curves were made for 2 areas, namely, DNV-3 and the Gulf of Mexico. The explanation of such choice is described in subsection 3.5. Results for DNV-3 are represented in the table below.

Table 4.2.2– Results of minimum required section modulus for FCS at DNV-3 for fatigue design curves

<i>Fast Crew Supplier</i>	<i>1905</i>	<i>2610</i>	<i>3307</i>	<i>4008</i>	<i>4207</i>	<i>5209</i>	Total sailing hours
<i>Length, [m]</i>	<i>19</i>	<i>26</i>	<i>33</i>	<i>40</i>	<i>42</i>	<i>52</i>	
<i>Analyzed frame</i>	<i>6</i>	<i>10</i>	<i>14</i>	<i>16</i>	<i>20</i>	<i>20</i>	
$H_s=1m$ $Z_{req}, [m^3]$	0.04	0.05	0.11	0.17	0.19	0.33	45 000
$H_s =2.5m$ $Z_{req}, [m^3]$	0.07	0.08	0.21	0.35	0.4	0.82	
$H_s =3m$ $Z_{req}, [m^3]$	0.07	0.09	0.23	0.38	0.42	0.9	
$H_s =3.5m$ $Z_{req}, [m^3]$	0.08	0.09	0.24	0.4	0.44	0.92	
$H_s =4m$ $Z_{req}, [m^3]$	0.08	0.1	0.26	0.41	0.45	0.94	
$H_s=1m$ $Z_{req}, [m^3]$	0.04	0.05	0.12	0.18	0.21	0.35	60 000
$H_s =2.5m$ $Z_{req}, [m^3]$	0.08	0.09	0.26	0.41	0.43	0.89	
$H_s =3m$ $Z_{req}, [m^3]$	0.08	0.1	0.28	0.44	0.47	0.97	
$H_s =3.5m$ $Z_{req}, [m^3]$	0.08	0.1	0.3	0.46	0.48	0.99	
$H_s =4m$ $Z_{req}, [m^3]$	0.08	0.1	0.31	0.48	0.49	1.01	
$H_s=1m$ $Z_{req}, [m^3]$	0.04	0.05	0.12	0.19	0.22	0.37	75 000
$H_s =2.5m$ $Z_{req}, [m^3]$	0.08	0.1	0.25	0.41	0.46	0.95	
$H_s =3m$ $Z_{req}, [m^3]$	0.09	0.1	0.27	0.44	0.5	1.03	
$H_s =3.5m$ $Z_{req}, [m^3]$	0.09	0.11	0.27	0.47	0.52	1.06	
$H_s =4m$ $Z_{req}, [m^3]$	0.09	0.11	0.3	0.49	0.54	1.08	
$H_s=1m$ $Z_{req}, [m^3]$	0.05	0.06	0.13	0.2	0.23	0.39	100 000
$H_s =2.5m$ $Z_{req}, [m^3]$	0.09	0.1	0.3	0.47	0.5	1.01	
$H_s =3m$ $Z_{req}, [m^3]$	0.09	0.11	0.32	0.51	0.54	1.11	
$H_s =3.5m$ $Z_{req}, [m^3]$	0.1	0.12	0.33	0.53	0.55	1.14	
$H_s =4m$ $Z_{req}, [m^3]$	0.1	0.12	0.34	0.55	0.56	1.16	
$H_s=1m$ $Z_{req}, [m^3]$	0.05	0.06	0.14	0.21	0.24	0.4	125 000
$H_s =2.5m$ $Z_{req}, [m^3]$	0.09	0.11	0.31	0.5	0.56	1.07	
$H_s =3m$ $Z_{req}, [m^3]$	0.1	0.12	0.33	0.54	0.58	1.18	
$H_s =3.5m$ $Z_{req}, [m^3]$	0.1	0.12	0.36	0.56	0.61	1.21	
$H_s =4m$ $Z_{req}, [m^3]$	0.1	0.13	0.37	0.58	0.63	1.23	

The results show a dramatic increase of minimum required section modulus with the growth of vessel length. In addition, a combination of increased time, limiting wave height and length of a vessel has a significant influence on Z. Based on the achieved results, the following diagram was plotted. In Figure 4.2.1 received lines are almost smooth, grey lines represent minimum required section modulus for limiting wave height 1m. Mentioned lines are represented 3 times, each with different total operation hours. On the graph in Figure 4.2.1 the first lowest line represents results with minimum sailing period 45000 hours (solid lines), second line with 75000 hours (dashed lines) and third with 125000 hours (dashed with dots line). So, the whole operation period is plotted and is easy to read. The interim periods are not plotted and can be used in future work. Then, black lines represent the minimum required

section modulus for limiting wave height specified in the standard requirement (in this case 2.5m) and are also represented 3 times. Design curves with all limiting wave heights are represented in Appendix E. As it was mentioned above, point (cycle) on the curve is actual section modulus of already built vessel, namely FCS 3307.

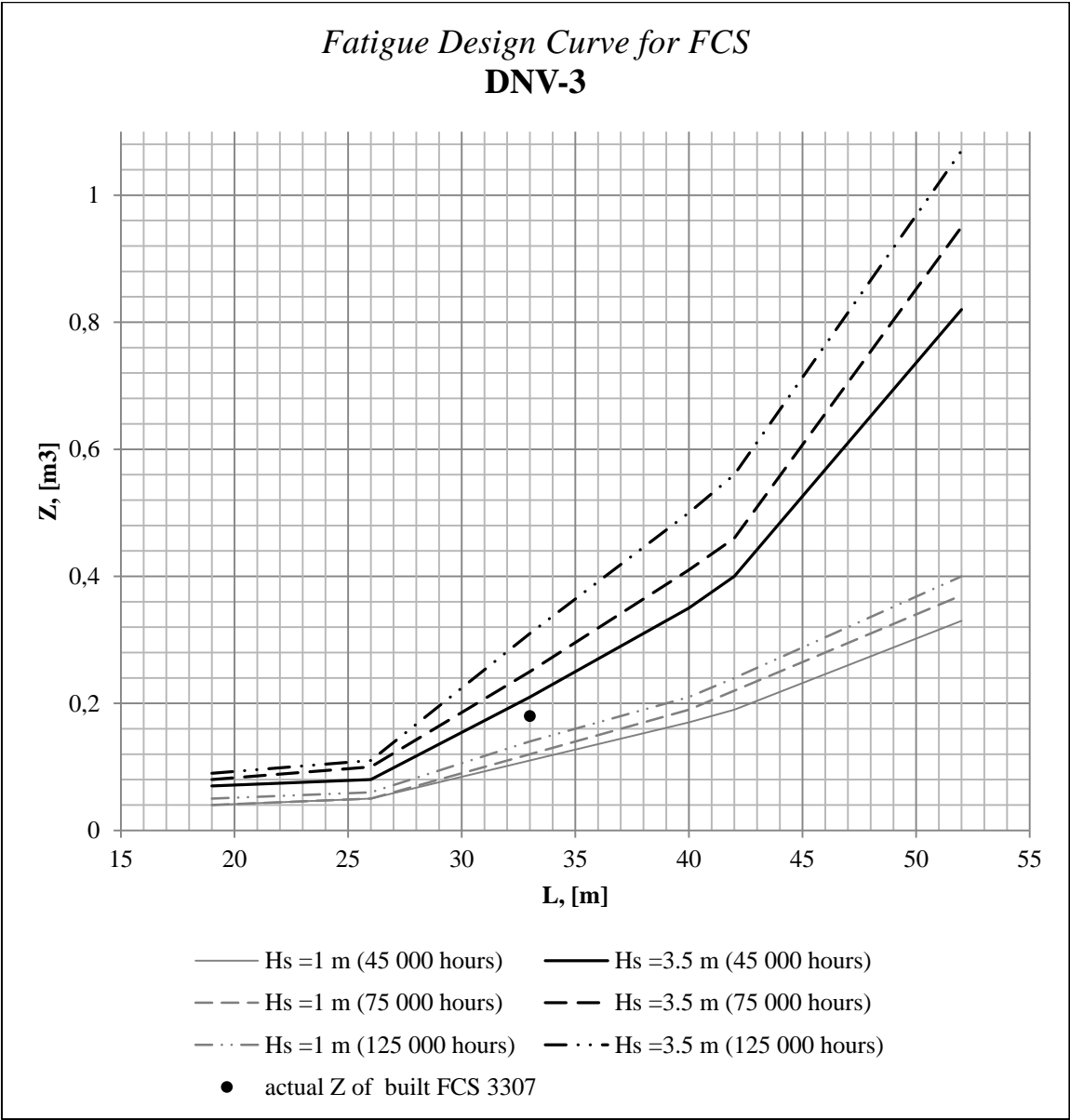


Figure 4.2.1– Fatigue design curve for FCS at DNV-3 with variable operational profile and constant service conditions

In Figure 4.2.1 it is easy to notice the large difference between the actual and minimum required section modulus for built vessel. This observation will be discussed in the next section. Similar approach was chosen for the Gulf of Mexico and the results are represented in the table below.

Table 4.2.3– Results of minimum required section modulus for FCS at Gulf of Mexico for fatigue design curves

<i>Fast Crew Supplier</i>	<i>1905</i>	<i>2610</i>	<i>3307</i>	<i>4008</i>	<i>4207</i>	<i>5209</i>	Total sailing hours
<i>Length, [m]</i>	<i>19</i>	<i>26</i>	<i>33</i>	<i>40</i>	<i>42</i>	<i>52</i>	
<i>Analyzed frame</i>	<i>6</i>	<i>10</i>	<i>14</i>	<i>16</i>	<i>20</i>	<i>20</i>	
$H_s=1m$ $Z_{req}, [m^3]$	0.04	0.05	0.14	0.21	0.24	0.37	45 000
$H_s =2.5m$ $Z_{req}, [m^3]$	0.1	0.11	0.34	0.56	0.63	1.13	
$H_s =3m$ $Z_{req}, [m^3]$	0.1	0.12	0.37	0.59	0.67	1.23	
$H_s =3.5m$ $Z_{req}, [m^3]$	0.11	0.13	0.39	0.62	0.69	1.3	
$H_s =4m$ $Z_{req}, [m^3]$	0.11	0.13	0.41	0.64	0.71	1.36	
$H_s=1m$ $Z_{req}, [m^3]$	0.04	0.06	0.14	0.22	0.25	0.39	60 000
$H_s =2.5m$ $Z_{req}, [m^3]$	0.1	0.12	0.34	0.59	0.67	1.2	
$H_s =3m$ $Z_{req}, [m^3]$	0.11	0.13	0.38	0.63	0.71	1.32	
$H_s =3.5m$ $Z_{req}, [m^3]$	0.11	0.14	0.4	0.66	0.74	1.4	
$H_s =4m$ $Z_{req}, [m^3]$	0.12	0.14	0.42	0.69	0.77	1.46	
$H_s=1m$ $Z_{req}, [m^3]$	0.05	0.06	0.15	0.23	0.26	0.41	75 000
$H_s =2.5m$ $Z_{req}, [m^3]$	0.11	0.13	0.39	0.63	0.71	1.28	
$H_s =3m$ $Z_{req}, [m^3]$	0.12	0.14	0.41	0.67	0.76	1.41	
$H_s =3.5m$ $Z_{req}, [m^3]$	0.12	0.14	0.43	0.7	0.79	1.5	
$H_s =4m$ $Z_{req}, [m^3]$	0.12	0.15	0.45	0.73	0.82	1.56	
$H_s=1m$ $Z_{req}, [m^3]$	0.05	0.06	0.16	0.24	0.27	0.43	100 000
$H_s =2.5m$ $Z_{req}, [m^3]$	0.12	0.14	0.42	0.67	0.76	1.37	
$H_s =3m$ $Z_{req}, [m^3]$	0.13	0.15	0.44	0.72	0.81	1.51	
$H_s =3.5m$ $Z_{req}, [m^3]$	0.13	0.16	0.47	0.75	0.85	1.59	
$H_s =4m$ $Z_{req}, [m^3]$	0.13	0.16	0.49	0.78	0.88	1.65	
$H_s=1m$ $Z_{req}, [m^3]$	0.05	0.06	0.17	0.25	0.29	0.45	125 000
$H_s =2.5m$ $Z_{req}, [m^3]$	0.12	0.15	0.43	0.7	0.8	1.45	
$H_s =3m$ $Z_{req}, [m^3]$	0.13	0.16	0.45	0.76	0.86	1.58	
$H_s =3.5m$ $Z_{req}, [m^3]$	0.14	0.16	0.48	0.79	0.9	1.66	
$H_s =4m$ $Z_{req}, [m^3]$	0.14	0.17	0.5	0.83	0.93	1.73	

The results show even more dramatic increase of Z with the growth of the vessel length, as compared with the results at DNV-3. The cause of this is stipulated by different dominating wave periods, wave lengths and operability of the vessel. Current results are plotted in Figure 4.2.2 where grey lines also represent Z for 1m limiting wave height and black lines represent the minimum required section modulus for 2.5m limiting wave height (requirement from the standard operational profile). All lines are represented 3 times with different total sailing hours (45 000h - solid lines, 75 000 - dashed lines and 125 000 h - dashed with dots lines). Visualization of Z for all wave heights from Table 4.2.3 is shown in Appendix E. As it was mentioned above, point (cycle) on the curve are actual section modulus for built vessel and there is still a big difference in Z between actual and required one, namely

0.16m³. This result is twice larger than for DNV-3. From Figure 4.2.1 and Figure 4.2.2 is seen that actual Z are located near 1m limiting wave height and thus, uncertainty with respect to the load and Z calculation are rather significant. The observation about uncertainty, their causes and possible improvements are discussed in section 5.

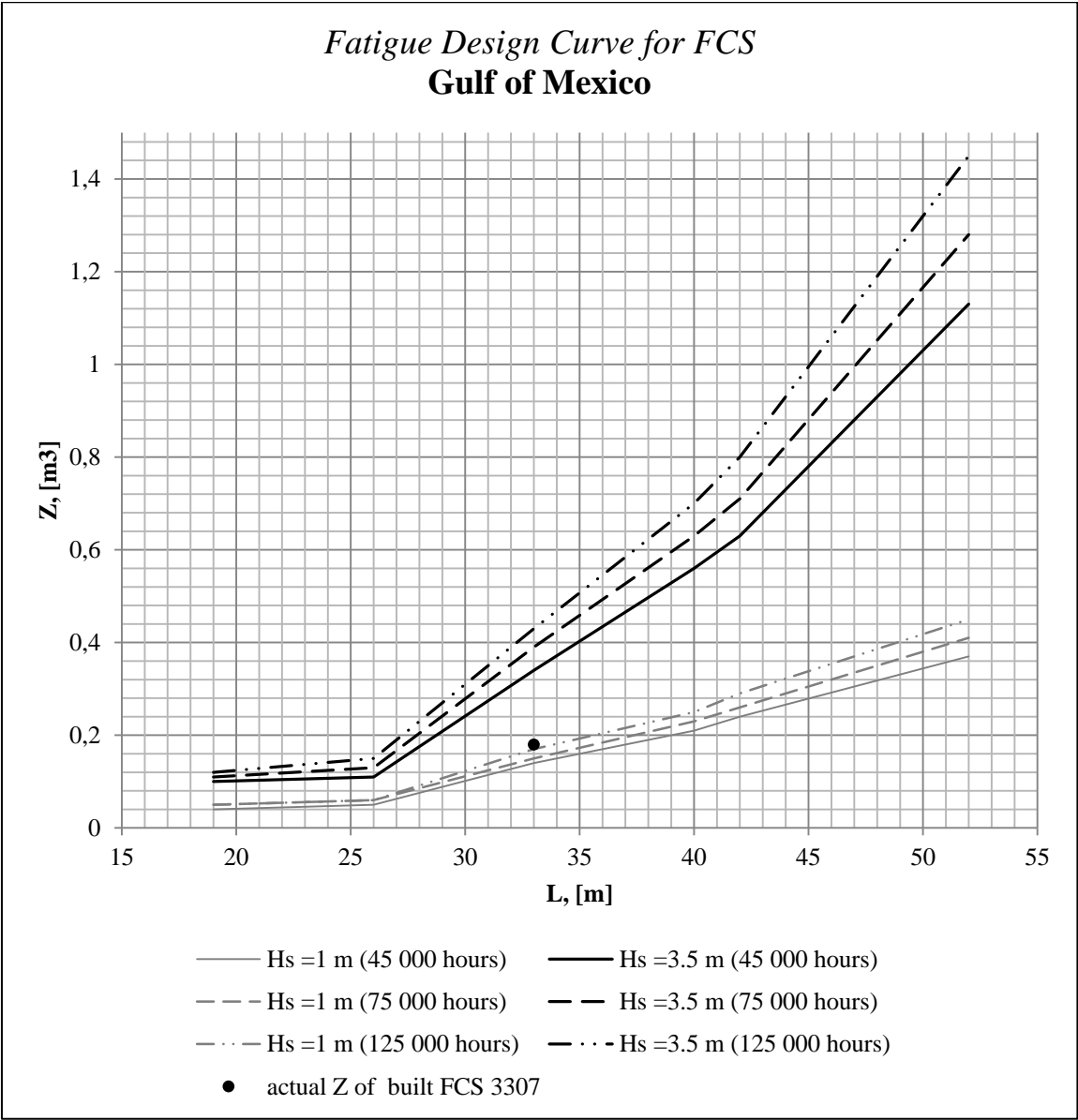


Figure 4.2.2– Fatigue design curve for FCS at Gulf of Mexico with variable operational profile and constant service conditions

Similar approaches were applied to Stan Patrol vessels while creating fatigue design curves. Tests for achieving Z at these curves were also carried out based on the standard operational profile, as seen in Table 3.6.3. Based on this standard, the required total operation time is 40000 hours which was also extended till 125000 hours but with different steepness,

as compared to FCS. The table below shows decoding of selected total sailing hours in fatigue design curves and in Table 4.2.5.

Table 4.2.4– Sailing periods used in fatigue design curves for Spa

Required lifetime, [years]	20 years		25 years		
Operating hours per years, [h/y]	2000	5000	2000	3000	5000
Total operation hours, [hours]	40 000	100 000	50 000	75 000	125 000

Other input parameters, such as limiting wave heights and alternate operational area, are the same as for FCS. The results of Z for SPA are represented as follows.

Table 4.2.5– Results of Z for SPa at DNV-3 for fatigue design curves

<i>Stan Patrol</i>		3007	3808	4207	4708	5009	Total sailing hours
<i>Length, [m]</i>		30	38	42	47	50	
<i>Analyzed frame</i>		11	16	18	20	24	
$H_s=1m$ $Z_{req}, [m^3]$		0,1	0,13	0,15	0,21	0,34	40 000
$H_s =2.5m$ $Z_{req}, [m^3]$		0,19	0,25	0,29	0,45	0,73	
$H_s =3m$ $Z_{req}, [m^3]$		0,2	0,27	0,31	0,49	0,8	
$H_s =3.5m$ $Z_{req}, [m^3]$		0,2	0,27	0,31	0,49	0,81	
$H_s =4m$ $Z_{req}, [m^3]$		0,2	0,27	0,31	0,5	0,82	
$H_s=1m$ $Z_{req}, [m^3]$		0,1	0,14	0,15	0,22	0,35	50 000
$H_s =2.5m$ $Z_{req}, [m^3]$		0,2	0,27	0,31	0,48	0,78	
$H_s =3m$ $Z_{req}, [m^3]$		0,21	0,29	0,33	0,52	0,85	
$H_s =3.5m$ $Z_{req}, [m^3]$		0,21	0,29	0,33	0,52	0,86	
$H_s =4m$ $Z_{req}, [m^3]$		0,21	0,29	0,34	0,53	0,87	
$H_s=1m$ $Z_{req}, [m^3]$		0,11	0,15	0,17	0,24	0,37	75 000
$H_s =2.5m$ $Z_{req}, [m^3]$		0,23	0,31	0,35	0,54	0,88	
$H_s =3m$ $Z_{req}, [m^3]$		0,24	0,33	0,37	0,59	0,96	
$H_s =3.5m$ $Z_{req}, [m^3]$		0,24	0,33	0,38	0,59	0,98	
$H_s =4m$ $Z_{req}, [m^3]$		0,24	0,33	0,38	0,6	0,99	
$H_s=1m$ $Z_{req}, [m^3]$		0,12	0,16	0,19	0,26	0,41	100 000
$H_s =2.5m$ $Z_{req}, [m^3]$		0,25	0,34	0,38	0,59	0,96	
$H_s =3m$ $Z_{req}, [m^3]$		0,26	0,36	0,41	0,64	1,05	
$H_s =3.5m$ $Z_{req}, [m^3]$		0,27	0,36	0,41	0,65	1,06	
$H_s =4m$ $Z_{req}, [m^3]$		0,27	0,36	0,41	0,65	1,07	
$H_s=1m$ $Z_{req}, [m^3]$		0,13	0,17	0,19	0,27	0,42	125 000
$H_s =2.5m$ $Z_{req}, [m^3]$		0,26	0,36	0,4	0,63	1,02	
$H_s =3m$ $Z_{req}, [m^3]$		0,28	0,38	0,43	0,67	1,1	
$H_s =3.5m$ $Z_{req}, [m^3]$		0,28	0,38	0,44	0,68	1,12	
$H_s =4m$ $Z_{req}, [m^3]$		0,28	0,38	0,44	0,69	1,13	

The results show approximately the same trend of Z toward the length of vessel, wave heights and sailing hours. The results of minimum required section modulus are plotted in

Figure 4.2.3. As it was also shown in previous curves, grey lines represent minimum required section modulus for 1m limiting wave height and another lines (black) represent Z for limiting wave height specified in the standard requirement (in this case 3.5m). In order to cover the whole operation period all lines are represented 3 times as for FCS. Design curves with all included limiting wave heights are represented in Appendix E. As it was mentioned above, point (cycle) on the curve are actual section modulus for built vessels.

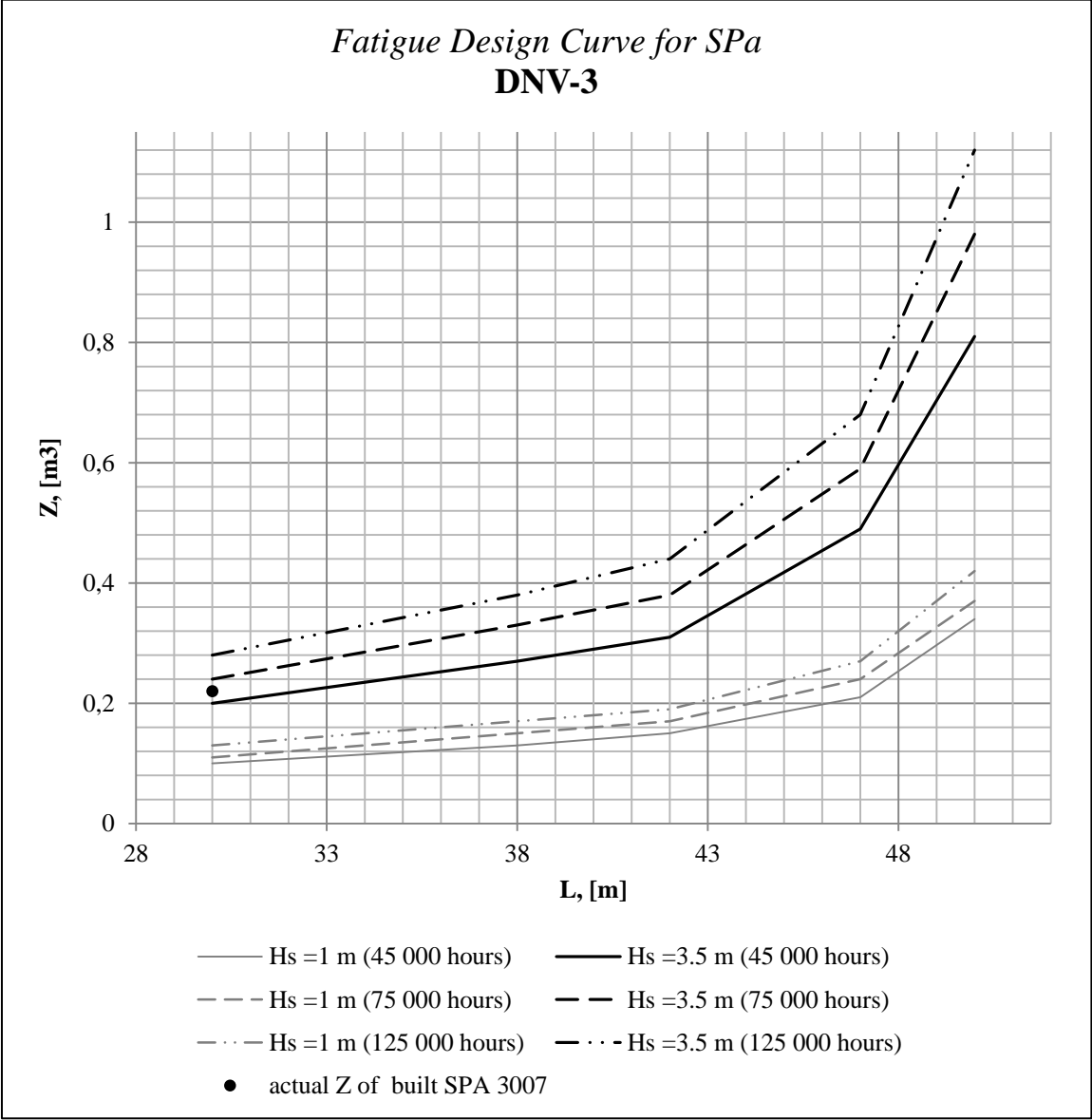


Figure 4.2.3– Fatigue design curve for SPa at DNV-3 with variable operational profile and constant service conditions

Figure 4.2.4 shows that all lines are almost smooth and have a dramatic increase of Z for vessel length more than 42m.

The same approach was used for the Gulf of Mexico and the results are represented in the table below. Visualization of Z for 1m limiting wave height and wave height specified in the standard requirement (3.5m) is plotted in Figure 4.2.3 and Z for all wave heights from Table 4.2.6 in Appendix E.

Table 4.2.6– Results of minimum required section modulus for SPa at the Gulf of Mexico for fatigue design curves

<i>Stan Patrol</i>		3007	3808	4207	4708	5009	Total sailing hours
<i>Length, [m]</i>		30	38	42	47	50	
<i>Analyzed frame</i>		11	16	18	20	24	
$H_s=1m$	$Z_{req}, [m^3]$	0,08	0,15	0,16	0,24	0,38	40 000
$H_s=2.5m$	$Z_{req}, [m^3]$	0,28	0,39	0,43	0,66	1,07	
$H_s=3m$	$Z_{req}, [m^3]$	0,3	0,41	0,46	0,7	1,14	
$H_s=3.5m$	$Z_{req}, [m^3]$	0,31	0,42	0,48	0,73	1,19	
$H_s=4m$	$Z_{req}, [m^3]$	0,32	0,44	0,49	0,76	1,23	
$H_s=1m$	$Z_{req}, [m^3]$	0,12	0,15	0,17	0,25	0,4	50 000
$H_s=2.5m$	$Z_{req}, [m^3]$	0,3	0,41	0,45	0,69	1,12	
$H_s=3m$	$Z_{req}, [m^3]$	0,32	0,43	0,48	0,74	1,2	
$H_s=3.5m$	$Z_{req}, [m^3]$	0,33	0,42	0,5	0,78	1,26	
$H_s=4m$	$Z_{req}, [m^3]$	0,34	0,46	0,52	0,8	1,31	
$H_s=1m$	$Z_{req}, [m^3]$	0,13	0,17	0,19	0,27	0,43	75 000
$H_s=2.5m$	$Z_{req}, [m^3]$	0,34	0,45	0,5	0,77	1,23	
$H_s=3m$	$Z_{req}, [m^3]$	0,36	0,48	0,54	0,82	1,33	
$H_s=3.5m$	$Z_{req}, [m^3]$	0,37	0,5	0,56	0,86	1,4	
$H_s=4m$	$Z_{req}, [m^3]$	0,39	0,51	0,58	0,9	1,46	
$H_s=1m$	$Z_{req}, [m^3]$	0,14	0,18	0,2	0,3	0,46	100 000
$H_s=2.5m$	$Z_{req}, [m^3]$	0,37	0,48	0,54	0,82	1,32	
$H_s=3m$	$Z_{req}, [m^3]$	0,39	0,52	0,59	0,89	1,44	
$H_s=3.5m$	$Z_{req}, [m^3]$	0,41	0,54	0,62	0,94	1,52	
$H_s=4m$	$Z_{req}, [m^3]$	0,42	0,56	0,64	0,97	1,58	
$H_s=1m$	$Z_{req}, [m^3]$	0,15	0,19	0,21	0,3	0,47	125 000
$H_s=2.5m$	$Z_{req}, [m^3]$	0,39	0,51	0,58	0,87	1,39	
$H_s=3m$	$Z_{req}, [m^3]$	0,42	0,55	0,62	0,94	1,52	
$H_s=3.5m$	$Z_{req}, [m^3]$	0,43	0,57	0,65	0,99	1,6	
$H_s=4m$	$Z_{req}, [m^3]$	0,45	0,59	0,68	1,03	1,66	

The figure shows the same trend of Z as for FCS in Gulf of Mexico. However, by comparing the trend of Z for SPa 3007 at DNV-3 it is easy to notice that actual Z is different from the minimum requirement, namely, $0.09m^3$. The cause of this is also explained by different dominating wave period, wave length and operability of vessel, see section 5.

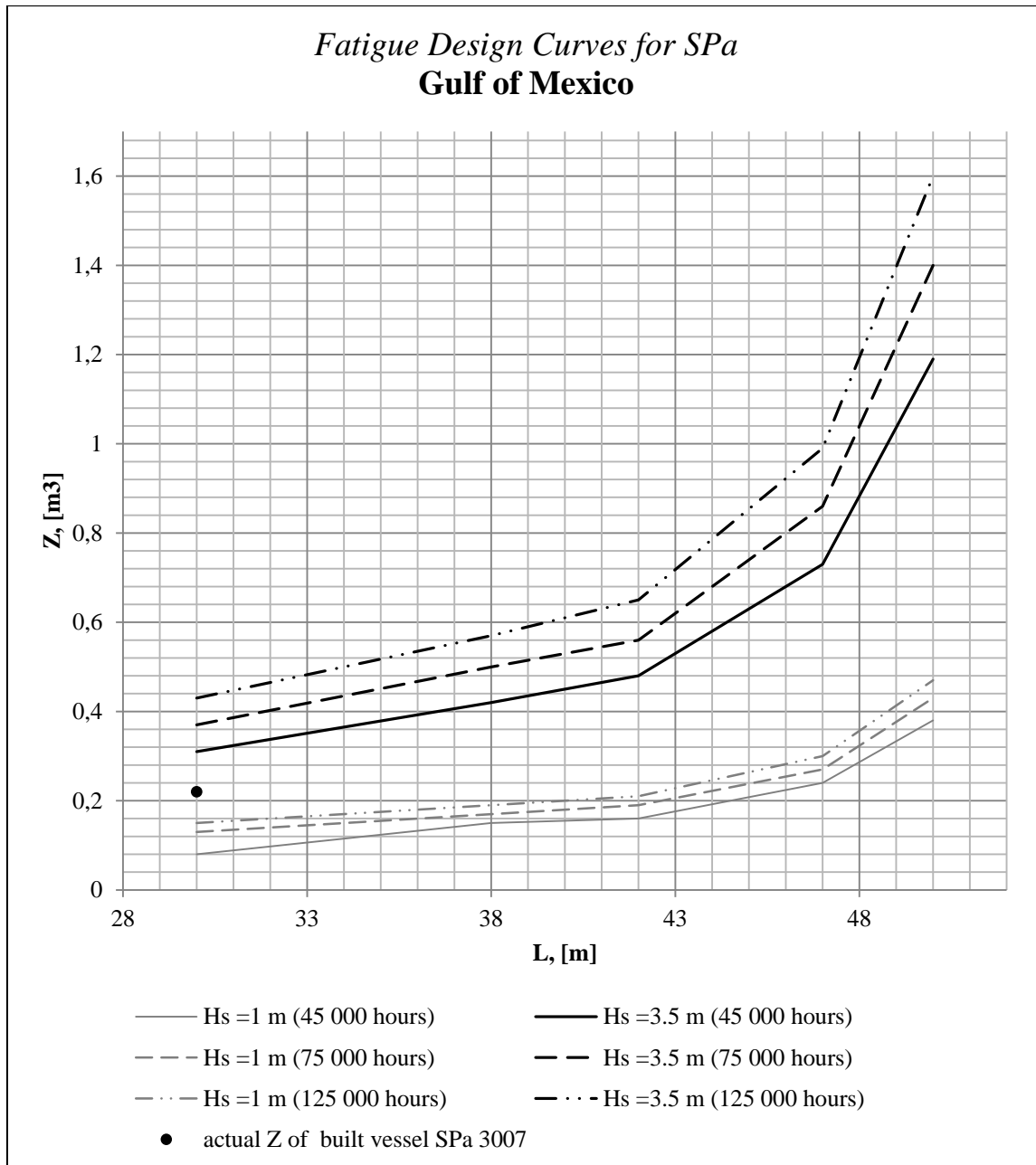


Figure 4.2.4– Fatigue design curve for SPa at the Gulf of Mexico with variable operational profile and constant service conditions

Current curves were established based on the standard operational profile where only wave height and required lifetime were variable. However, more powerful engines which give new higher speeds for each vessel can be set. Thus, another fatigue curve, namely for FCS, was created based on the standard operational profile ($H_s=2.5$ m, 75000 hours, DNV-3) where engines are only variable. All previous tests were carried out with minimum engine (power) set on the vessel. This led to minimum speeds and minimum hull girder bending moments. Thus, alternate engine was selected (see subsection 3.6.3), with maximum engine power and

maximum vessel speeds correspondingly. The results of archived Z for different engines are represented in the table below and are plotted in Figure 4.2.5.

Table 4.2.7– Results of Z for variable engine power

<i>Fast Crew Supplier</i>	1905	2610	3307	4008	4207	5209
<i>Length, [m]</i>	19	26	33	40	42	52
<i>Analyzed frame</i>	6	10	14	16	20	20
Used engine power in previous tests	0.08	0.1	0.25	0.41	0.46	0.95
Minimum engine power of vessel	0.08	0.1	0.25	0.41	0.46	0.95
Maximum engine power of vessel	0.08	0.1	0.36	0.7	0.79	1.5

Figure 4.2.5 shows the range of possible received Z for each vessel with respect to the whole range of engine power (from minimum to maximum).

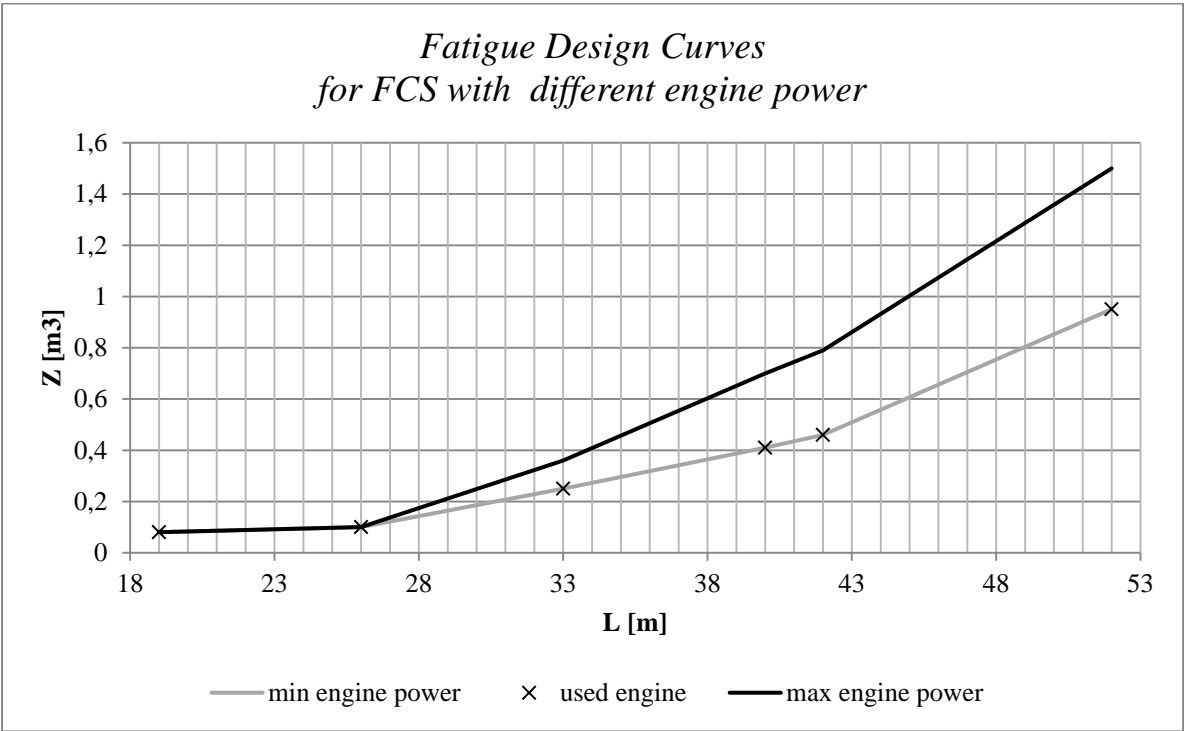


Figure 4.2.5 – Fatigue design curve for FCS at DNV-3 with different engine power

In current figure, grey line represents minimum required section modulus of each vessel on which the smallest and least powerful engine has been set. Crosses (x) on this line represent Z received in the previous tests. The black line shows minimum required section modulus of each vessel on which the largest and most powerful engine has been set.

As seen from the curve, two smallest vessels (FCS 1905 and 2610) do not have choice in different engines and thus the range of Z is 0. However, for other vessels there is a range

and it grows with increasing of the length of the vessel, namely, for FCS 3307 the range is 0.11m^3 and for FCS 5209 is 0.55m^3 . The table below shows the increased Z in percentage.

Table 4.2.8– Increase of Z in percentage

<i>Fast Crew Supplier</i>	1905	2610	3307	4008	4207	5209
<i>Length, [m]</i>	19	26	33	40	42	52
Increase Z in percentage	0	0	31%	41%	42%	37%

As it is clear from Table 4.2.8, the range of increase Z is from 31% to 42%, but in chaotic order and is not a constant value. In order to know if such dependency is present in the speeds estimation, speeds were compared and the results are as follows.

Table 4.2.9– Increase of speed in percentage

FCS	Engine	Speeds [kn]			Changes in %			Average
3307	A (original)	21.5kn	16kn	8kn	23%	18%	23%	$\approx 20\%$
	B (new)	27.9kn	19.6kn	11kn				
4008	A (original)	24.7kn	17.5kn	8kn	29%	38%	33%	$\approx 34\%$
	B (new)	35kn	28kn	12kn				
4207	A (original)	24kn	18kn	8kn	31%	33%	38%	$\approx 34\%$
	B (new)	35kn	27kn	13kn				
5209	A (original)	25.5kn	19.8kn	11.1kn	27%	24%	26%	$\approx 25\%$
	B (new)	35kn	26kn	15kn				

The results show unique values out of three speeds for each vessel (for FCS 3307 the increased speeds are in the range between 18-23%) and such dependency is true for all the vessels. In addition, each vessel received a unique percentage of increased speed on average (FCS 3307 – 20% approximately, FCS 4008 – 34% approximately). Moreover, the results show no dependency between increased speeds and Z, for example, the increased speed by 20% for FCS 3307 led to increased Z by 31% (11% of difference), while the increased speed by 34% for FCS 4207 led to increased Z by 42% (7% of difference). It may be concluded that each set engine has a unique influence on speeds and finally on Z. Thus, estimated range of Z for a particular vessel length is unique and valid only for specified vessels and their conditions.

Fatigue design curves with different engine (power) have been done for SPa as well. As alternate engine (power), the most and least powerful ones were selected, where the highest and lowest speeds were obtained, as seen in subsection 3.6.3. All previous tests were carried out with average engine (power) set on the vessels. Current tests for SPa were created

based on the standard operational profile ($H_s=3.5\text{m}$, 40000 hours, DNV-3). The results of received Z for different engines are shown in the table below and plotted in Figure 4.2.6.

Table 4.2.10– Results of Z for variable engine power

<i>Stan Patrol</i>	3007	3808	4207	4708	5009
<i>Length, [m]</i>	30	38	42	47	50
<i>Analyzed frame</i>	11	16	18	20	24
Used engine power in previous tests	0.2	0.27	0.31	0.49	0.81
Minimum engine power of vessel	0.14	0.21	0.27	0.44	0.72
Maximum engine power of vessel	0.22	0.32	0.4	0.59	0.94

Figure 4.2.6 shows the range of possible received Z for each vessel with respect to the whole range of engine power (from minimum to maximum).

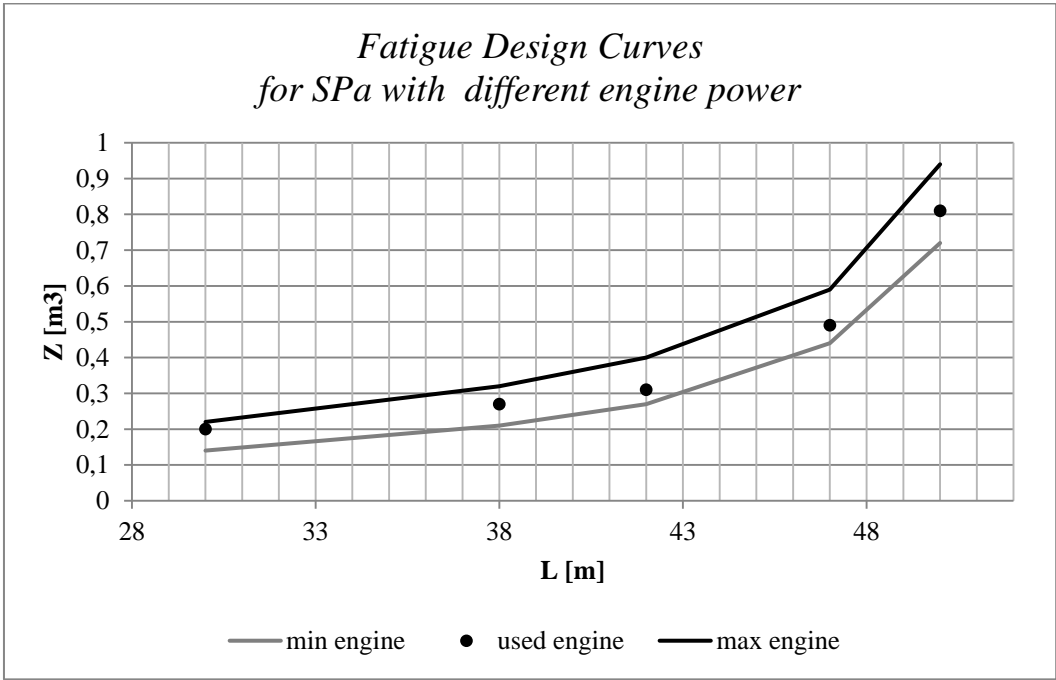


Figure 4.2.6– Fatigue design curve for SPa at DNV-3 with different engine power

In current figure, the grey line represents minimum required section modulus of each vessel on which the smallest and least powerful engine has been set. The black line shows a minimum required section modulus of each vessel on which the largest and most powerful engine has been set. Black points (cycles) between these two lines are Z received in previous tests. Unfortunately, most of these vessels are only at the design stage and that is why the largest and smallest engines (power) were only assumed based on the data for existing vessels. Due to the presence of assumptions and uncertainties in the results, no comparison

has been performed for FCS. Achieved results are useful for an additional research as future work.

The third type of fatigue design curves is made to determine the influence of length, displacement and speed of vessels on the minimum required section modulus. Thus, in current experiment three vessels with different lengths and displacements were analyzed, namely, FCS 3307, FCS 4008 and FCS 5209. Two smallest vessels (FCS 1905 and FCS 2610) are out of consideration because bending moments are not significant for such a short length, as stresses are governed by local loading. So, each tested vessel was extended or shortened to the length of two other vessels and the same was done for the displacements. With regards to the speeds, current tests were done for 2 speeds (20kn and 26kn) with the assumption that vessels go only at top speeds 100% of time, as the top speed out of three service conditions influences the most. The results of achieved minimum required section modulus are represented as follows.

Table 4.2.11– Results of Z for the third type of fatigue 3D curves

Δ , [t]	FCS 3307 L=33m			FCS 4008 L=40m			FCS 5209 L=52m		
	135	168	339	135	168	339	135	168	339
Vs= 20kn	0.36	0.4	0.53	0.37	0.49	0.69	0.39	0.56	0.84
Vs = 26kn	0.41	0.41	0.89	0.44	0.6	0.99	0.47	0.65	1.09

The results are plotted at Figure 4.2.7 and also see Appendix G.

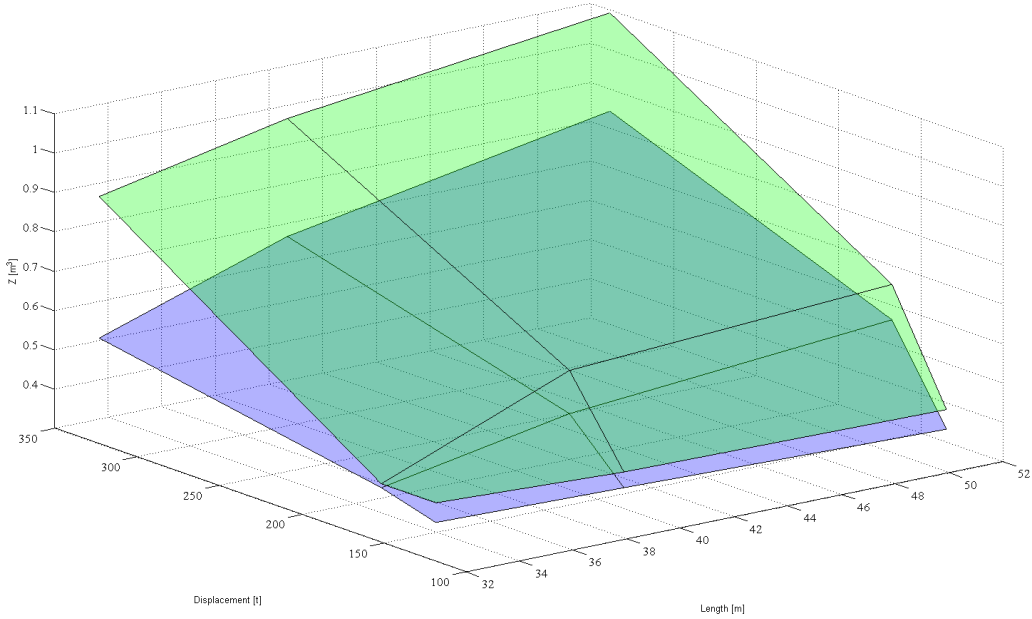


Figure 4.2.7– 3D fatigue curve (lower surface – Z at 20kn; upper surface – Z at 26kn)

The tests were carried out based on the standard operation profile which means 2.5 limiting wave height, DNV-3, 75 000 hours. The assumption to consider only top speed 100% of time leads to overstated results but with one speed it is easier to follow the influence of this parameter on Z. The lower surface represents results for the speed of 20 knots and upper surface for 26 knots. In general, the results show that the increase of displacement influences more significantly than extending the length of the vessel. In addition, when the speed was increased by 6 knots, vessels with largest displacements showed the peak values. The cause of this is explained by large mass distribution to each frame and highest accelerations in heave and pitch which cause significant force (bending moment), as compared with other displacements. The detail observation of this process is described in section 5.

In order to understand the behavior of influence input parameters on Z, the following tests were conducted. In the first test, mentioned vessels were tested with their own length and displacement, but with constant speed of 26 knots. The results of peak bending moment and achieved Z are represented in the table and figure below.

Table 4.2.12– Results of Z for FCS with constant speed

FCS	3307	4008	5209
Vs, [kn]	26	26	26
Mb max	$5.33 \cdot 10^3$	$7.85 \cdot 10^3$	$1.22 \cdot 10^4$
Z	0.38	0.6	1.09

The results show nonlinear dependency between these parameters. However, in order to estimate exact relationship current test results are not sufficient. Thus, influence of speed on bending moments for different vessels should be analyzed further (see section 5), and more tests should be conducted where different parameters or their ratio are constant.

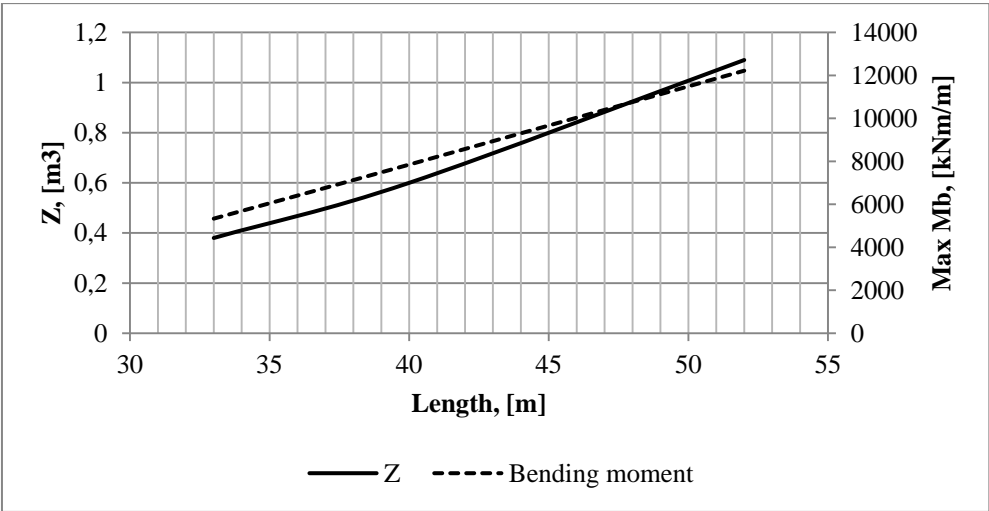


Figure 4.2.8– Results of Z for FCS with constant speed

Thus, three more cases were considered: 1. All vessels have constant speed (26 kn) and displacement (168 ton); 2. All vessels have constant speed (26 kn) and L/D ratio (0.24); 3. All vessels have the same L/D (0.24) and L/Vs (1.538) ratio. Estimated constant ratios were taken from FCS 4008 as a basis. The results are as follows.

Table 4.2.13– Results of Z for mentioned conditions

	FCS	3307	4008	5209
	L [m]	33	40	52
1	Z	0,41	0,6	0,65
2	New Δ	138	167	217
	Z	0,41	0,6	0,84

	FCS	3307	4008	5209
	L [m]	33	40	52
3	New Δ	138	167	217
	New Vs	21,45	26	33,8
	Z	0,34	0,6	0,97

Figure 4.2.9 shows the results of Z for specified conditions and a nonlinear behavior is seen again and for all cases. All lines are crossed at 40m because as mentioned above all ratios were taken from 4008 as a basis. However, all lines have their unique behavior and it is not repetitive for any line.

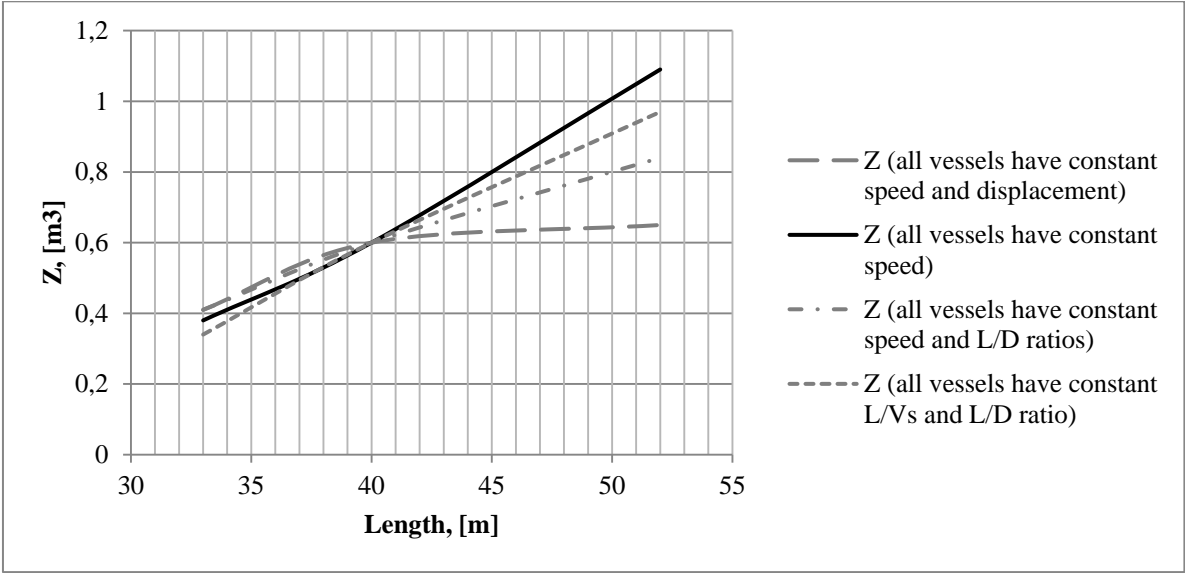


Figure 4.2.9– Results of Z for FCS with constant speed and displacement

Thus, it may be concluded that even reducing variable parameters to constant or neglected and keeping only the most influenced parameters, it is still impossible to estimate the exact behavior of the influence. The reason of this is lie in a unique influence of the main parameter on others which seems invisible and unimportant from the first site but which influences are significant, such as a dominating wave frequency, an encounter frequency, the wave length, maximum accelerations at heave and pitch and finally location of frame with largest bending moment. Detailed observation of the mentioned influences can be found in Discussion section 5.

5 Discussion

This study has analyzed the influence of different parameters on fatigue lifetime of details on vessels, accuracy of achieving results and occurred uncertainty with respect to the load calculation on the vessel and minimum required section modulus. The structure of this section is consistent and follows the structure of section 4. The sensitivity analysis was conducted in order to investigate how combination of different parameters influence fatigue lifetime and which input parameter influence the most. The fatigue design curves helped to understand if there is any trend between input parameters and the minimum required section modulus in order to develop standard fatigue curves. In addition, these curves helped to assess the accuracy of the results and identify uncertainties associated with estimation of fatigue lifetime.

5.1 Sensitivity analysis

As mentioned in subsection 4.1 the sensitivity analysis was carried out for SPa 3007 for 3 frames where the frame with largest bending moment was identified as most prone to fatigue cracks. If a vessel is considered as a beam with hinged supports, applied load gives the largest bending moment approximately in the middle of the vessel. However, the fore part of SPa is very narrow and thus, there are no high loads. In addition, axe bow (see Figure 3.4.1) allows excluding green seas for the vessel. So, the fore hinged support is transferred several frames aft. Taken this into account the highest bending moment is transferred to “a new middle” of the craft and this is frame 11, as seen in Figure 5.1.1. Thus, all other tests were conducted for frames only with largest bending moment.

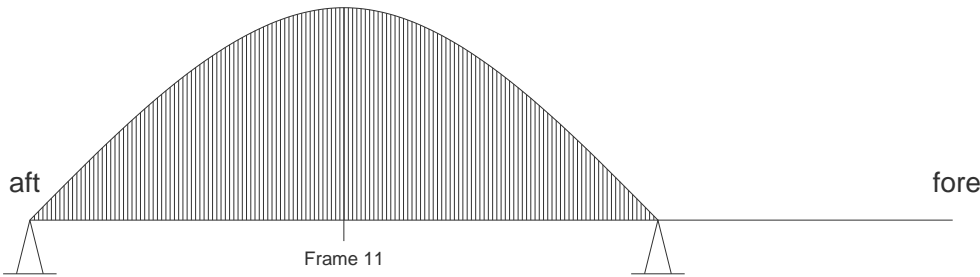


Figure 5.1.1– Bending moment distribution along the length of vessel

With regards to severity of different operational areas, two scatter diagrams with different wave behavior were compared, namely, the North Sea and the Northern part of the Arabian Sea. These two scatter diagrams represented in Appendix (table A2 and A10).

From both scatter diagrams (WSD) it is seen that the total number of waves is approximately the same. However, the North Sea contains higher waves (up to 9.5 meters), compared with the N-Arabian Sea (up to 6.5m). As mentioned in subsection 3.3.2 in the preliminary analysis, the wave height is limited (2,5m or 3m or 3.5m or 4m) which means that all waves above selected are removed from the scatter diagram. For example, if the limiting wave height is 3.5, then WSD will be as follows:

Table 5.1.1– Scatter diagram for the North Sea

	22	157	306	255	116	38	8	2	0	0	0	901
Sign. wave height Hs (m)	12.5											0
	11.5											0
	10.5											0
	9.5				1							1
	8.5			1	1	1						3
	7.5		1	2	2	1						6
	6.5		2	4	4	2	1					13
	5.5	1	4	9	8	4	1					27
	4.5	2	11	19	15	6	2					55
	3.5	6	27	39	26	10	3	1				112
	2.5	1	17	63	74	40	13	3	1			212
	1.5	3	48	121	100	40	10	2				324
	0.5	18	86	95	42	10	2					253
		3.5	4.5	5.5	6.5	7.5	8.5	9.5	10.5	11.5	12.5	13.5
		Zero crossing period T2 (s)										

The small experiment showed that total number of waves in the N-Arabian Sea became 966 (cut by 37 waves in total) and in the North Sea - 901(cut by 105 in total). So, the new number of wave occurrence is also the reason of such estimated severity of seas.

Table 5.1.2– Scatter diagram for the N-Arabian Sea

	132	336	309	139	40	9	1	0	0	0	0	966
Sign. wave height Hs (m)	12.5											0
	11.5											0
	10.5											0
	9.5											0
	8.5											0
	7.5											0
	6.5		1	1	1							3
	5.5	1	3	3	1	1						9
	4.5	4	9	8	3	1						25
	3.5	2	14	26	19	8	2					71
	2.5	7	44	66	39	13	3	1				173
	1.5	26	116	125	56	15	3					341
	0.5	97	162	92	25	4	1					381
		3.5	4.5	5.5	6.5	7.5	8.5	9.5	10.5	11.5	12.5	13.5
		Zero crossing period T2 (s)										

In addition to the wave height limitation, most waves in the North Sea meet at longer wave periods, while in the N-Arabian Sea most waves meet more frequently (every 4.5-5 seconds). Thus, two analyzed areas were tested for dominating wave length and compared with the vessel length. The length of vessels is 30 meters. In current study the water was considered as deep, so the wave length, λ , was calculated by following formula:

$$\lambda = \frac{g}{2\pi} \cdot T^2 \tag{Eq. 5.1.1}$$

where T – is a wave period, (Journee & Massie, 2001).

The remaining total number of occurrence waves at specific wave length was calculated as summation of waves for each wave period. The results are plotted in figure below and numerical results are represented in Appendix F.

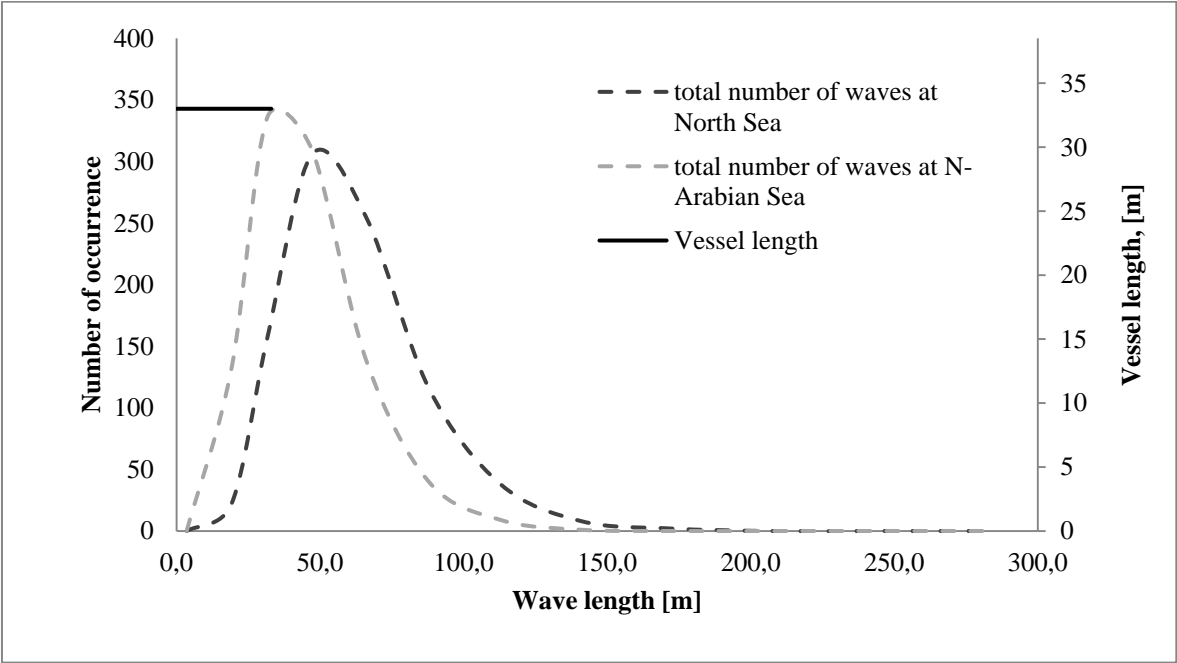


Figure 5.1.2– Comparison of dominating wave length and vessel length in two areas

Figure 5.1.2 showed that the dominating wave length is located around ship length in the N-Arabian Sea, which corresponds to dominating wave period 4.5 seconds, while in the North Sea the dominating wave length does not coincide with the vessel length, with corresponded wave period of 5.5 seconds. This means that while operating in the N-Arabian Sea the vessel is in the resonance with wave length in pitch, which entails higher forces (bending moments) and leads to faster occurrence of fatigue cracks. This explains the reason of such estimated severity of seas in subsection 4.1. The similar approach happens while comparing DNV-3 and the Gulf of Mexico; these two areas were used in analysis in

subsection 4.2. In order to lower the response of the vessel, it is proposed to lengthen it to the value different from the wave length which excludes appeared resonance. This will decrease stress concentrations induced by the waves.

Moreover, if the resonant period in heave coincides with the dominating wave period in wave energy spectrum, the structure response gives very high values, as seen in Appendix I. Thus, operation area significantly affects not only the pitch motion where the wave length may coincide with the vessel's length but also for the heave motion. In order to avoid the resonance, the wave spectrum and vessel geometry should be analyzed and optionally the vessel should be lengthened or shortened. Then, the vessel will have a new natural frequency and a corresponding new dominating natural period.

5.2 Fatigue design curves

As mentioned above, the fatigue design curves were created for both types of vessels in order to help engineers at the design stage to make right selection regarding the vessel length for specific operational profile or individual customer requirement. These curves were designed for two operational areas with different wave behavior, as seen in section 4 and subsection 5.1.

All curves are complemented with points of actual Z for already built vessels. FCS 3307 is made of aluminum and there is a large difference in Z with actual and minimum required (based on the standard operational profile), namely 0.07m^3 of a discrepancy at DNV-3. However, for SPa 3007 (which is also made of aluminum) minimum required and actual Z are almost coinciding, only 0.02m^3 at DNV-3. The fatigue design curve with added hybrid material is shown in Appendix H, and even there the distance is rather large. Therefore, causes of uncertainty and accuracy of results are discussed here.

Different uncertainties are associated with fatigue life prediction of the structures. (Wirsching, 1983), (Gran, 1980). They also refer to several most influenced parameters which are load and stress calculations.

The uncertainty regarding the load calculation greatly depends on available vessel data, weight distribution, calculation procedure, distribution of waves and hydrodynamic coefficients (Lotsberg et al., 1985). With respect to the weight distribution, the Seaway Octopus gives absolutely the same results when weight is distributed evenly and unevenly along the length of vessel. This finding in the program should be taken into consideration and the large distance in curves between actual and required Z can be the result of inaccurate

calculation of transfer function (bending moments). In order to figure out how valid are the calculated bending moments as compared with the actual ones, special measuring instruments (strain gauges) should be installed on the vessels, data should constantly be observed and strains be recorded, measuring the structure response. Moreover, the fatigue lifetime is very sensitive to distribution of waves (Lotsberg et al., 1985). During the study of Alufastship program, a major assumption referring to the wave distribution was identified. Since most fatigue damage is caused by forward incoming waves between -45 to +45 degrees for high speed crafts (see Figure 5.2.1), a factor 0.5 is used to take into account the wave distribution in Alufastship, which considers reduction on number of cycles by 50 %. This assumption can lead to some uncertainty of fatigue lifetime calculation and thus, additional tests should be conducted.

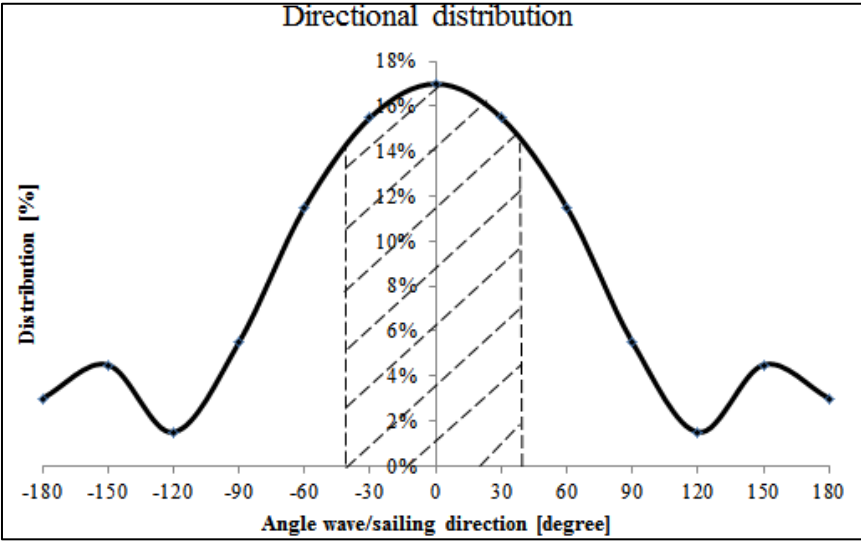


Figure 5.2.1–Directional distribution based on DNV report 97-0152

In addition, there are several uncertain points with respect to stress calculation which depend on structural response, FAT class and calculation of stress concentration factor. The SCF in this study was estimated as 1.15 due to butt welds corresponding to FAT class 6 (Germanisher Lloyd). However, such category can be very conservative. In order to accurately determine SCF the finite element analysis should be carried out rather than assume or use parametric equations which were established several years ago (Lotsberg et al., 1985).

With respect to the 3D-fatigue curve and small experiments with input parameters nonlinear behavior of Z is observed. However, it is difficult to estimate exact dependency of parameters and even create a formula because many parameters impact Z and three vessels are not sufficient for this research. In addition, during tests the changes in length and displacement of vessels were done manually, thus several parameters were roughly calculated

and assumed (such as VCG for each frame and roll radius of gyration), in order to determine bending moments. Therefore, it is not possible to provide accurate results for bending moments in current tests. In case the length and displacement remain original for each vessel and concerning influence of speed on bending moments several dependencies were found.

Firstly, for each vessel with original parameters the speed was considered from 8 to 30 knots with a step of 2kn. The results present largest bending moment for a corresponding frame. They are as follows.

Table 5.2.1– Largest bending moments for specified speeds

Speed, [kn]	FCS 3307		FCS 4008		FCS 5209	
	Max M_b [kNm/m]	Increased M_b in %	Max M_b [kNm/m]	Increased M_b in %	Max M_b [kNm/m]	Increased M_b in %
8	2328		3799		7123	
10	2521	8%	4102	7%	7540	6%
12	2736	8%	4477	8%	7936	5%
14	2957	7%	4801	7%	8419	6%
16	3263	9%	5297	9%	8966	6%
18	3533	8%	5707	7%	9439	5%
20	3939	10%	6306	9%	10090	6%
22	4275	8%	6778	7%	10760	6%
24	4742	10%	7534	10%	11290	5%
26	5103	7%	7903	5%	12220	8%
28	5707	11%	9114	13%	13100	7%
30	6048	6%	9829	7%	13650	4%

**Colored part of “Max M_b ” results means that frame with largest bending moment shifted to one aft.*

Table 5.2.1 showed that there is an approximate constant dependency between the speed and the bending moment, namely, increase of speed by 2kn led to the increase of maximum bending moment on average by 8-10% for FCS 3307, 7-9% for FCS 4008 and 5-6% for FCS 5209. However, the value of dependency is unique for each vessel, so influence of speed on bending moments in intervals between considered vessels remains unknown. In addition, tests showed that increasing speed shifts frame with largest bending moment. This event was investigated in more details.

The next test was conducted for FCS 3307 for all frames; two speeds (8 and 28 knots) and 2 wave frequencies corresponded to largest bending moment at each speed. Unfortunately, the program provides a natural frequency of ship only in heave and pitch

motions. So, this value is out of consideration in current analysis. The results have been plotted in the figure below and numerical results in Appendix J.

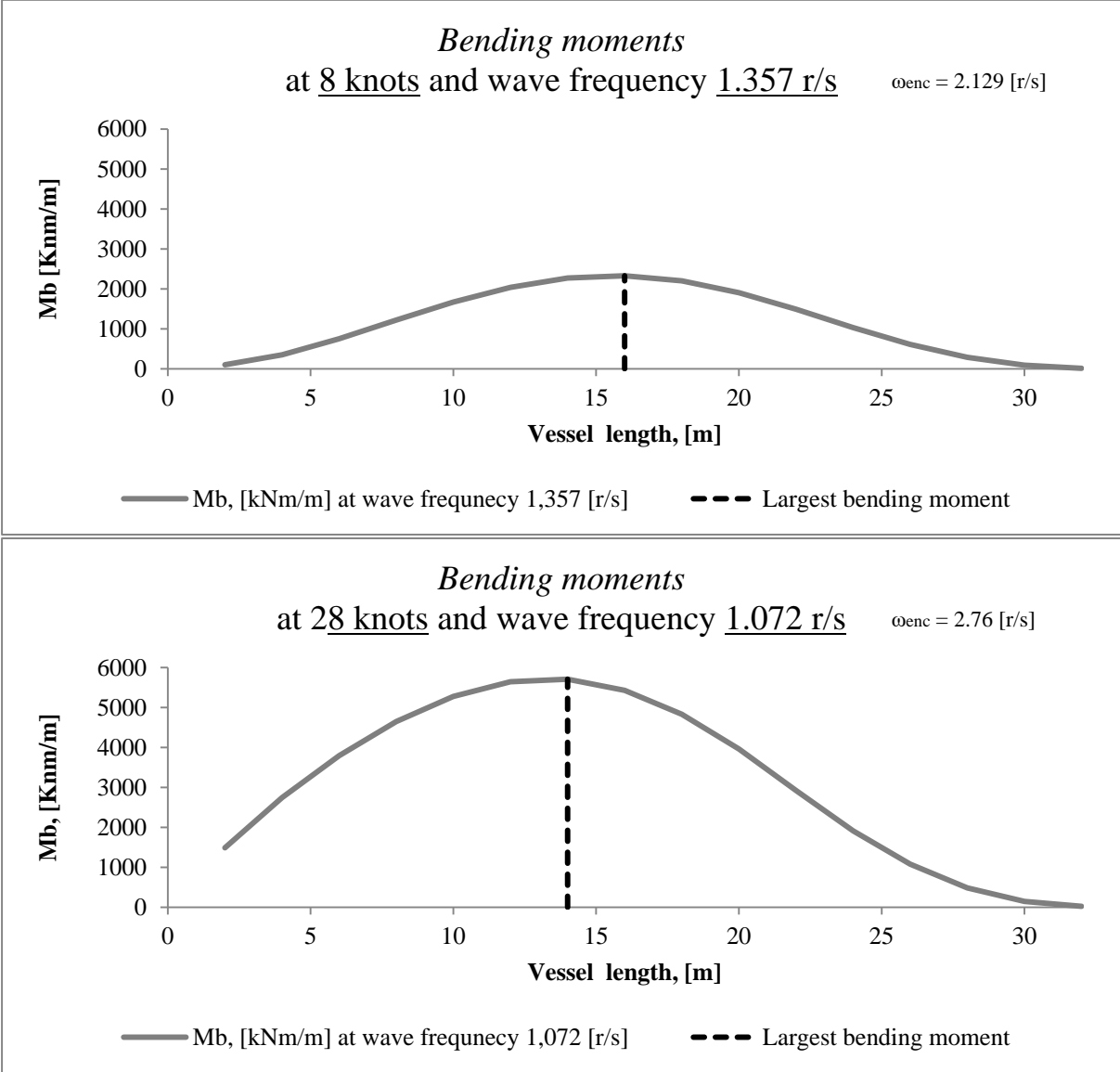


Figure 5.2.2– Behavior of bending moments along the vessel length at 8 and 28kn

Figure 5.2.2 shows behavior of bending moments in both diagrams (first mode of vibrations). Since the largest bending moment at 8 knots was achieved for frame 16 and corresponds to wave frequency $\omega=1.357$ [r/s], it was assumed as constant in the upper diagram. As the largest bending moment at 28 knots was achieved for frame 14 and corresponds to wave frequency $\omega=1.072$ [r/s], that frequency was assumed as constant in the lower diagram. In addition, the program calculated the encounter frequency (by Eq.5.2.1) for corresponding speed and wave frequency. The results in the upper right corner of the diagrams show that with increased speed, the encounter frequency also increased.

The encounter frequency in head seas can be found as follows:

$$\omega_e = \omega + \frac{\omega^2 \cdot V_s}{g} \quad (\text{Eq. 5.2.1})$$

where ω is a wave frequency [r/s] and V_s is the vessel speed [kn].

Overall, while considering behavior of bending moments through the whole length of the vessel, it is seen that increased speed shifts the maximum bending moment toward the stern and largest bending moment is at the lower wave frequency. Such trend was followed for other vessels, for example, for containership 175m in the Offshore Hydrodynamics book (Journey & Massie, 2001), as seen in figure below.

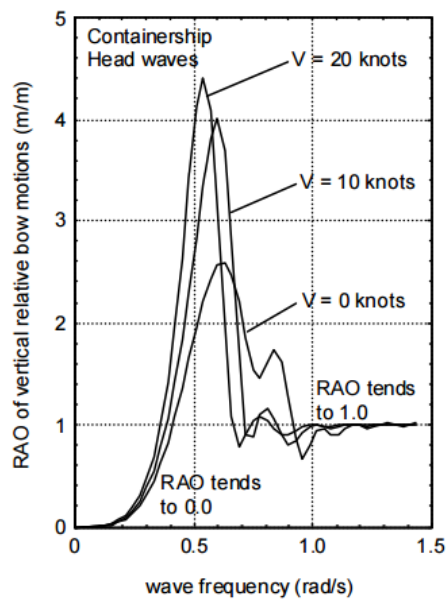


Figure 5.2.3– Vertical motions at the bow,(Journey & Massie, 2001)

However, due to limited resources and information, the reasons for such event should be investigated in future work.

6 Conclusion

6.1 Conclusion of the thesis

This thesis looks at several targets. The first goal was to investigate the sensitivity of fatigue analysis for one of high speed crafts developed by Damen, namely Stan Patrol 3007. Based on the general arrangement of the vessels, several allegedly weak locations subject to fatigue were selected for the analysis. As only limited initial data was available, it seemed relevant to conduct preliminary fatigue analysis in order to receive a minimum required section modulus of a hull section. This parameter reflects fatigue lifetime and was used as a comparative value in the sensitivity study.

Overall, the vessel parts that are mostly prone to fatigue failure are the details located at the frames with the transition from the hull to the superstructure and with the calculated largest hull girder bending moment. In addition, the sensitivity analysis showed that it is speed that influences mostly the fatigue lifetime while less important parameters are: time spent at the top speed, time spent at the average speed, an intended service period and the operating area. With respect to the impact of different operating areas on minimum required section modulus, additional analysis showed that seemingly modest areas like N-Arabian Sea can be more dangerous for fatigue lifetime of a vessel than the North Sea due to several reasons. Firstly, coincidence of the dominating wave length with the vessel length causes resonance in pitch and need to reinforce. Secondly, coincidence of the dominating wave period in the wave energy spectrum with the dominating period of the transfer function in heave also causes resonance and results in an additional requirement to increase the strength. Finally, due to the assumption of wave limitation in calculation, a certain number of waves are taken out from the calculation which leads to manual lowering severity of several operation areas like the North Sea.

The second goal was to create fatigue design curves in order to facilitate proper selection of the main particulars of the vessel for a specific required operational profile. For this purpose, 11 high speed crafts were investigated where six of them were Fast Crew Suppliers and the rest were the Stan Patrol type. All of them are assumed to be made of aluminum only. The curves for FCS and SPa were performed separately. All fatigue design curves showed behavior of minimum required section modulus influenced by different parameters and include points of actual section modulus for already built vessels. To summarize, the fatigue design curves were performed of three types, namely: fatigue curves

with variable operational profile and constant service conditions, fatigue curves with variable engine power and 3D-fatigue curves.

Based on the results achieved in the sensitivity study, for the first type of the curves several mostly influenced variable parameters have been selected, such as multi-axes for the fatigue design curves; one of these axes was the length of the vessel. Current curves cover the total sailing period from 45000h (for FCS)/40000h (for SPa) till 125000h for both types. All curves contain lines with achieved Z for 1m limiting wave height in order to understand the lower wave influence and for limiting wave height specified in the standard requirement. These curves were designed for two operational areas with different wave behavior, DNV-3 and the Gulf of Mexico. All included tests were carried out based on a standard operational profile. The results showed a dramatic increase of minimum required section modulus with the growth of the vessel length. In addition, curves showed large difference in Z with actual and minimum required parameters for both aluminum and hybrid vessels and thus, the accuracy of fatigue life prediction were assessed. On balance, the weight distribution in Seaway Octopus gives absolutely the same results if the weight is distributed evenly and unevenly along the length of vessel. This finding in the program should be taken into consideration and checked using special measuring instruments (strain gauges) installed on the vessels. Another finding was identified during the study of the Alufastship program, namely, the actual wave distribution. Since most fatigue damage is caused by forward incoming waves between -45 to +45 degrees for high speed crafts, a factor 0.5 is used to take into account the wave distribution in Alufastship which considers reduction in number of cycles by 50 %. So, additional tests should be conducted. Finally, the estimated SCF factor based on FAT class can be very conservative. Thus, the finite element analysis should be carried out.

Second type of the curves was studied based on the standard operational profile except of the engine power. In this case alternate engines were selected from minimum to maximum in order to show the whole range of Z allowable for specified length of the vessel based on the total power range. However, fatigue curves for FCS showed that each set engine had a unique influence on speeds and finally on Z. Thus, estimated range of Z for particular length of vessels is unique and is valid only for specified vessels and their conditions. With respect to the fatigue curve for SPa, unfortunately, most of SPa crafts are only at the design stage and that is why the largest and smallest engines (power) were only assumed, based on the data for the existing vessels. Due to the available assumptions and uncertainties in the results, no

comparison has been performed as for FCS. The results achieved might be useful for future study.

In the third type of the fatigue curves only Fast Crew Suppliers were investigated except of two smallest ones (FCS 1905 and FCS 2610) because the bending moments were not significant for such a short length as stresses were governed only by local loading. Tests were carried out based on the standard operation profile, but only top speed was used as the service condition.

The tests showed that an increased displacement tend to be more significant than an extended length of the vessel. In addition, keeping only the most influenced parameters such as speed, length and displacement, it was still impossible to estimate the exact dependency of the parameters and even to find a formula due to the nonlinear behavior of Z and unique influence of the input parameters. As changes in length and displacement of vessels were done manually, several parameters were roughly calculated and assumed (such as VCG for each frame and roll radius of gyration), in order to obtain the bending moments. Therefore, it was not possible to provide accurate results for bending moments.

Another observation showed approximately constant dependency between the speed and the bending moment, but the value of dependency is unique for each vessel, so influence of speed on bending moments in intervals between considered vessels remained unknown. In addition, current observation showed that increased speed shifted the largest bending moment toward stern and at lower wave frequency.

6.2 Suggestions for future study

To summarize, there were several uncertainties in the study which should be further investigated, such as a calculated response of the vessel and output sensitivity to weight distribution in Seaway Octopus software. In addition, the way of wave distribution in Alufastship should be checked and if necessary improved. Finally, the behavior of largest bending moments at low wave frequencies with increased speed should be investigated in the future work.

References

- Allday, B. (1993). Aluminium alloys - design for fatigue. *Ship & Boat International*, 25-39.
- API_RP_2A. (1982). Recommended Practice for Planning, Designing and Constructing Fixed Offshore Platforms—Working Stress Design (13 ed., pp. 242). Washington DC: American Petroleum Institute
- Bendat, J. S., & Piersol, A. G. (1971). *Random Data: Analysis and Measurement Procedures*: Wiley - Interscience.
- Berge, S. (1985). *Basic Fatigue properties of Welded Joints*. Trondheim: Tapir.
- Biot, M., Marino, A., & Susmel, F. (2005). *A Proposal For a Simple Fatigue Design Check Procedure*. Paper presented at the International Conference on Fast Sea Transportation FAST 2005, St. Petersburg, Russia.
- Capanoglu, C. C. (1993). fatigue Technology Assessment and Strategies For Fatigue Avoidance in Marine Structures (pp. 412). Washington DC.
- D.En. (1983). Offshore Installations: Guidance on Design and Construction. New Fatigue Design Guidance for Steel Welded Joints in Offshore Structures: Department of Energy "Guidance Notes"
- Dijkstra, O. D. (2004). Ontwerpmethodiek voor aluminium hogesnelheidsschepen met lange levensduur Beshrijving MathCAD rekenprocedure (pp. 13). Delft: Netherlands Organisation for Applied Scientific Research.
- DNV. (1996). Fatigue Assessment of Ship Structures (DTP, Trans.) (pp. 154). Høvik, Norway.
- DNV. (1997). Proposal For Classification Note Fatigue Analysis of HSLC (pp. 88): Det Norske Veritas.
- DNV. (2010). Fatigue Assessment of Ship Structures (pp. 108). Høvik, Norway: Det Norske Veritas.
- DNV. (2012). Direct Calculation Methods. In L. C. a. N. S. C. High Speed (Ed.), *Structures, Equipment* (pp. 15). Det Norske Veritas.
- Fines, S. (1985). *Loads on Ocean Structures*. Oslo: Tapir.
- Gibstein, M. B., & T.Moe, E. (1985). *Fatigue of Tubular Joints*. Oslo: Tapir.
- GL. (2007). Fatigue Strength. In S. I - Part 1 (Ed.), (pp. 20). Hamburg: GL
- Gran, S. (1980). Fatigue and Crack Failure Prediction Methods in Marine Structures (DNV, Trans.): Det Norske Veritas.
- Hall, T., Violette, D. F., & Chung, H. (1998). *Fatigue Design Assessment of Aluminium Fast Craft*. Paper presented at the AUSMARINE - CONFERENCE '98, Fremantle; Australia. Print retrieved from <http://products.damen.com/en>. (April 2016). A VESSEL FOR EVERY PURPOSE *Damen Products*.
- Hydra, R. (2013). SPa 3007 - Preliminary fatigue analysis (pp. 5). Damen Shipyards Gorinchem: Damen Shipyards Gorinchem.
- Hydra, R., & Jorinus, K. (2010). Guideline to fatigue analysis (pp. 21). Damen Shipyards Gorinchem: Damen Shipyards Gorinchem.

- Journee, J. M. J. (2001). User Manual of Seaway (F. o. M. E. a. M. Technology, Trans.) (pp. 142). Delft University of Technology: Delft University of Technology.
- Journee, J. M. J., & Massie, W. W. (2001). *Offshore Hydrodynamics* (first edition ed.). Delft: Delft University of Technology.
- Langen, I., & Sigbjørnsson, R. (1979). *Dynamisk Analyse av Konstruksjoner*. Trondheim: Tapir.
- Lotsberg, I., A. Almer-Næss, & Veritec, A. S. (1985). *Fatigue Life Calculations*. Trondheim: Tapir.
- Lyngstad, O. A. (2002). Fatigue of High Speed Craft - In Service Experience (pp. 306 - 328).
- Moan, T. (1985). *Overview of Offshore Steel Structures*. Trondheim: Tapir.
- Newland, D. E. (1975). *Random Vibrations and Spectral Analysis*. London: Longman.
- Roylance, D. (2001). Fatigue (pp. 9). Cambridge MA: Massachusetts Institute of Technology.
- Segers, G. (2004). *Validation "Alufastship" Mathcad application*. . (Bachelor Science Thesis Report), Inholland University of Technology, Damen Shipyards Gorinchem.
- Veritas, D. N. (1977). *Rules for the design, construction and inspection of offshore structures, 1977 / Det Norske Veritas*. Oslo: Det Norske Veritas.
- Wirsching, P. H. (1983). Probability - Based Fatigue Design Criteria for Offshore Structures (D. o. A. a. M. Engineering, Trans.). Tucson: University of Arizona.

Appendix A: Standard wave scatter diagrams

Table A.1 – Scatter diagram for DNV-3

1.285	1	2	3	4	5	6	7	8	9	10	11	12	13	14
0.5	0	0	15	70	104	85	50	24	10	4	1	1	0	0
1	0	0	1	17	51	65	49	27	12	5	2	1	0	0
1.5	0	0	0	4	24	44	43	28	13	5	2	1	0	0
2	0	0	0	1	9	24	30	22	12	5	2	1	0	0
2.5	0	0	0	0	3	11	18	16	9	4	1	1	0	0
3	0	0	0	0	1	5	10	10	6	3	1	0	0	0
3.5	0	0	0	0	0	2	5	5	4	2	1	0	0	0
4	0	0	0	0	0	1	2	3	2	1	1	0	0	0
4.5	0	0	0	0	0	0	1	1	1	1	0	0	0	0
5	0	0	0	0	0	0	0	1	1	0	0	0	0	0
5.5	0	0	0	0	0	0	0	0	0	0	0	0	0	0
6	0	0	0	0	0	0	0	0	0	0	0	0	0	0

Table A.2 – Scatter diagram for the North Sea

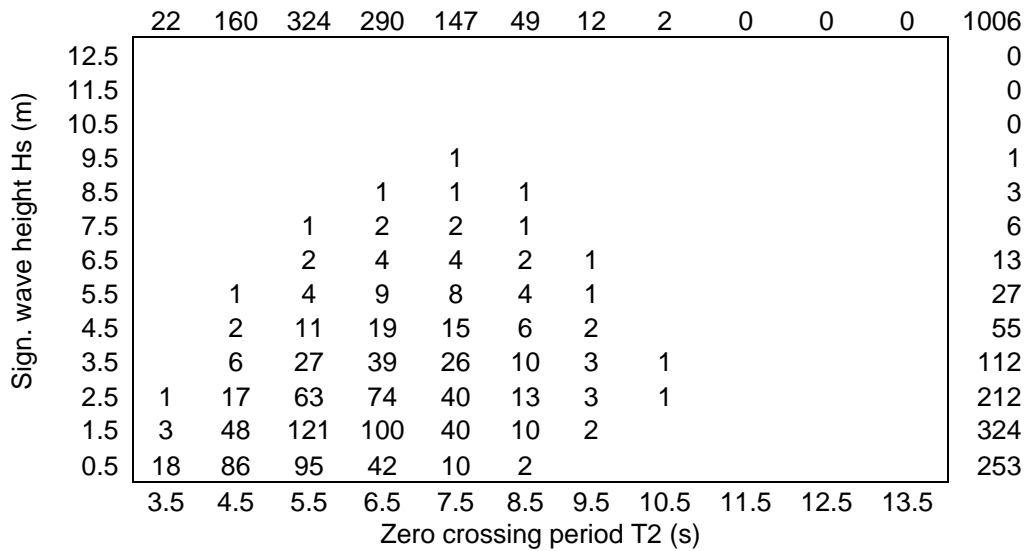


Table A.3 – Scatter diagram for the Gulf of Mexico

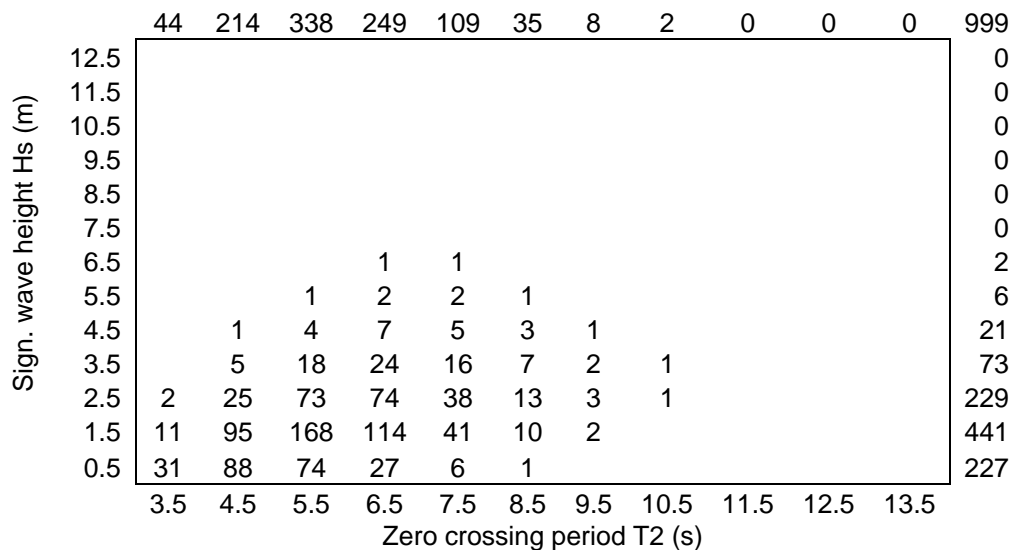


Table A.4 – Scatter diagram for the Northern part of Brazil

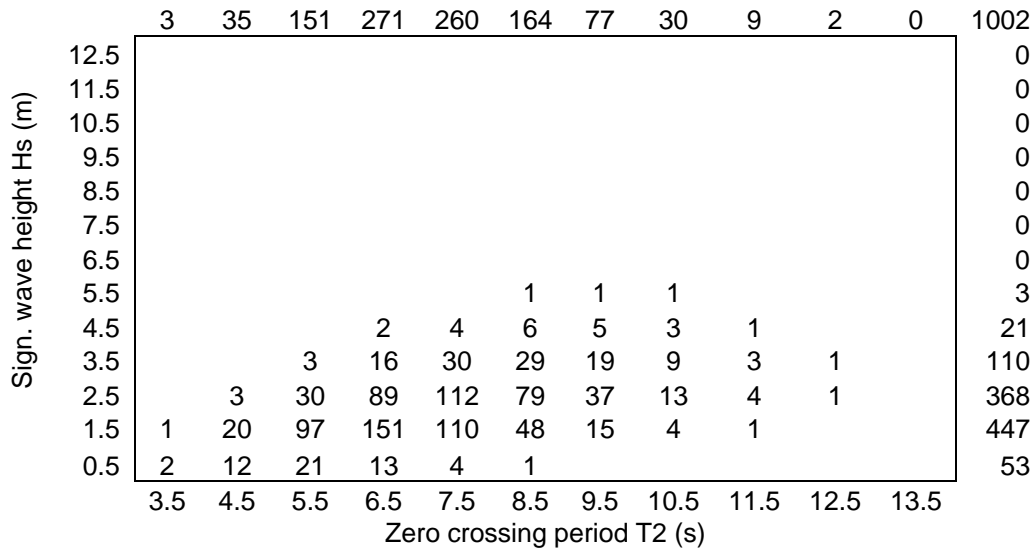


Table A.5 – Scatter diagram for Southern Brazil

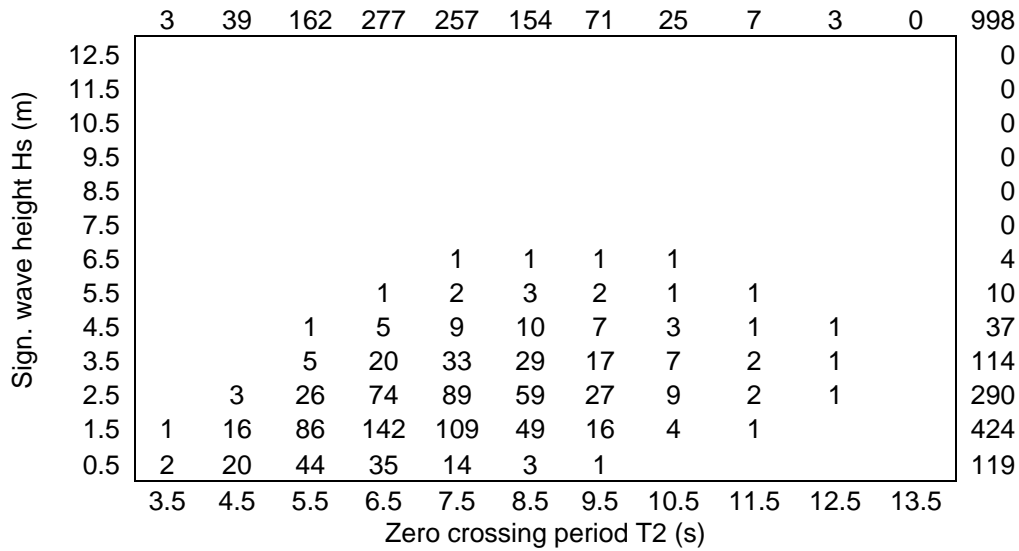


Table A.6 – Scatter diagram for Nigeria

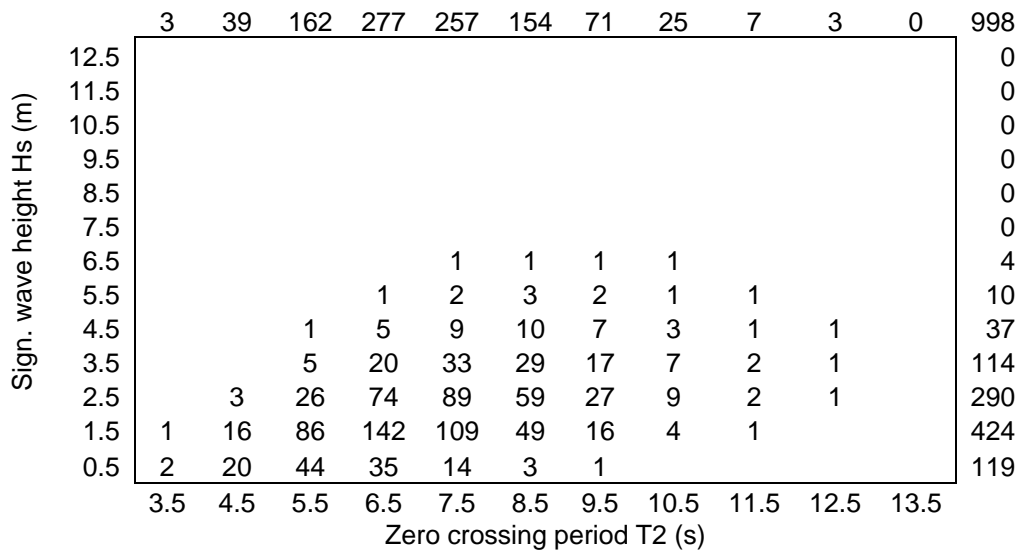


Table A.7 – Scatter diagram for Angola

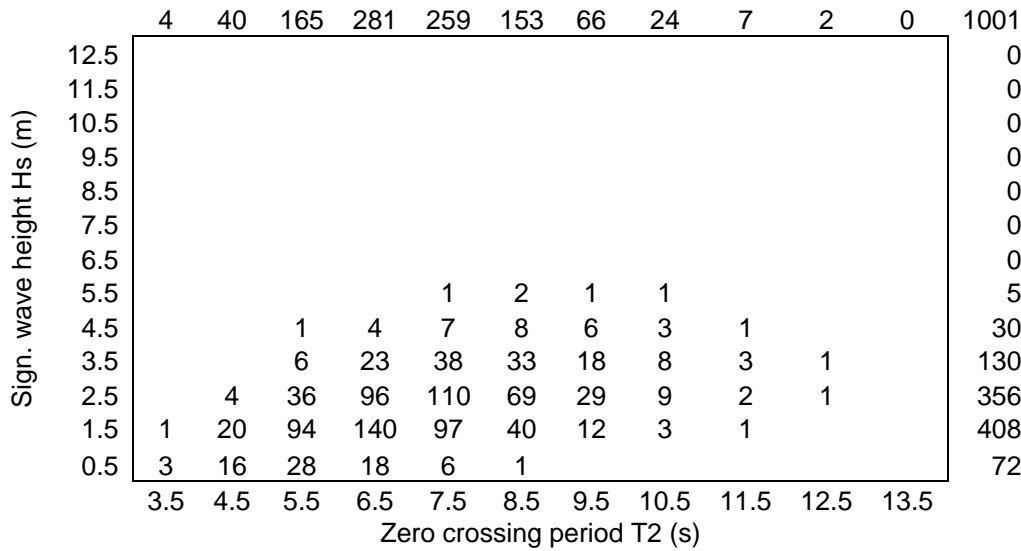


Table A.8 – Scatter diagram for the Red Sea

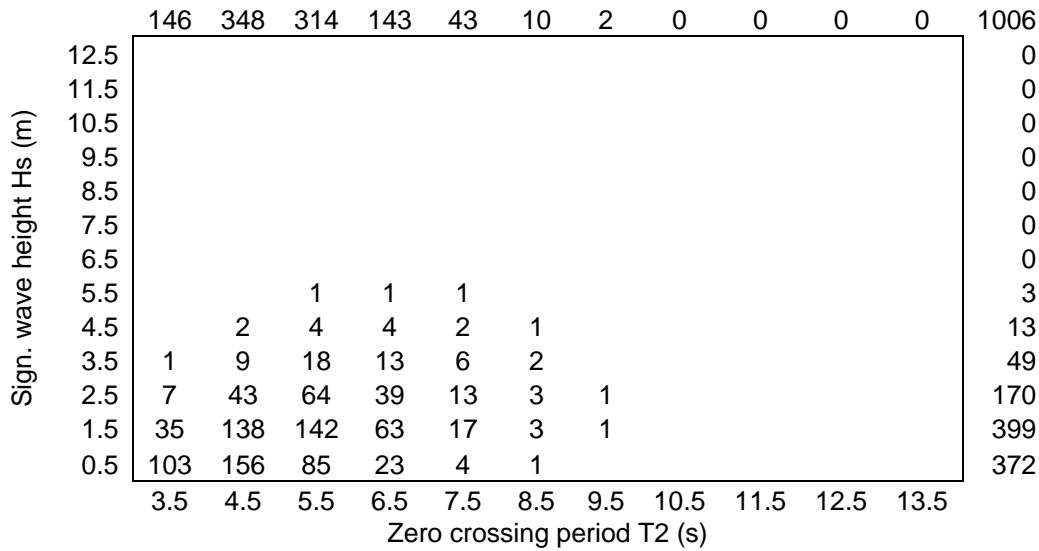


Table A.9 – Scatter diagram for the Persian Gulf

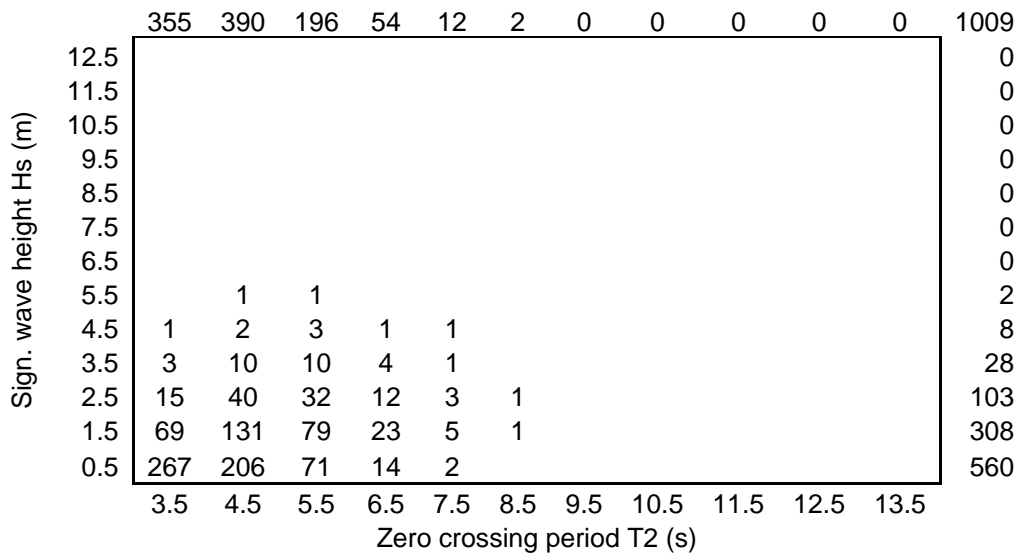


Table A.10 – Scatter diagram for the North Arabian Sea

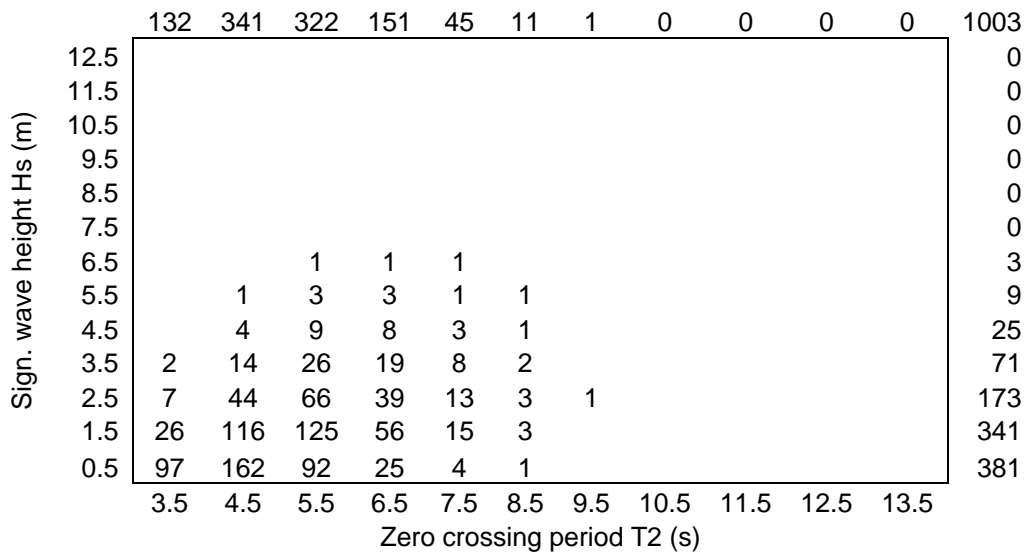


Table A.11 – Scatter diagram for the Bengal Sea

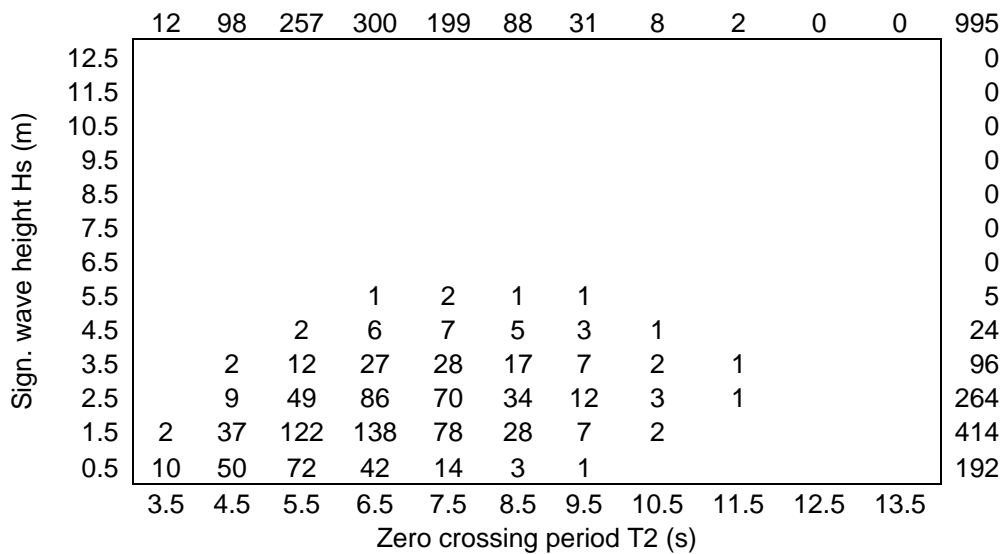


Table A.12 – Scatter diagram for the Northern part of the Chinese Sea

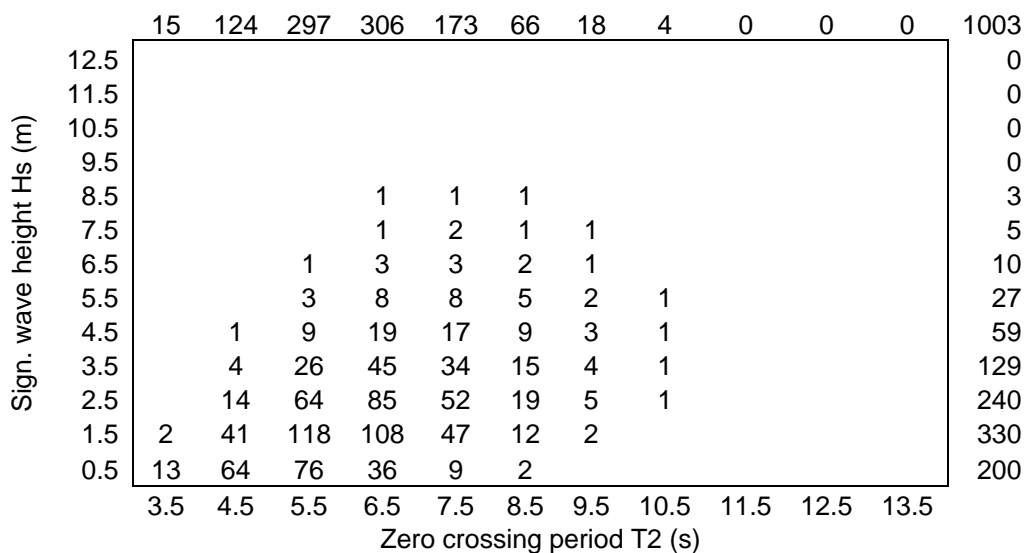


Table A.13 – Scatter diagram for the Southern part of the Chinese Sea

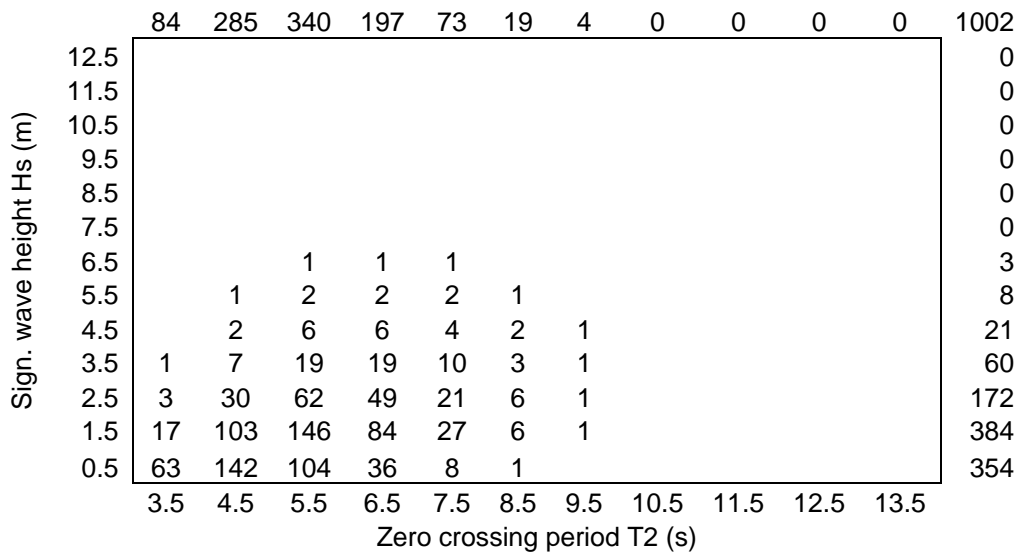


Table A.14 – Scatter diagram for the West Pacific Sea

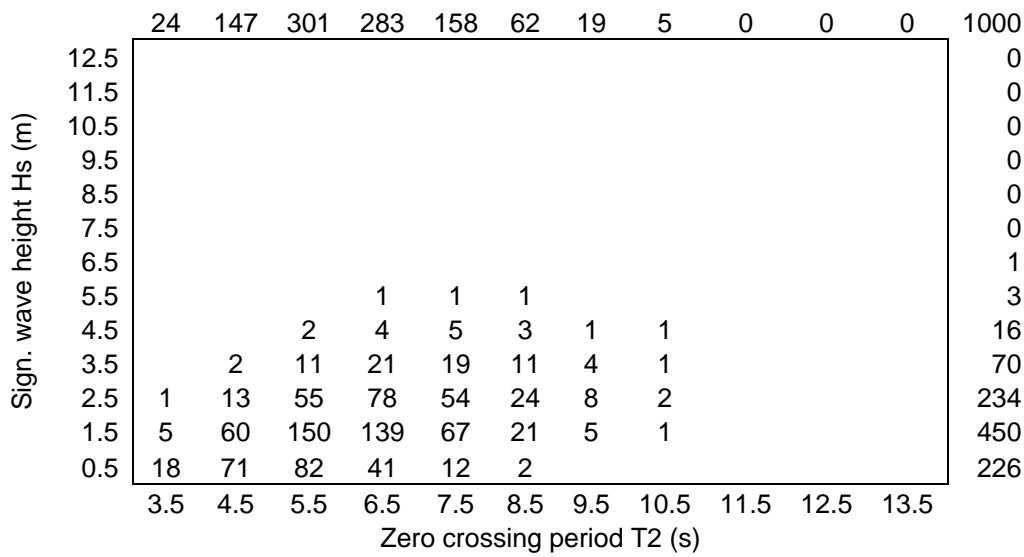


Table A.15 – Scatter diagram for the West Mediterranean Sea

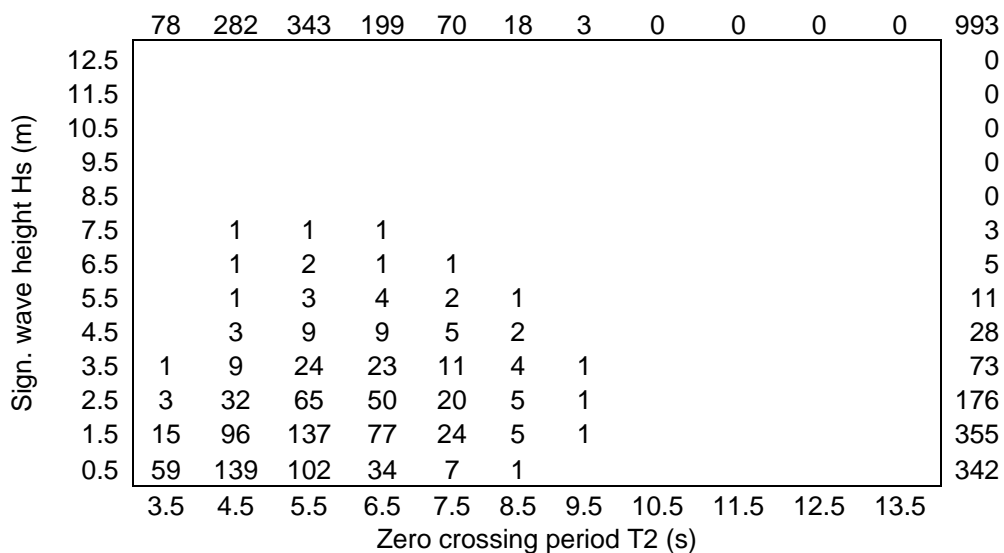
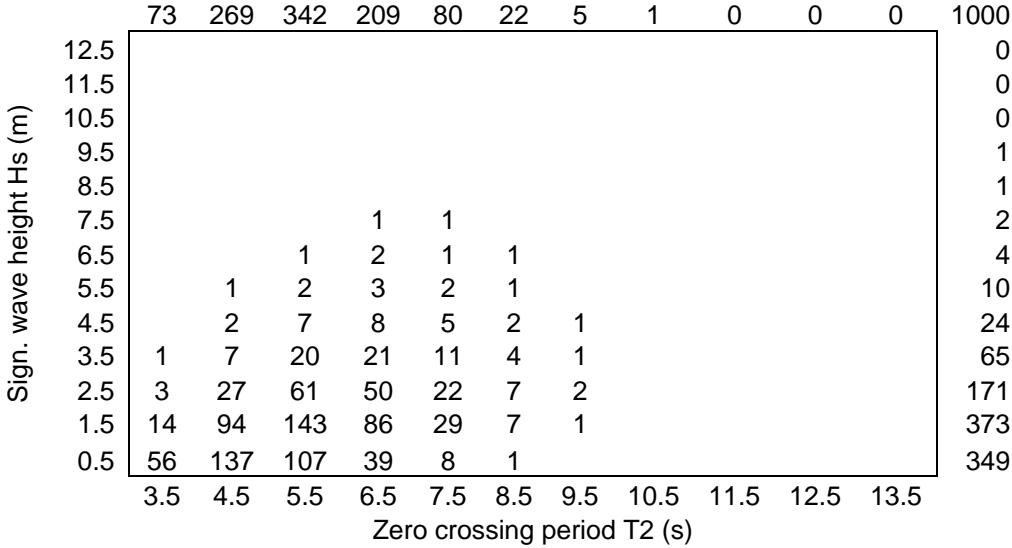


Table A.16 – Scatter diagram for the East Mediterranean Sea



Appendix B: Report from Alufastship (Spa 3007, standard operation profile)

Unit conversion

Input parameters

1 Usage profile

Required lifetime

$$L_{req} := 20 \cdot \text{yr}$$

Operating hours per year

$$Hr_{yr} := 2000 \cdot \frac{\text{hr}}{\text{yr}}$$

Total operating time in seconds

$$T_{op} := L_{req} \cdot Hr_{yr} \quad T_{op} = 144000000 \text{ s}$$

Directional distribution reduction
(on number of cycles)

$$Ddr := 0.5$$

2 Ship details for global stress range

Rule length of the ship

$$L_s := 35 \cdot \text{m}$$

Location of detail from bow

$$L_d := 13 \cdot \text{m}$$

Borders of moment envelope - Only for Lloyds
(relative length from bow)

$$l_f := 0\%$$

$$l_r := 100\%$$

Effective moment of inertia of the ship at detail location

$$I_s := 560 \cdot 10^9 \text{ mm}^4$$

Position neutral axis above base

$$h_{na} := 2000 \cdot \text{mm}$$

Position detail above base

$$h_{dt} := 5000 \cdot \text{mm}$$

3 Stress Concentration Factor

SCF as determined from FEA

$$SCF_{glo} := 1.15$$

SCF range for SCF-Life plot

$$SCF_{range} := 1..7 \quad \text{not yet implemented}$$

5 Sea-Speed conditions

Wave scatter diagram - speed matrix (6 x 6)

$$WSD_S := \begin{pmatrix} 0 & 1 & 2 & 3 & 4 & 5 \\ 30 & 0.05 & 0.00 & 0.00 & 0.00 & 0 \\ 20 & 0 & 0.75 & 0.00 & 0.00 & 0 \\ 9 & 0.00 & 0.00 & 0.20 & 0.00 & 0 \\ 0 & 0.00 & 0.00 & 0.00 & 0.00 & 0 \\ 0.00 & 0.00 & 0.00 & 0.00 & 0.00 & 0.00 \end{pmatrix}$$

Correction on waveheight (irregular waves)

$$cw := 71\%$$

6 Safety Factors

Partial safety factor on stress range (Ds)

$$\gamma_{\Delta\sigma} := 1.0$$

Partial safety factor on number of cycles (n)

$$\gamma_n := 1.0$$

Partial safety factor on S-N curve (additional)

$$\gamma_{S-N} := 1.0$$

Input parameters

☑ Moments & Wave scatter diagrams

Sum operation time
$$\text{Sum_op_tm} := \sum_{i=2}^6 \sum_{j=2}^6 \text{WSD_S}_{i,j} \quad \text{Sum_op_tm} = 1$$

Check on Sum operation time
$$f_s(\text{Sum_op_tm}) := \begin{cases} (\text{error}(\text{"Sum operation time must be unity"})) & \text{if Sum_op_tm} \neq 1 \\ \text{Sum_op_tm} & \text{otherwise} \end{cases}$$

$f_s(\text{Sum_op_tm}) = 1$

Number of wave scatter diagrams $n_WSD := \text{cols}(\text{WSD_S}) - 1 \quad n_WSD = 5$

Number of speeds $n_S := \text{rows}(\text{WSD_S}) - 1 \quad n_S = 5$

Counters $j_WSD := 1..n_WSD \quad i_S := 1..n_S$

Speed of the ship $V_Ship_{i_S} := \text{WSD_S}_{i_S+1,1} \cdot \text{knots}$

Relative operation time (WSD_S combination) $\alpha_{i_S, j_WSD} := \text{WSD_S}_{i_S+1, j_WSD+1}$

Data acquisition

Read moments from input file "DM_Vs_WSD.xls" $M :=$
(DM_Vs_WSD.)

Read WSD_1 from input file "DM_Vs_WSD.xls" $WSD_1 :=$
(DM_Vs_WSD.)

Read WSD_2 from input file "DM_Vs_WSD.xls" $WSD_2 :=$
(DM_Vs_WSD.)

Read WSD_3 from input file "DM_Vs_WSD.xls" $WSD_3 :=$
(DM_Vs_WSD.)

Read WSD_4 from input file "DM_Vs_WSD.xls" $WSD_4 :=$
(DM_Vs_WSD.)

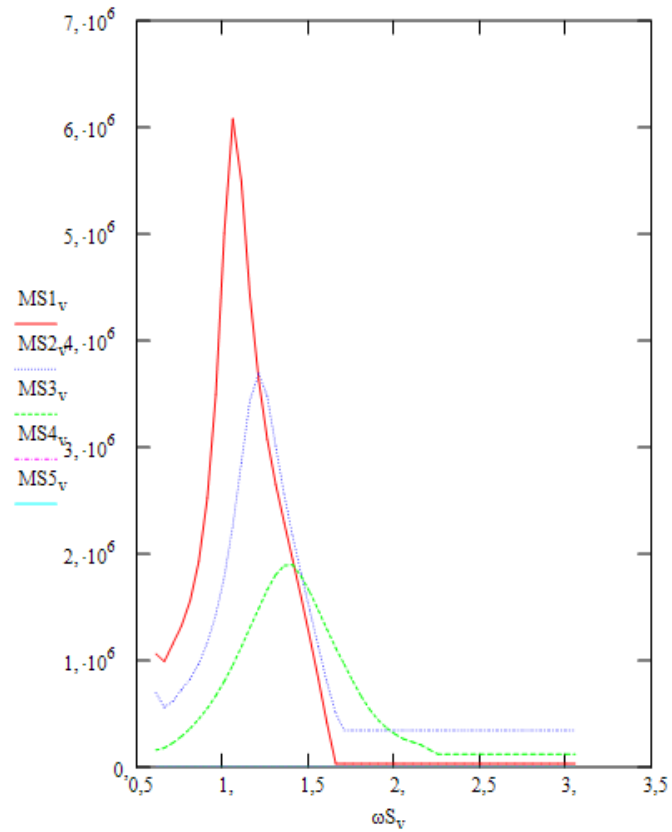
Read WSD_5 from input file "DM_Vs_WSD.xls" $WSD_5 :=$
(DM_Vs_WSD.)

Read transferfunction from file. rows(M) - 1 $\omega S_v := M_{v+1,1} \cdot \frac{\text{rad}}{\text{s}}$

$$MS1_v := M_{v+1,2} \cdot \text{kN} \cdot \frac{\text{m}}{\text{m}} \quad MS2_v := M_{v+1,3} \cdot \text{kN} \cdot \frac{\text{m}}{\text{m}} \quad MS3_v := M_{v+1,4} \cdot \text{kN} \cdot \frac{\text{m}}{\text{m}} \quad MS4_v := M_{v+1,5} \cdot \text{kN} \cdot \frac{\text{m}}{\text{m}} \quad MS5_v := M_{v+1,6} \cdot \text{kN} \cdot \frac{\text{m}}{\text{m}}$$

	1	2
1	"Omega"	30
2	0.611	1.063·10 ³
3	0.661	990.659
4	0.711	1.159·10 ³
5	0.761	1.325·10 ³
6	0.811	1.563·10 ³
7	0.861	1.928·10 ³
8	0.911	2.524·10 ³
9	0.96	3.499·10 ³
10	1.01	5.007·10 ³
11	1.06	6.082·10 ³
12	1.11	5.498·10 ³
13	1.16	4.426·10 ³
14	1.21	3.632·10 ³
15	1.26	3.077·10 ³
16	1.31	2.648·10 ³
17	1.36	2.293·10 ³
18	1.41	1.942·10 ³
19	1.459	1.59·10 ³
20	1.509	1.216·10 ³
21	1.559	828.974
22	1.609	416.839
23	1.659	33.072
24	1.709	33.072

M =

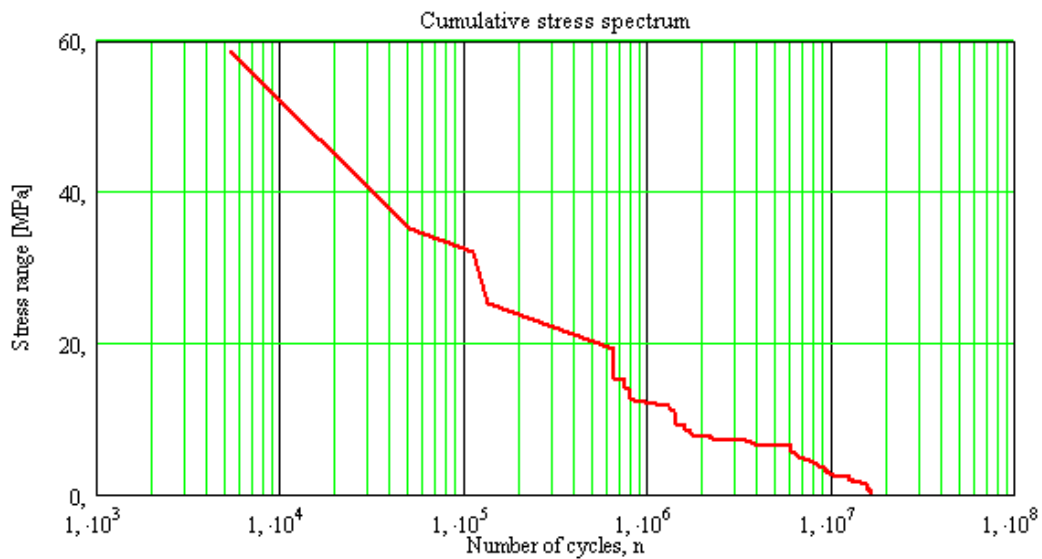
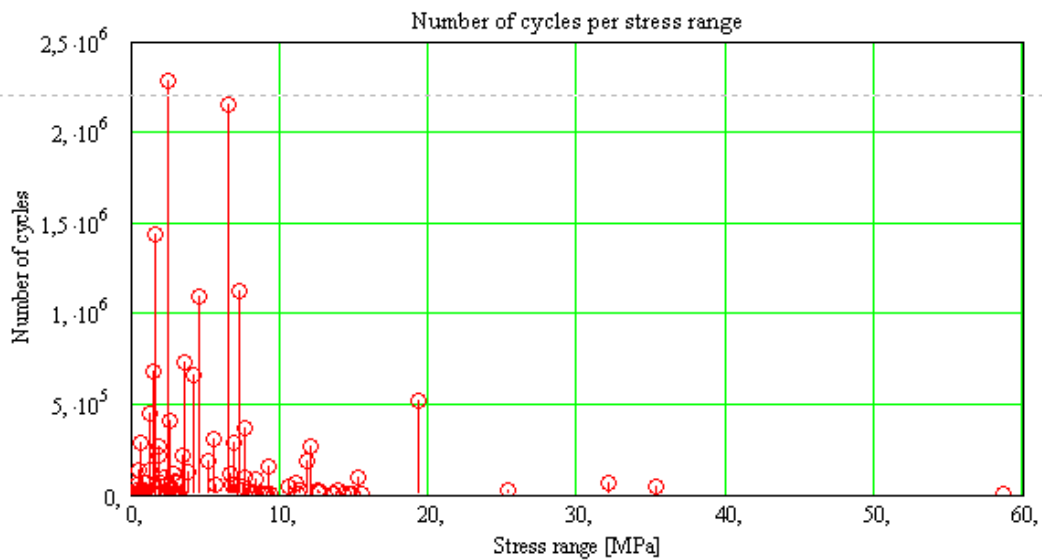


5 Analysis of stress spectrum

Reference: H:\tests\Spa 3007\not equally distributed\20 years - original\DNV-3 (Hs=2.5m)\loc2\sub_wsd_101.mcd(R)

Total number of cycles with stress levels up to $\sigma_{max} = 58.6 \text{ MPa}$

Total number of cycles $N_{c_Total} = 1.647 \times 10^7$



▶ EC 9

▶ DNV TR 97-152

▶ NEN 2063

▼ GL 2004

GL2004 code

$\Delta\sigma_C := 18 \text{ MPa}$

$m_1 := 3$

▶ Reference: H:\tests\Spa 3007\not equally distributed\20 years - original\DNV-3 (Hs=2.5m)\loc2\Miner-GL2004_102.mcd(F)

Fatigue damage in

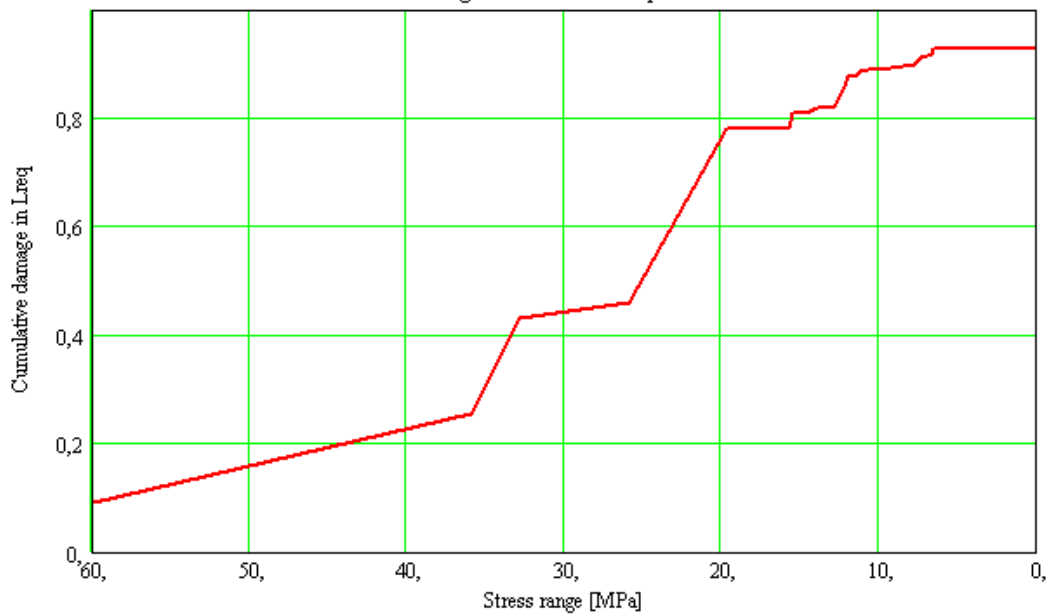
$L_{req} = 20 \text{ yr}$

$D_{totGL} = 0.928324$

Calculated life in years

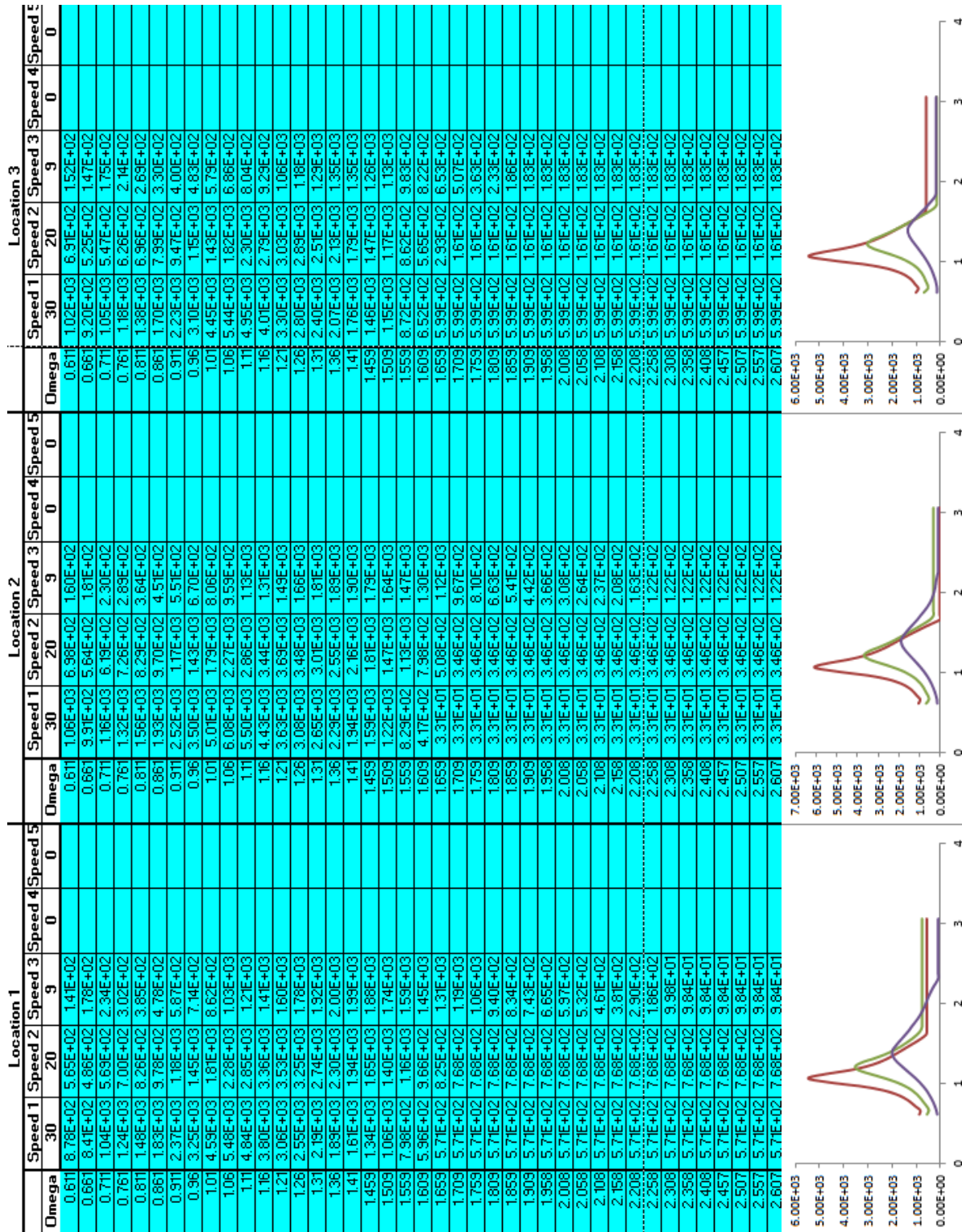
$L_{desGL} = 21.544 \text{ yr}$

Damage accumulation in spectrum






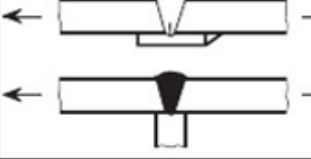
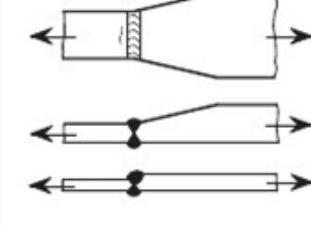

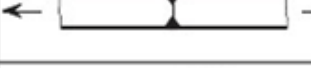
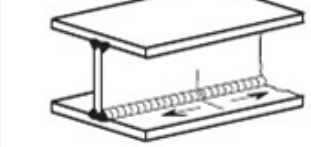
▶ GL 2004

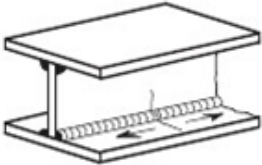
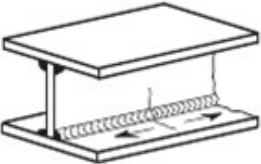
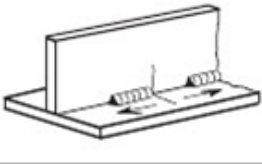
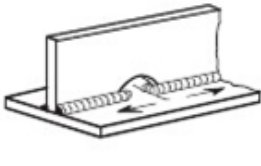
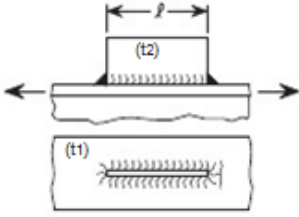
Appendix C: Standard format of Bending moments for Alufastship

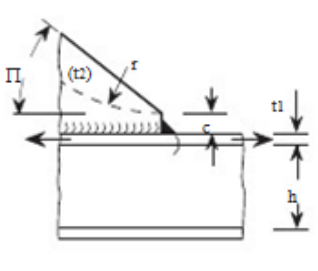
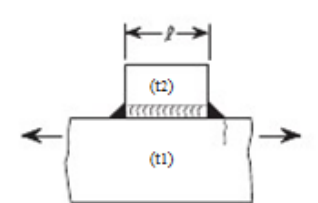
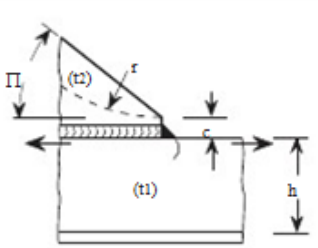
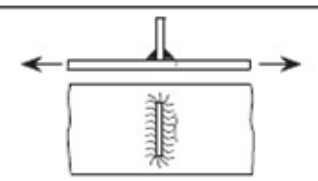
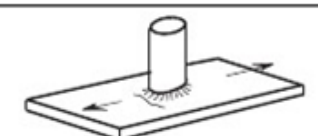


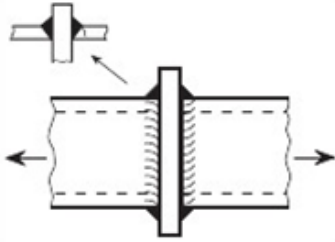
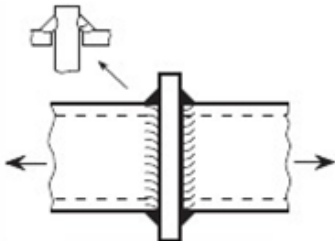
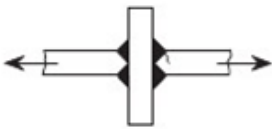
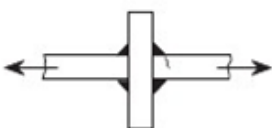
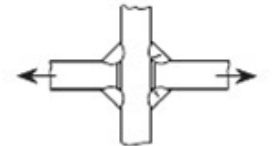
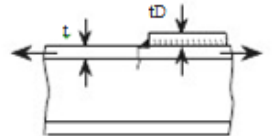
* Current hull girder bending moments were achieved for Spa 3007.

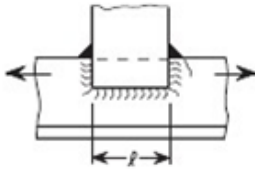
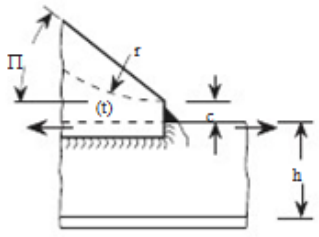
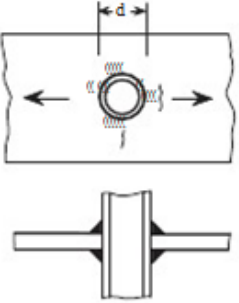
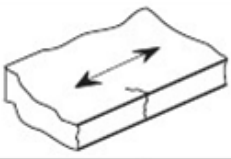

Appendix D: Catalogue of details

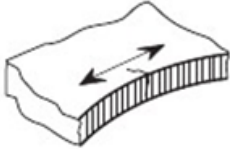
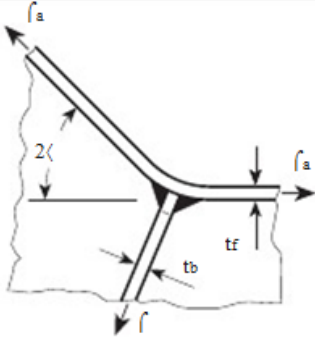
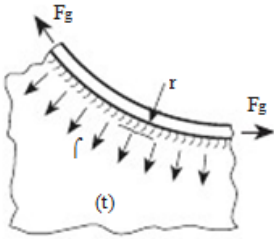
Type No.	Joint configuration showing mode of fatigue cracking and stress \hat{f} considered	Description of joint	Detail category $\Delta\sigma_R$	
			Steel	Al
1		Transverse butt weld ground flush to plate, 100 % NDT (Non-Destructive Testing)	125	50
2		Transverse butt weld made in shop in flat position, max. weld reinforcement 1 mm + 0,1 · weld width, smooth transitions, NDT	100	40
3		Transverse butt weld not satisfying conditions for joint type No. 2, NDT	80	32
4		Transverse butt weld on backing strip or three-plate connection with unloaded branch	71	25
5		<p>Transverse butt welds between plates of different widths or thickness, NDT</p> <p>as for joint type No. 2, slope 1 : 5 as for joint type No. 2, slope 1 : 3 as for joint type No. 2, slope 1 : 2</p> <p>as for joint type No. 3, slope 1 : 5 as for joint type No. 3, slope 1 : 3 as for joint type No. 3, slope 1 : 2</p> <p>For the third sketched case the slope results from the ratio of the difference in plate thicknesses to the breadth of the welded seam. Additional bending stress due to thickness change to be considered, see also B.1.3.</p>	<p>100 90 80</p> <p>32 28 25</p>	<p>32 28 25</p> <p>25 22 20</p>
6		<p>Transverse butt welds welded from one side without backing bar, full penetration root controlled by NDT not NDT</p> <p>For tubular profiles \square \hat{f}_R may be lifted to the next higher detail category.</p>	71 45	28 18
7		Partial penetration butt weld; the stress is to be related to the weld throat sectional area, weld overfill not to be taken into account	45	16
8		Continuous automatic longitudinal fully penetrated butt weld without stop/start positions (based on stress range in flange adjacent to weld)	125	50

Type No.	Joint configuration showing mode of fatigue cracking and stress f considered	Description of joint	Detail category $\Delta\sigma_R$	
			Steel	Al
9		Continuous automatic longitudinal fillet weld without stop/start positions (based on stress range in flange adjacent to weld)	100	40
10		Continuous manual longitudinal fillet or butt weld (based on stress range in flange adjacent to weld)	90	36
11		Intermittent longitudinal fillet weld (based on stress range in flange at weld ends) In presence of shear τ in the web, the detail category has to be reduced by the factor $(1 - \Delta\tau/\Delta\sigma)$, but not below 36 (steel) or 14 (Al).	80	32
12		Longitudinal butt weld, fillet weld or intermittent fillet weld with cut outs (based on stress range in flange at weld ends) If cut out is higher than 40 % of web height	71	28
		In presence of shear τ in the web, the detail category has to be reduced by the factor $(1 - \Delta\tau/\Delta\sigma)$, but not below 36 (steel) or 14 (Al). Note For Ω -shaped scallops, an assessment based on local stresses is recommended.	63	25
13		Longitudinal gusset welded on beam flange, bulb or plate:		
		$l < 50 \text{ mm}$	80	28
		$50 \text{ mm} < l < 150 \text{ mm}$	71	25
		$150 \text{ mm} < l < 300 \text{ mm}$	63	20
		$l > 300 \text{ mm}$	56	18
		For $t_2 < 0,5 t_1$, $\Delta\sigma_R$ may be increased by one category, but not over 80 (steel) or 28 (Al); not valid for bulb profiles. When welding close to edges of plates or profiles (distance less than 10 mm) and/or the structural element is subjected to bending, $\Delta\sigma_R$ is to be decreased by one category.		

Type No.	Joint configuration showing mode of fatigue cracking and stress σ considered	Description of joint	Detail category $\Delta\sigma_R$	
			Steel	Al
14		<p>Gusset with smooth transition (sniped end or radius) welded on beam flange, bulb or plate; $c < 2 t_2$, max. 25 mm</p> <p>$r > 0,5 h$ $r < 0,5 h$ or $\varphi < 20^\circ$ $\varphi > 20^\circ$ see joint type 13</p> <p>For $t_2 < 0,5 t_1$, $\Delta\sigma_R$ may be increased by one category; not valid for bulb profiles.</p> <p>When welding close to the edges of plates or profiles (distance less than 10 mm), $\Delta\sigma_R$ is to be decreased by one category.</p>	71 63	25 20
15		<p>Longitudinal flat side gusset welded on plate or beam flange edge</p> <p>$l < 50 \text{ mm}$ $50 \text{ mm} < l < 150 \text{ mm}$ $150 \text{ mm} < l < 300 \text{ mm}$ $l > 300 \text{ mm}$</p> <p>For $t_2 < 0,7 t_1$, $\Delta\sigma_R$ may be increased by one category, but not over 56 (steel) or 20 (Al).</p> <p>If the plate or beam flange is subjected to in-plane bending, $\Delta\sigma_R$ has to be decreased by one category.</p>	56 50 45 40	20 18 16 14
16		<p>Longitudinal flat side gusset welded on plate edge or beam flange edge, with smooth transition (sniped end or radius); $c \leq 2 t_2$, max. 25 mm</p> <p>$r > 0,5 h$ $r < 0,5 h$ or $\varphi < 20^\circ$ $\varphi > 20^\circ$ see joint type 15</p> <p>For $t_2 < 0,7 t_1$, $\Delta\sigma_R$ may be increased by one category.</p>	50 45	18 16
17		<p>Transverse stiffener with fillet welds (applicable for short and long stiffeners)</p>	80	28
18		<p>Non-load-carrying shear connector</p>	80	28

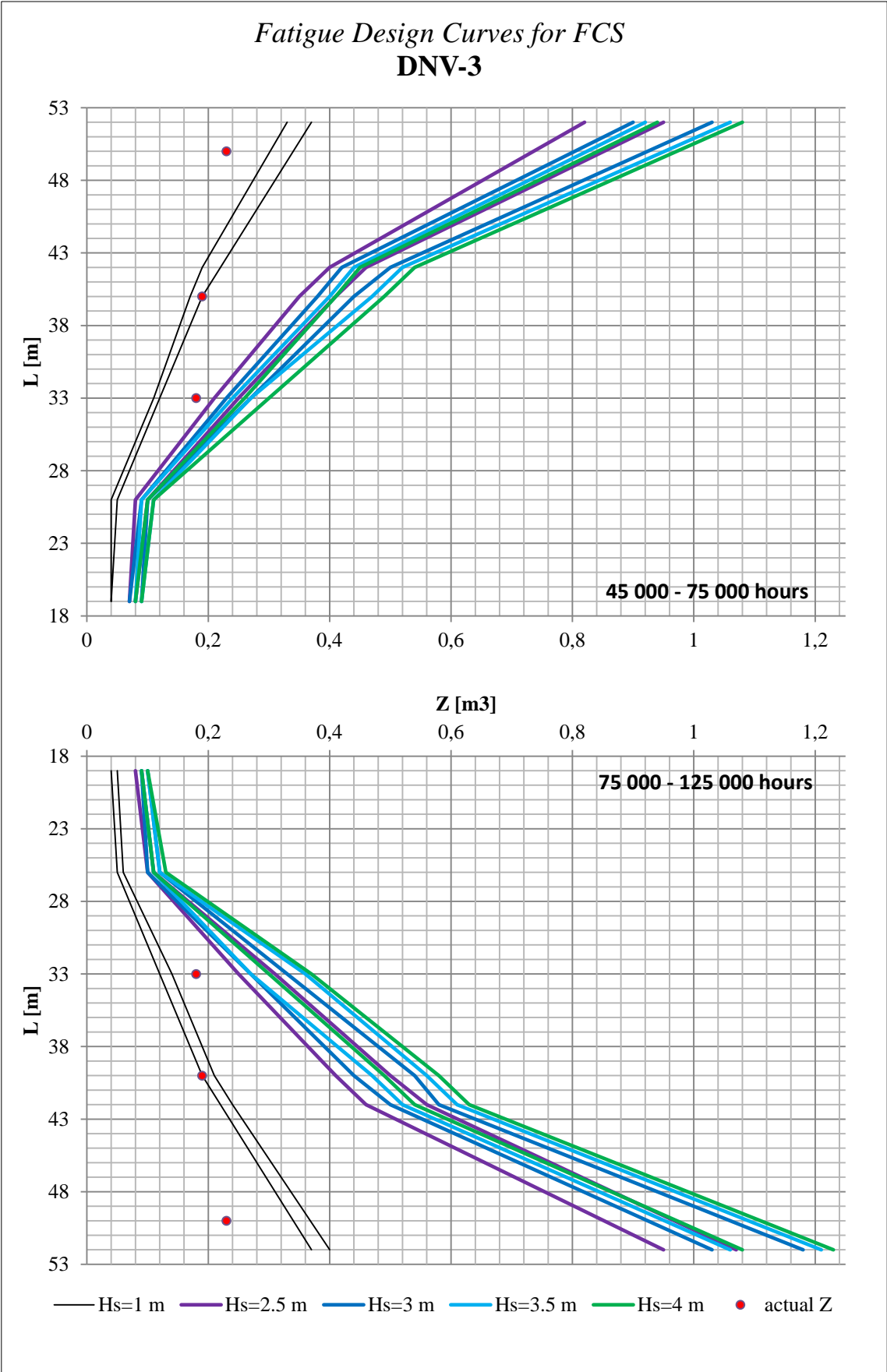
Type No.	Joint configuration showing mode of fatigue cracking and stress σ considered	Description of joint	Detail category $\Delta\sigma_R$	
			Steel	Al
19		Full penetration weld at the connection between a hollow section (e.g. pillar) and a plate, for tubular section for rectangular hollow section	56 50	20 18
20		Fillet weld at the connection between a hollow section (e.g. pillar) and a plate, for tubular section for rectangular hollow section The stress is to be related to the weld sectional area.	45 40	16 14
21		Cruciform or tee-joint K-butt welds with full penetration or with defined incomplete root penetration according to Fig. 19.9. cruciform joint tee-joint	71 80	25 28
22		Cruciform or tee-joint with transverse fillet welds, toe failure (root failure particularly for throat at thickness $a < 0,7 t$, see joint type 23) cruciform joint tee-joint	63 71	22 25
23		Welded metal in transverse load-carrying fillet welds at cruciform or tee-joint, root failure (based on stress range in weld throat), see also joint type No. 22	45	16
24		End of long doubling plate on beam, welded ends (based on stress range in flange at weld toe) $t_D < 0,8 t$ $0,8 t < t_D < 1,5 t$ $t_D > 1,5 t$ The following features increase $\Delta\sigma_R$ by one category accordingly: – reinforced ends according to Fig. 19.4 – weld toe angle $< 30^\circ$ – length of doubling $< 150 \text{ mm}$	56 50 45	20 18 16

Type No.	Joint configuration showing mode of fatigue cracking and stress σ considered	Description of joint	Detail category $\Delta\sigma_R$	
			Steel	Al
25		<p>Fillet welded non-load-carrying lap joint welded to longitudinally stressed component.</p> <ul style="list-style-type: none"> - to bulb section or flat bar - to angle section <p>For $l > 150$ mm, $\Delta\sigma_R$ has to be decreased by one category, while for $l < 50$ mm, $\Delta\sigma_R$ may be increased by one category.</p> <p>If the component is subjected to bending, $\Delta\sigma_R$ has to be reduced by one category.</p>	56 50	20 18
26		<p>Fillet welded lap joint with smooth transition (sniped end with $\phi < 20^\circ$ or radius) welded to longitudinally stressed component.</p> <ul style="list-style-type: none"> - to bulb section or flat bar - to angle section <p>$c < 2t$, max. 25 mm</p>	56 50	20 18
27		<p>Continuous butt or fillet weld connecting a pipe penetrating through a plate</p> <p>$d < 50$ mm $d > 50$ mm</p> <p><i>Note</i> For large diameters an assessment based on local stress is recommended.</p>	71 63	25 22
28		<p>Rolled or extruded plates and sections as well as seamless pipes, no surface or rolling defects</p>	160 ($m_0 = 5$)	71 ($m_0 = 5$)
29		<p>Plate edge sheared or machine-cut by any thermal process with surface free of cracks and notches, cutting edges broken or rounded. Stress increase due to geometry of cut-outs to be considered</p>	140 ($m_0 = 4$)	40 ($m_0 = 4$)

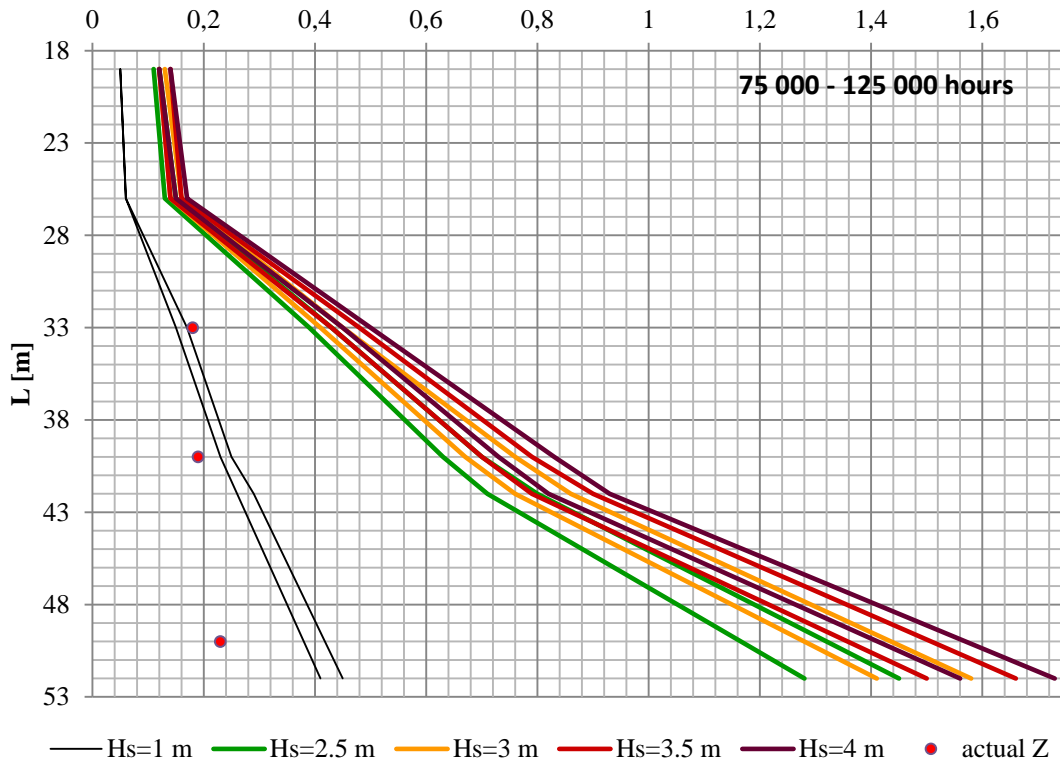
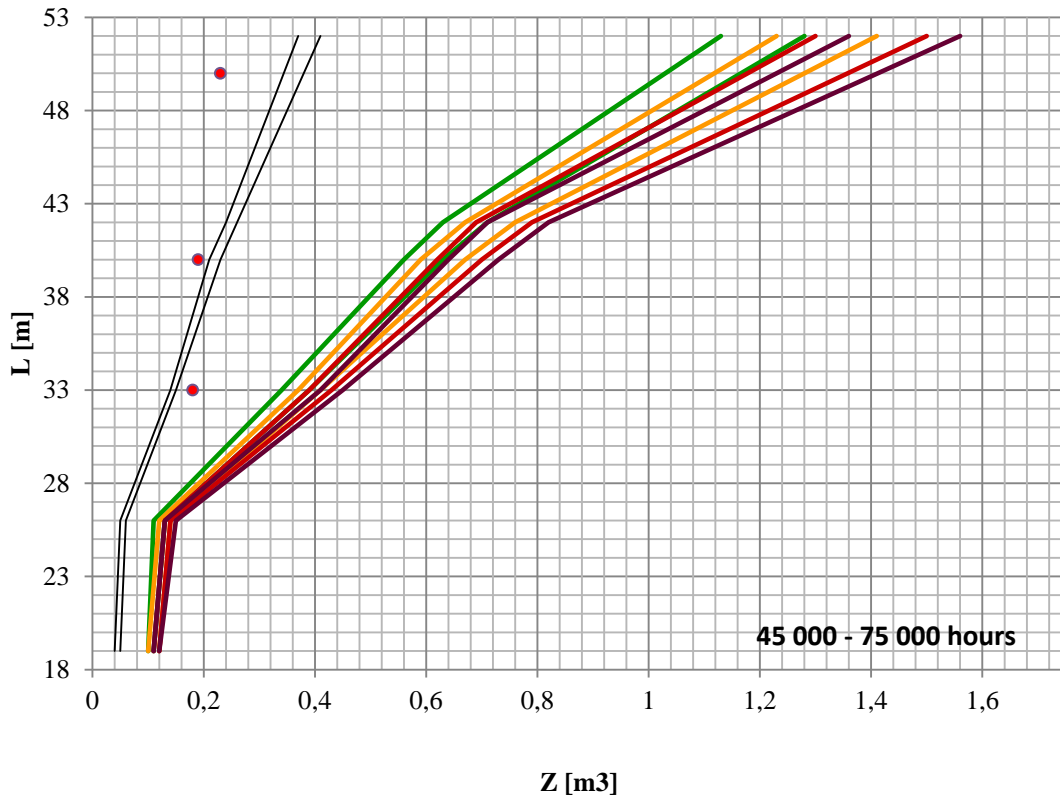
Type No.	Joint configuration showing mode of fatigue cracking and stress f considered	Description of joint	Detail category $\Delta\sigma_R$	
			Steel	Al
30		<p>Plate edge not meeting the requirements of type 29, but free from cracks and severe notches.</p> <p>Machine cut or sheared edge:</p> <p>Manually thermally cut:</p> <p>Stress increase due to geometry of cut-outs to be considered.</p>	<p>125 ($m_0 = 3,5$)</p> <p>100 ($m_0 = 3,5$)</p>	<p>36 ($m_0 = 3,5$)</p> <p>32 ($m_0 = 3,0$)</p>
31		<p>Joint at stiffened knuckle of a flange, to be assessed according to type 21, 22 or 23, depending on the type of joint. The stress in the stiffener at the knuckle can normally be calculated as follows:</p> $\sigma = \sigma_2 \frac{t_f}{t_b} 2 \sin \alpha$	—	—
32		<p>Unstiffened flange to web joint, to be assessed according to type 21, 22 or 23, depending on the type of joint. The stress in the web is calculated using the force F_g in the flange as follows:</p> $\sigma = \frac{F_g}{r \cdot t}$ <p>Furthermore, the stress in longitudinal weld direction has to be assessed according to type 8 – 10. In case of additional shear or bending, also the highest principal stress may become relevant in the web, see B.1.4.</p>	—	—

Partly based on Recommendations on Fatigue of Welded Components, reproduced from IIW document XIII-1539/96 / XV-845/96, by kind permission of the International Institute of Welding.

Appendix E: Fatigue Design curves

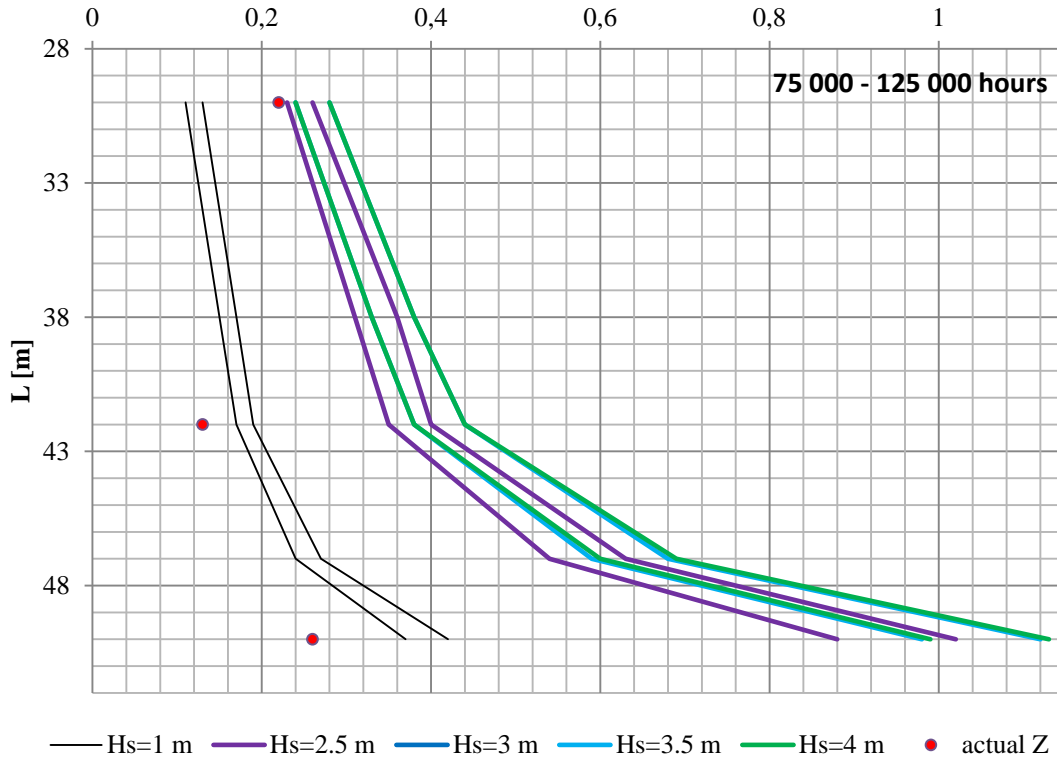
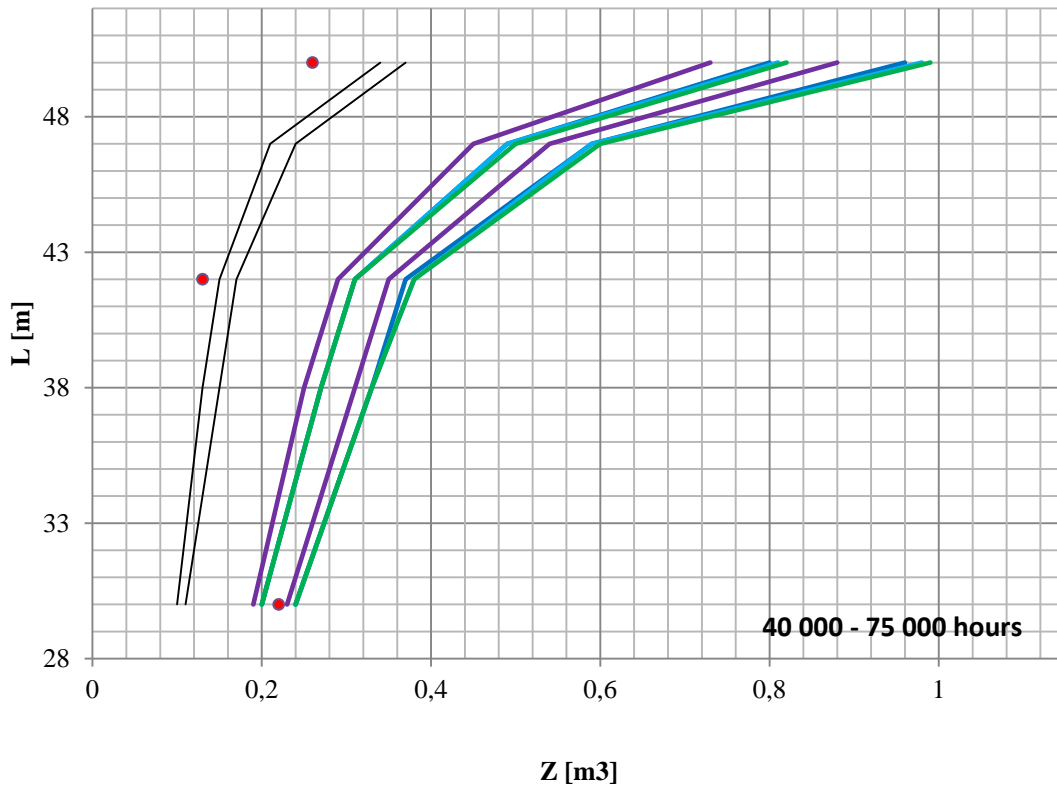


Fatigue Design Curves for FCS Gulf of Mexico

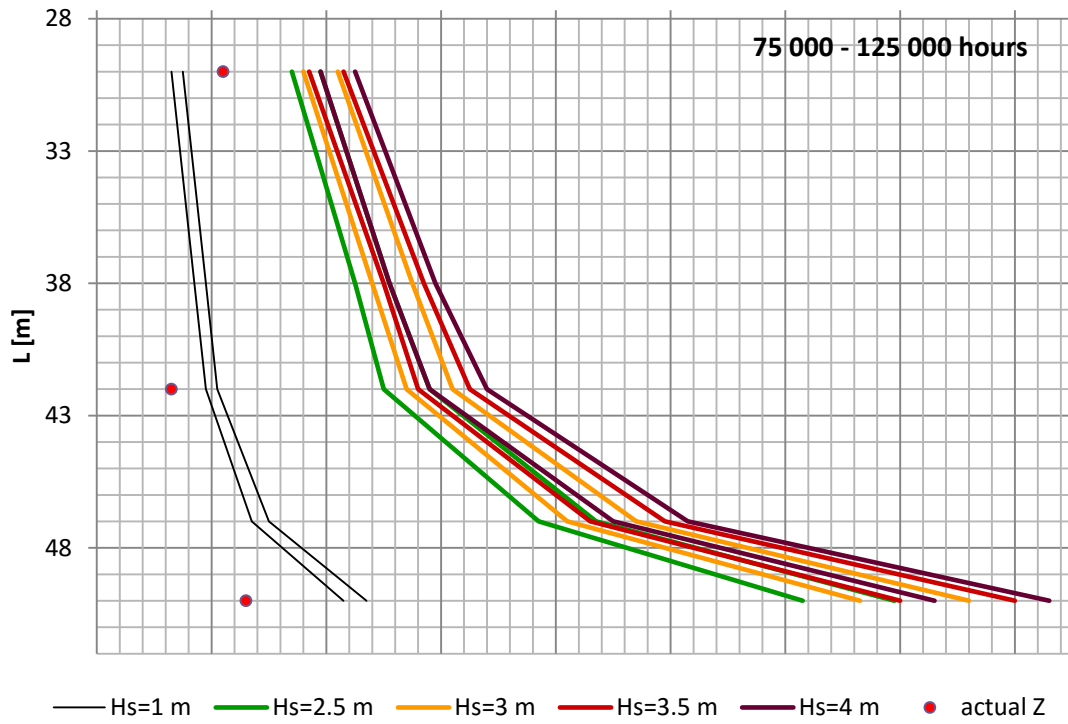
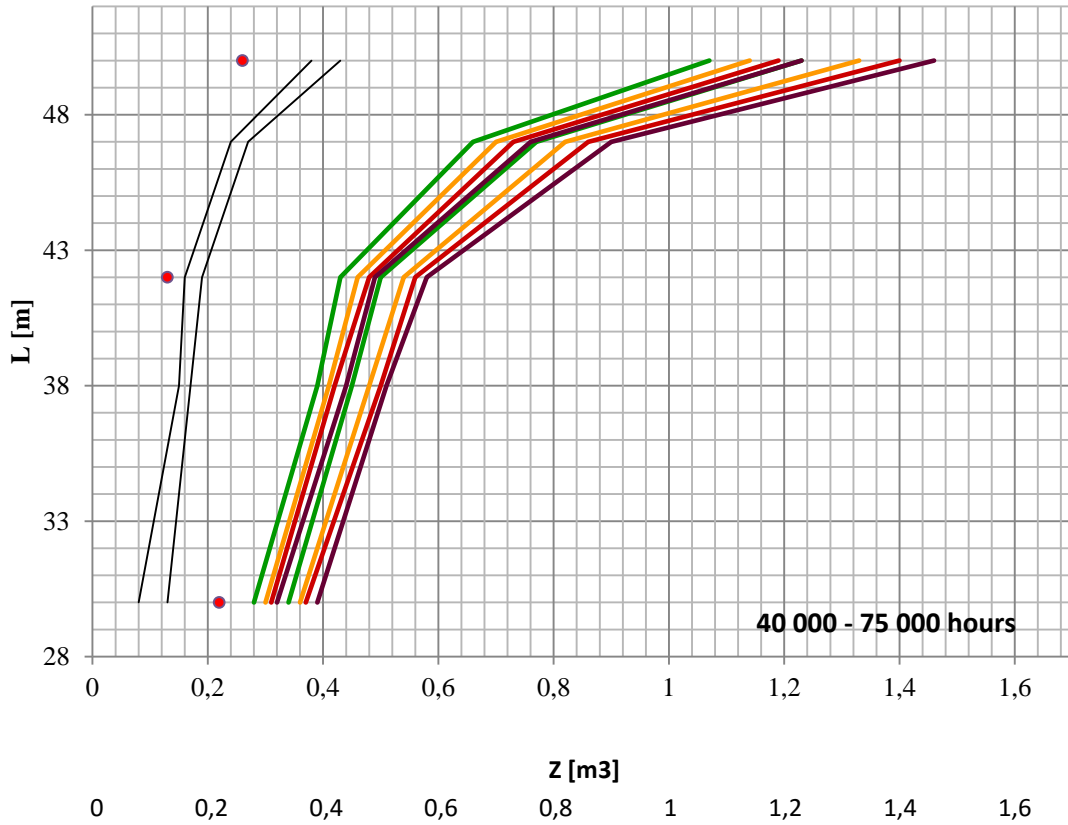


— $H_s=1$ m — $H_s=2.5$ m — $H_s=3$ m — $H_s=3.5$ m — $H_s=4$ m • actual Z

Fatigue Design Curves for SPa DNV-3



Fatigue Design Curves for SPa Gulf of Mexico



Appendix F: Comparison of dominating wave length and vessel length in two areas

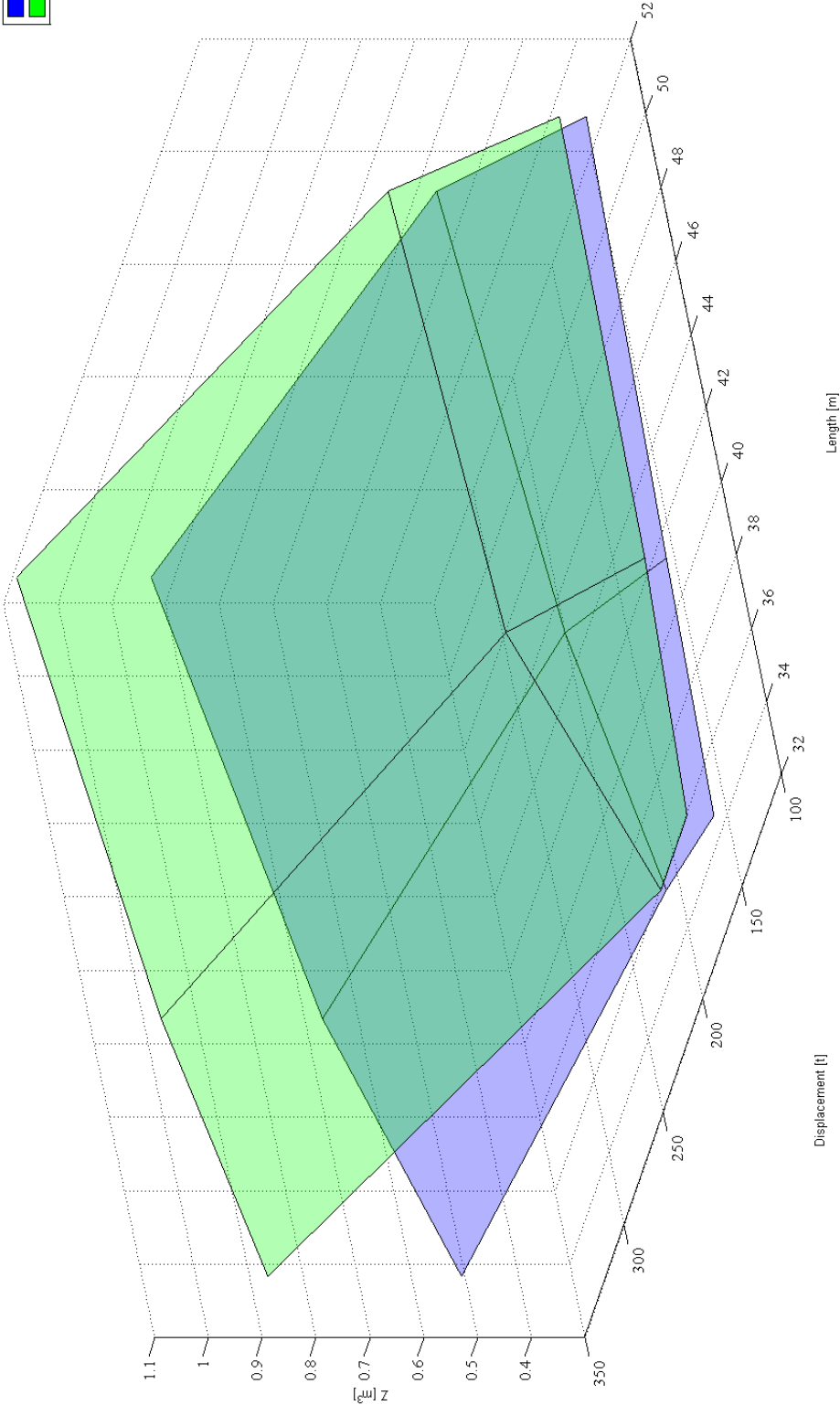
Table F.1– Results of wave length and number of occurrence for corresponded wave period at North Sea

<i>NORTH SEA</i>		
<i>Wave period (T), [s]</i>	<i>Wave length (λ), [m]</i>	<i>Number of occurrence</i>
1.5	3.5	0
3.5	19.1	22
4.5	31.6	157
5.5	47.3	306
6.5	66.0	255
7.5	87.9	116
8.5	112.9	38
9.5	141.0	8
10.5	172.2	2
11.5	206.6	0
12.5	244.1	0
13.5	284.7	0

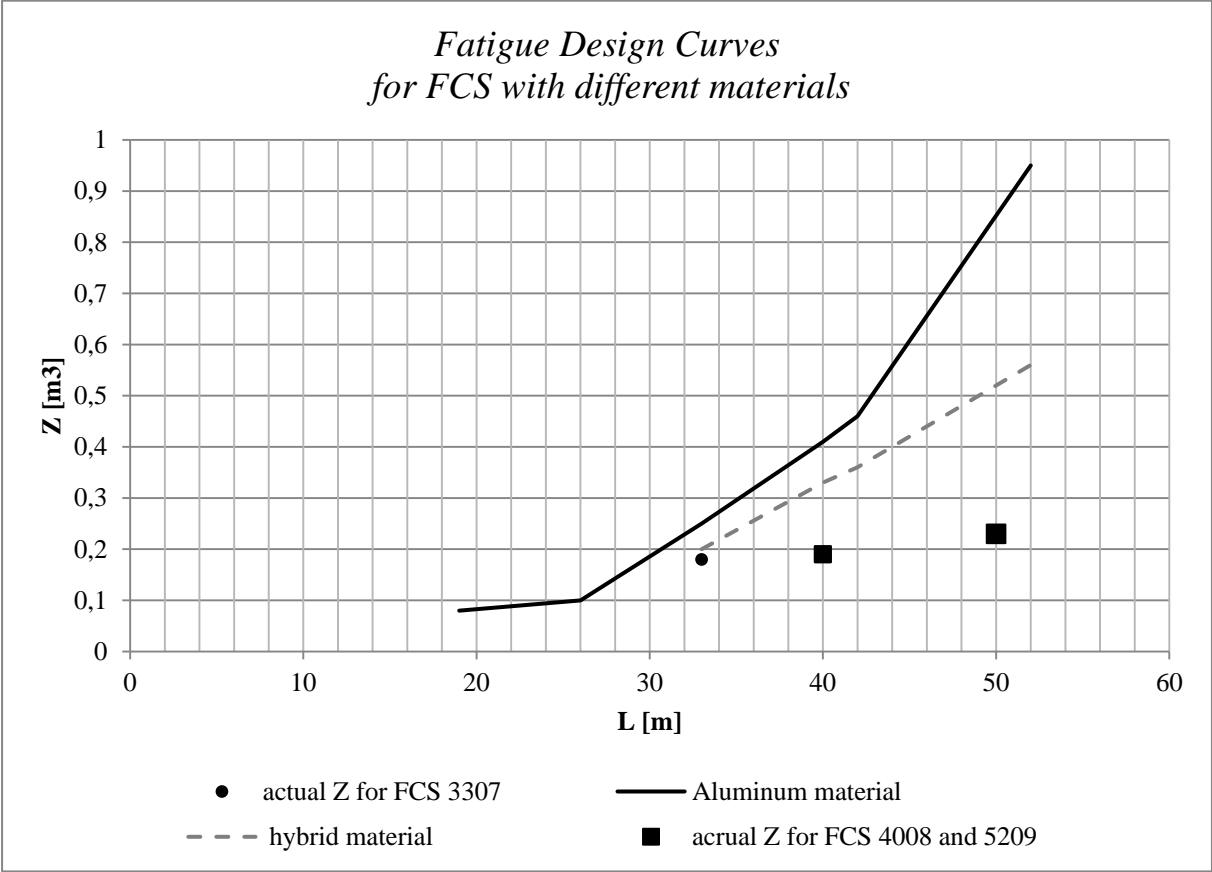
Table F.2 – Results of wave length and number of occurrence for corresponded wave period at N-Arabian Sea

<i>N-Arabian Sea</i>		
<i>Wave period (T), [s]</i>	<i>Wave length (λ), [m]</i>	<i>Number of occurrence</i>
1.5	3.5	0
3.5	19.1	132
4.5	31.6	336
5.5	47.3	309
6.5	66.0	139
7.5	87.9	40
8.5	112.9	9
9.5	141.0	1
10.5	172.2	0
11.5	206.6	0
12.5	244.1	0
13.5	284.7	0

Appendix G: 3D fatigue curve



Appendix H: The fatigue design curve with aluminum and hybrid construction materials



* Based on the standard operational profile for FCS

Appendix I: Effect of Wave Periods on a response spectrum in heave

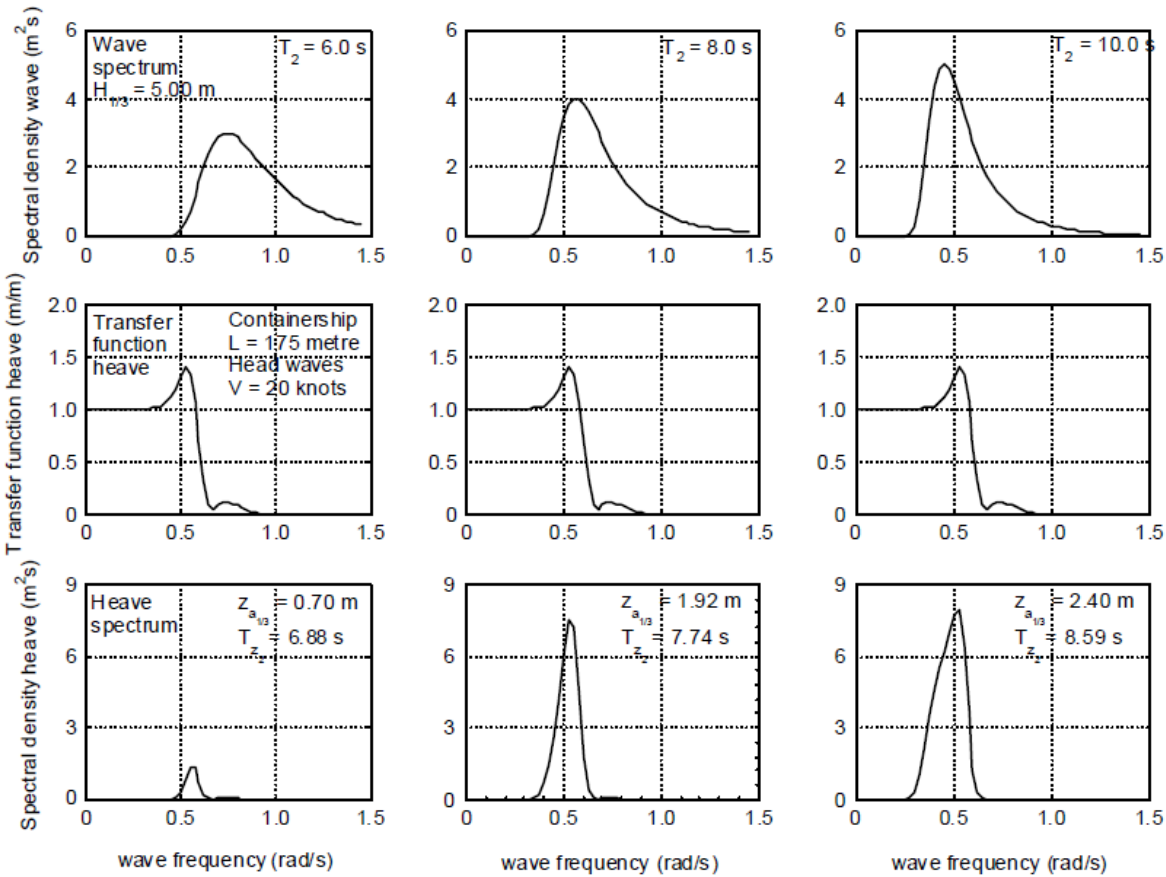


Figure I.1 – example of response spectrum in heave affected by periods from chapter 8 in (Journee & Massie, 2001). As a tested vessel, a 175 meter container ship sailed at 20 knots in head waves with 5.0 m significant wave height

Appendix J: Vertical bending moments for FCS 3307

Table J.1– Vertical bending moments for FCS 3307 at 8 knots

Encounter frequency	Wave frequency	Frame 2	Frame 4	Frame 6	Frame 8	Frame 10	Frame 12	Frame 14	Frame 16	Frame 18	Frame 20	Frame 22	Frame 24	Frame 26	Frame 28	Frame 30	Frame 32	
		My	My	My	My	My	My	My	My	My	My	My	My	My	My	My	My	My
[r/s]	[r/s]	[kNm/m]	[kNm/m]	[kNm/m]	[kNm/m]	[kNm/m]	[kNm/m]	[kNm/m]	[kNm/m]	[kNm/m]	[kNm/m]	[kNm/m]	[kNm/m]	[kNm/m]	[kNm/m]	[kNm/m]	[kNm/m]	[kNm/m]
0.692	0.56	54.17	78.62	83.6	81.16	82.38	91.87	104.8	113.5	112.8	100.2	76.81	51.73	31.21	15.11	4.845	0.5404	
0.777	0.617	32.73	44.06	54.2	78.35	111.9	145.2	170.9	184	181.5	162.8	130.2	92.54	57.87	28.8	9.303	0.6343	
0.864	0.674	24.8	40.64	73.7	121.2	171.8	216.3	248.1	262.1	255.6	228.6	184.6	133	83.82	42.23	13.79	0.8609	
0.955	0.731	31.06	55.77	103.4	167.3	233.4	290.6	330.5	347.3	338	302.8	246	178.5	112.7	56.97	18.77	1.217	
1.048	0.788	39.01	74.66	140	224.5	310.1	383	432.8	452.4	438.6	392.7	320.3	233.4	147.5	74.91	24.98	1.822	
1.144	0.845	54	102.8	187.7	296.9	407.4	501	564.2	587.8	568.1	507.3	413.4	301.2	190.1	96.46	32.45	2.713	
1.242	0.901	65.47	132	245.4	387.4	529.3	648.4	727.6	755.6	727.7	647.1	524.7	380.2	238.5	120.5	40.65	3.854	
1.344	0.958	77.77	165.1	311.6	491.8	670.6	819.8	918.3	952	914.9	811.4	655.4	472.3	293.8	146.9	49.45	5.454	
1.448	1.015	89.91	201	385.3	608.6	828.9	1012	1133	1173	1126	997.3	804	578	358.2	177.7	59.38	7.141	
1.554	1.072	101	238.9	465.4	736.4	1003	1223	1368	1415	1357	1200	966.2	693.5	429.3	213	70.93	9.031	
1.664	1.129	110.1	275.9	545.3	865	1178	1437	1606	1660	1589	1403	1126	805.8	497.2	246.2	82.18	10.6	
1.776	1.186	115.9	309.2	620.7	987.4	1345	1640	1831	1889	1805	1587	1268	901.8	552.2	270.8	89.39	11.92	
1.891	1.243	117.2	335.9	686.5	1096	1495	1822	2032	2093	1994	1746	1387	979.4	594.6	288.5	94.06	12.78	
2.009	1.3	112.5	351.6	733.5	1178	1610	1963	2187	2248	2133	1858	1466	1026	616.2	294.9	94.58	13.06	
2.129	1.357	100.1	351.4	753.1	1220	1672	2040	2271	2328	2200	1905	1490	1032	611.5	287.8	90.42	12.66	
2.252	1.413	78.44	330.3	735.2	1206	1663	2034	2263	2315	2177	1872	1450	991.3	578.4	266.9	81.89	11.74	
2.378	1.47	47.4	285.1	673.3	1129	1572	1933	2155	2201	2062	1760	1349	910.6	522.4	236	70.78	10.63	
2.506	1.527	9.053	217.7	568.9	989.4	1405	1747	1959	2005	1875	1593	1211	808.1	456.7	202.6	59.89	9.717	
2.637	1.584	32.96	135	431	802.5	1181	1500	1706	1760	1653	1404	1064	705.6	395.3	173.6	51.47	9.162	
2.771	1.641	72.91	56.57	278.6	595.3	934.9	1234	1439	1511	1435	1228	934.6	620.3	347.3	152.7	46.03	8.855	
2.908	1.698	107.5	65.39	125.7	388.8	692.5	976	1186	1280	1241	1077	828.1	554.2	312.6	138.9	43	8.806	
3.047	1.755	133.5	132	131.01	213.2	485	754.7	969.6	1086	1079	954.6	744.9	504.8	288.2	130.1	41.56	8.95	
3.189	1.812	150.3	187.4	124.5	126.8	341.3	588.4	800.4	929.7	948.3	855.2	678.2	466.2	270.2	124.4	41.04	9.179	
3.334	1.869	170.7	243.5	230.4	204.7	311.1	509.1	701.1	827.8	856.4	781.6	627	436.1	256.1	119.9	40.49	9.276	
3.482	1.926	154.5	231.5	238.2	222.4	284.8	428.4	586.8	702	739.2	687.8	563	399.6	239.2	114	39.03	9.095	
3.632	1.982	141.6	221.6	240.3	212.8	207.2	296.7	434	551	609.3	590.6	500.9	366.3	224.5	108.8	37.7	8.985	
3.785	2.039	127.7	195.6	212.9	186.9	146.9	172.1	278.7	396.9	478.3	493.6	439.2	332.6	209	103.2	36.58	9.206	
3.94	2.096	118.4	164.6	164.7	139.1	99.18	72.17	140.3	253.3	351.7	398.7	379.3	301	195.4	98.85	35.98	9.505	
4.099	2.153	116.7	141.1	106.6	74.86	86.18	73.97	34.62	127.5	243.5	319.4	330	275.5	184.9	95.99	36.08	10.22	
4.26	2.21	122	138.2	70.29	39.29	133.4	165.1	121.2	75.19	171	264.5	294.7	257.6	178	94.44	36.45	10.9	
4.424	2.267	129.7	154.4	97.39	98.77	199.7	252.2	221.4	143.8	154.6	237.9	274.4	243.6	171.5	92.29	36.12	10.91	
4.59	2.324	135.2	174.5	142.1	155.1	250.5	311.5	289.6	208.3	172	227.8	261.9	231.5	162.9	87.35	34.02	10.57	
4.76	2.381	136.3	187.2	173	189.4	276.7	340.2	325.9	247.1	188.4	218.5	246.5	213.3	142.6	77.59	31.29	10	
4.931	2.438	131	180.3	167.4	175.3	245.9	300	288.1	217.5	153.6	174	208	188.6	127.5	66.79	28.11	9.495	
5.106	2.495	125.2	160.9	134.4	134.2	183.9	205.2	173.6	108	50.37	78.1	124.7	134.6	104.8	60	26.61	9.943	
5.284	2.551	125.6	153.8	124.9	141.5	181.4	162.5	83.97	5.615	49.75	36.94	51.53	89.8	88.44	58.3	28.83	11.15	
5.464	2.608	129.5	160.8	147.3	189.2	231	197	114.7	113	143	101.2	14.86	67.98	86.76	62.49	31.46	12.07	
5.647	2.665	132.5	171.1	175.7	234	280.5	248.1	182.5	190	207.8	151.9	60.62	75.56	92.48	65.19	31.38	11.84	
5.832	2.722	132.2	175.2	187.4	245.9	290.6	262	204.8	214.5	225.4	164.1	74.62	80.65	91.2	61.54	28.56	11.45	
6.02	2.779	125.4	162.5	169.8	216.2	247.3	217.6	169.7	185.7	192.9	136.8	56.71	68.52	77.44	51.53	24.97	11.62	

Table J.2– Vertical bending moments for FCS 3307 at 28 knots

Encounter frequency	Wave frequency	Frame 2	Frame 4	Frame 6	Frame 8	Frame 10	Frame 12	Frame 14	Frame 16	Frame 18	Frame 20	Frame 22	Frame 24	Frame 26	Frame 28	Frame 30	Frame 32	
		My	My	My	My	My	My	My	My	My	My	My	My	My	My	My	My	My
[r/s]	[r/s]	[kNm/m]	[kNm/m]	[kNm/m]	[kNm/m]	[kNm/m]	[kNm/m]	[kNm/m]	[kNm/m]	[kNm/m]	[kNm/m]	[kNm/m]	[kNm/m]	[kNm/m]	[kNm/m]	[kNm/m]	[kNm/m]	[kNm/m]
1.021	0.56	570	1005	1316	1518	1620	1635	1569	1432	1235	997.9	740.2	494.4	290.9	141.8	50.63	12.42	
1.176	0.617	445.7	792.2	1048	1225	1329	1365	1334	1237	1079	874.1	643.9	427.1	249.9	120.9	41.76	9.752	
1.341	0.674	328.9	596.3	810	977.6	1100	1172	1188	1139	1021	840.7	619.7	407.5	236.9	113.1	36.85	6.841	
1.515	0.731	371.3	667.8	904.6	1095	1241	1338	1374	1342	1232	1046	794.4	528.9	305.1	142.7	43.33	4.642	
1.699	0.788	431.1	767.6	1034	1252	1426	1547	1602	1577	1465	1267	995.1	689.7	404.9	190.1	58.23	3.677	
1.892	0.845	532.1	940.5	1262	1525	1737	1887	1956	1926	1786	1541	1211	851.8	517	246	76.16	5.199	
2.095	0.901	700.2	1234	1652	1993	2265	2454	2535	2482	2285	1951	1512	1047	631.4	305	94.76	6.676	
2.307	0.958	973.5	1727	2320	2801	3177	3429	3521	3422	3122	2636	2013	1371	810.3	383.4	119.7	14.42	
2.529	1.015	1336	2410	3275	3974	4506	4840	4931	4746	4279	3566	2681	1793	1038	479.6	146.5	21.06	
2.76	1.072	1488	2746	3795	4647	5278	5646	5707	5431	4830	3961	2922	1911	1078	483.4	144.1	24.55	
3.001	1.129	1234	2347	3313	4108	4688	5009	5033	4745	4167	3365	2438	1562	859.2	375.6	111.6	22.79	
3.252	1.186	928.7	1828	2645	3329	3829	4101	4111	3854	3355	2680	1919	1212	657.4	285.2	87.74	20.84	
3.511	1.243	703	1435	2129	2723	3162	3402	3415	3196	2772	2203	1569	987.3	535	234.7	76.22	20.02	
3.781	1.3	542.9	1143	1732	2247	2635	2853	2875	2697	2340	1860	1327	837.4	457.1	204.3	69.27	19.37	
4.06	1.357	438.8	919.6	1397	1820	2146	2337	2369	2233	1948	1557	1119	712.5	393.7	179.3	62.82	18.86	
4.348	1.413	378.2	737.7	1082	1393	1645	1812	1865	1787	1585	1288	940.8	609.3	342.6	159.2	57.6	18.53	
4.646	1.47	381.8	647.9	843.4	1002	1142	1260	1331	1329	1232	1044	790.4	528.4	305.5	144.9	54.41	17.95	
4.954	1.527	429.5	656	723.6	693.5	658.1	699.2	808	908.8	937.2	863.2	695.9	487.7	292.7	145.5	55.59	18.15	
5.27	1.584	499.1	744.7	768	609.1	331	132.2	406.7	668.3	811.7	815.8	694.1	504.3	311	157.4	62.01	20.06	
5.597	1.641	572	873.8	938.1	810.9	581	433.3	564.9	787.5	920.2	913.5	779	568.8	353.4	181.3	73.45	25.76	
5.933	1.698	659.9	1058	1232	1236	1152	1038	1099	1187	1205	1106	904.5	646.2	395.4	200	78.82	25.07	
6.278	1.755	435.9	678.7	782.6	796.4	800.3	859.6	991.6	1126	1196	1222	945.9	644.9	382.6	188.1	72.61	23.06	
6.633	1.812	734.2	1242	1556	1717	1784	1811	1818	1781									

FATIGUE TOOL SENSITIVITY ANALYSIS AND DESIGN CURVES

Kateryna Tymofieienko

Norwegian University of Science and Technology
Department of Maritime Technology and Operations
Alesund, 6005, Møre og Romsdal, Norway
tym.postbox@hotmail.com

ABSTRACT

The paper looks at the fatigue tool sensitivity analysis and design curves for aluminum high speed crafts. Spectral fatigue method developed by Det Norske Veritas was used to achieve the objective. As only limited initial data was available, the preliminary fatigue analysis was relevant to be conducted in order to receive a minimum required section modulus of a hull section. This parameter impacts the fatigue lifetime and was used as a comparative value in current study.

To summarize, the results showed behavior of a minimum required section modulus influenced by different parameters while several other findings were made during the study. All of them are described in the Sensitivity analysis and Fatigue design curves sections. Finally, this paper contains recommendations that may facilitate better design results.

INTRODUCTION

One of the main requirements for high speed crafts is light weight which is absolutely feasible due to use of aluminum as a primary material for hull structures. However, such sensitive structure is exposed to higher operational stress levels and thus to reduced structural redundancy. Therefore, the fatigue strength of aluminum vessels is approximately one-third of the construction steel. Furthermore, fatigue cracks in the vessel structures normally have a self-limiting nature. That is why the fatigue design of many structures in the vessel that are very critical to dynamic loads is a very challenging task and requires accuracy in prediction of the fatigue lifetime.



Fig. 1: An aluminum high speed supply vessel

Damen has already been engaged into the fatigue analysis of aluminum hulls for more than 15 years. During these years several developments have taken place (within and outside Damen) in the analysis procedure and questions have been raised about prediction accuracy and input parameters for the analysis. Therefore, an internal research project was initiated to investigate these aspects.

The first objective was to conduct a sensitivity analysis for one of the high speed crafts designed in Damen and indicate which vessel details are most prone to the fatigue failure. The second objective was to develop fatigue design curves for the range of vessels designed in Damen. A specific objective was to assess the accuracy of the fatigue lifetime prediction based on the results of these curves.

Structurally, the report contains a short introduction which is given above. The next part is dedicated to the basic knowledge about fatigue and common locations of crack initiation. The methodology part covers description of the spectral method developed by DNV and the implemented method in actual calculating procedure. Next section presents results and discussion of the sensitivity analysis and fatigue design curves. Finally, conclusion summarizes up all the findings of the research.

BASIC KNOWLEDGE ABOUT FATIGUE AND COMMON LOCATIONS OF CRACK INITIATION

A process of accumulative damage due to repetitive loading application of a structure at stresses well below yield stress is defined as a fatigue. The important feature of the fatigue is that the applied loads do not cause immediate crash of the structure. Instead, over a number of cyclic loads, the accumulative damage reaches the critical level that causes the fatigue failure [1].

The most common places where the fatigue initiation occurs are locations with high ratio of dynamic to static load, for example, high load application with low frequency or low load application with high frequency. Secondly, at the locations of stress concentration, such as holes, changes of section, discontinuous welded structures with different plate thickness etc. [2]. So, attention should be paid to make smooth

geometrical transitions and locate weld joints outside of the highest stress consecration areas.

The picture below shows the most common reasons and damages occurring in high speed crafts.

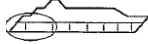



Aft ship	Hull general	Fore ship	Superstructure
			
Damages	Damages	Damages	Damages
- Cracks - Corrosion	- Cracks - Corrosion - Buckling	- Cracks - Corrosion - Buckling	- Cracks - Loosening of windows
Loads / factors	Loads / factors	Loads / factors	Loads / factors
- Vibrations - Cyclic loads - Galvanic currents	- Cyclic bending - Cyclic sea loads - Humid environment	- Cyclic sea loads - Slamming loads - Contact - Humid environment	- Global Deflections

Fig.2: Common damages and main influencing factors [3]

The need for the fatigue analysis of aluminum fast crafts therefore is of high priority both from safety and maintenance points of view [4].

SPECTRAL METHOD

The fatigue design is usually performed by the methods based on the fatigue tests and estimation of the cumulative damage. In this project the spectral method developed by DNV was selected as it allows calculating long term stress from the assumed wave climate. The spectral method implies simultaneous appearance of different load effect areas retained during the calculations. Thus, this method indicates a significant reduction of uncertainties as compared with other methods [5].

In general, this method is based on the theory of stochastic process for response calculation. For a specific sea state, the spectrum of stress response is defined as a combination of the wave spectrum ($S_x(\omega)$) with the transfer function (1), which expresses the relation between heading and frequency. The transfer function ($T(\omega)$) may be defined by the time history approach [6].

$$S_y(\omega) = |T(\omega)|^2 \cdot S_x(\omega) \quad (1)$$

The long term distribution of stress ranges due to variable amplitude loading may be defined through a short term Rayleigh distribution for a particular sea state (2).

$$\Delta\sigma = \Delta\sigma_{100} \cdot \left(1 - \frac{\log N}{\log N_{100}}\right)^k \quad (2)$$

where $\Delta\sigma_{100}$ is the stress range summomed by 100 year wave;
 N – the total number of years;
 N_{100} – total number of waves during 100 years.

When the long term stresses are defined, the fatigue damage for one-slope S-N curve may be calculated [5]. S-N curve is a plot representing the relation of the fatigue life versus constant cyclic stress amplitude S . The basic design S-N curve is given as:

$$\log N = \log \bar{a} - m \cdot \log \Delta\sigma \quad (3)$$

where $\log \bar{a}$ is the intercept of curve with $\log N$ axis;

m – negative inverse slope;

$\Delta\sigma$ – stress range.

In some materials, such as ferrous alloys, S-N curve begins to flatten out and this means that σ_e failure will never occur below certain endurance limit. However, aluminum is a material with no existed fatigue limit [7].

Using S-N data, the cumulative damage (the development of fatigue damage under the repeated fluctuating loads) can be calculated by the Miner-Palmgren formula (4).

$$D = \sum_{i=1}^k \frac{n_i}{N_i} \quad (4)$$

where k – number of stress blocks;

n_i – number of stress cycles in stress block i with constant stress range;

N_i – number of cycles to failure at constant stress range [8].

In case damage D is larger than 1, the design is not acceptable and should be modified [9].

OVERVIEW AND WORK FLOW FOR FATIGUE ANALYSIS

In general, at the design stage only limited initial data is available, so preliminary fatigue analysis (PFA) is relevant to conduct. The main target of this analysis is to calculate the minimum required section modulus at the particular cross sections of the vessel. This parameter impacts the fatigue lifetime and was used as a comparative value in current study.

The calculation is conducted in 2 programs: Seaway Octopus and Alufastship. The first program is based on the strip theory and allows measurement of the hull girder bending moments due to encountered waves for each location in the vessel. The desired bending moments RAO are acquired for a vertical plane (combination of heave and pitch motions) and are produced in regular waves, speed, wave frequency relative to 1m significant wave height. Basically, the output from “Seaway” is the transfer function – one of the input parameters for Alufastship program.

Other input parameters necessary for fatigue calculation in Alufastship are as follows:

- The wave scatted diagram;
- Usage profile (the operational lifetime, operating hours per year and sailing directions);
- Speeds and time spent for particular speed in combination with wave height and wave period;
- Structural parameters (initial moment of inertia, location of neutral axis and stress concentration factor);
- Safety factor.

Having obtained the data, spectral analysis may be launched carried out by several iterations in order to receive an appropriate moment of inertia and, finally, the required section modulus (Z).

SENSITIVITY ANALYSIS

The achieved value of the required section modulus is very sensitive to different input parameters. Thus, the sensitivity analysis will give the insight of how variable parameters influence the fatigue lifetime and which of them affects the most.

As a test vessel for this analysis the Stan Patrol 3007 was selected and as analyzed locations three frames were defined, as seen in the figure below.

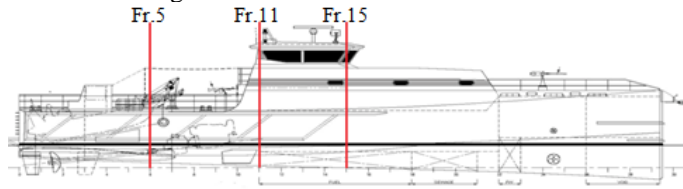


Fig.3: General layout SPa 3007 with locations for the sensitivity analysis

Frame 5 was selected due to presence of the slipway; at frame 11 the highest calculated bending moment was identified. Frame 15 contains a superstructure and it was selected to get an idea of the section modulus sufficiency.

All tests were carried out based on the standard operational profile (see Appendix A). Input parameters which are included there were decided to test for sensitivity. They are as follows:

- Weight distribution;
- Speed;
- Service conditions;
- Wave height constraint;
- Operating area;
- Intended service period and sailing hours per year.

As the operation areas, 16 seas were considered in addition to the standard one, namely DNV-3. They are: the North Sea; South Brazil; Nigeria; North Brazil; the Gulf of Mexico; Angola; the North Arabian Sea; the Red Sea; the Bengal Sea; the Persian Gulf; the South Chinese Sea; the North Chinese Sea; the West Mediterranean Sea; the East Mediterranean Sea and the West Pacific Sea. Current areas were selected to investigate, because most customers in Damen require them for these types of vessels.

Overall, conducting the first test for the mentioned three frames, results for frame 11 were the highest. For example, a minimum required section modulus for 4m limiting wave height in the North Sea is 0.22m^3 while for frame 5 and 15 the value is 0.21m^3 and 0.19m^3 respectively, as seen in the figure below.

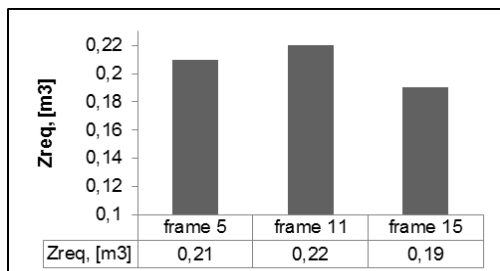


Fig.4: Results of Z for 3 frames in North Sea and 4m wave height

Therefore, it may be concluded that the largest hull girder bending moment makes the frame the weakest for fatigue for these types of vessels. That is why all subsequent tests on the sensitivity analysis were carried out for only frame 11.

Second test showed how the results are sensitive to the operating areas and wave heights. As it is evident from the figure below, Z grows with increasing significant wave height, but the growth rate is unique for each operational area and it depends primarily on dominating wave periods, wave length and operability of the vessel. So, the largest values of Z for 4m wave height were achieved in the N-Arabian Sea (0.39m^3), while the lowest values were for the South Brazil Sea (0.16m^3).

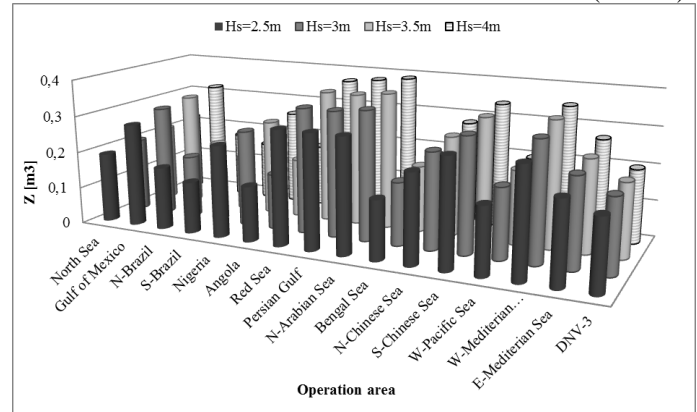


Fig.5: Results of Z for frame 11

With respect to the impact of different operating areas on the minimum required section modulus, additional analysis showed that seemingly modest areas like the N-Arabian Sea can be more dangerous for the fatigue lifetime of a vessel than the North Sea due to several reasons.

Although the North Sea contains higher waves (up to 9.5m), in preliminary analysis the wave height is limited (2,5m or 3m or 3.5m or 4m) which means that all waves above selected one are removed from the scatter diagram. This results in large portion of cut waves in the North Sea.

Moreover, the remaining total number of occurrence waves at a specific wave length was calculated as a summation of waves for each wave period. The length of the vessel is 30m and the wave length (in current study the water was considered as deep) was calculated for a corresponding wave period (T) by the following formula:

$$\lambda = \frac{g}{2\pi} \cdot T^2 \quad (5)$$

The results plotted in Fig. 6 below show that the dominating wave length is located around ship length in the N-Arabian Sea which corresponds to the dominating wave period 4.5 seconds while in the North Sea the dominating wave length does not coincide with the vessel length. This means that while operating in the N-Arabian Sea the vessel is in the resonance with wave length in pitch, which entails higher forces (bending moments) and leads to faster occurrence of fatigue cracks.

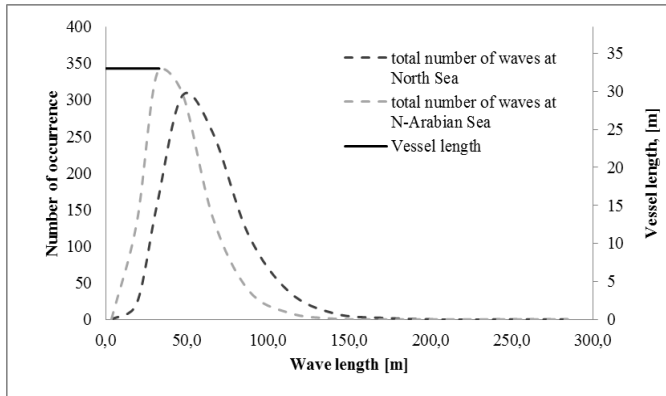


Fig.6: Comparison of dominating wave length and vessel length in two areas

Furthermore, the coincidence of the dominating wave period in the wave energy spectrum with the dominating period of the transfer function in heave also causes resonance and results in higher forces and an additional requirement to increase the strength. In order to lower the response of the vessel, it is proposed to lengthen or shorten the vessel length to a safe value.

Returning to the sensitivity analysis, the following test was conducted in order to finally evaluate which input parameter is the most significant. So, each input parameter was increased independently from others by a constant value, namely 25% and the results are as follows.

Table 1 Results of Z for final evaluation

No	Input parameter	Original value	New value	Z, [m ³]
1	Original	----	----	0,37
2	Intended service condition	20 [years]	25 [years]	0,4
3	Time at top speed	5 [% of time]	6,25 [%t]	0,39
4	Time at average speed	75 [% of time]	93,75 [%t]	0,38
5	Top speed	30 [kn]	37,5 [kn]	0,43
6	Average speed	20 [kn]	25 [kn]	0,43
7	Vessel length	30 [m]	37,5 [m]	0,42
8	Displacement	94 [t]	117,5 [t]	0,42

This vivid example (Fig. 7) definitely shows that speed influences fatigue lifetime most of all. Next significant parameters (in the descending order) are the vessel length and displacement, but these two parameters were increased manually and such rough modification cannot provide accurate results. Less important parameters are intended service period and time spent at the top speed. However, increased intended service period till 25 years is a rational upper limit for such vessels but time spent at the top speed can be increased by 4 times or even more and thus, this parameter and speed will influence the fatigue time most of all. Finally, time spent at an average speed and intended service periods provide the least influence.

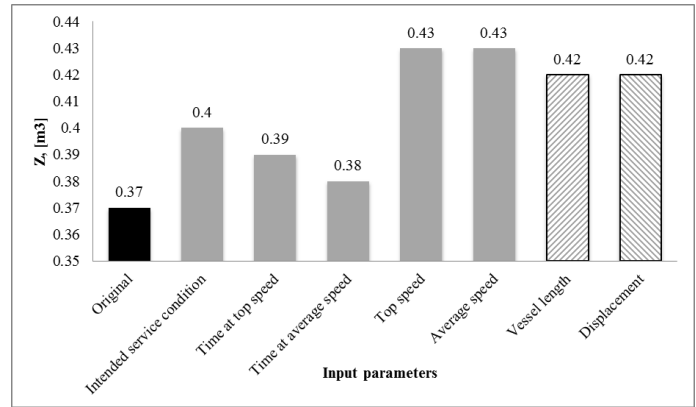


Fig.7: Results of Z for final evaluation for frame 11 at DNV-3

FATIGUE DESIGN CURVES

The main target of creating the fatigue design curves was to help engineers at the design stage to make a proper selection regarding main particles of the vessel for a specific operational profile or an individual customer's requirement. In addition, such curves can help to identify any dependency between input parameters and minimum required section modulus.

For this purpose, 11 high speed crafts were investigated where six of them were Fast Crew Suppliers (FCS) and the rest were the Stan Patrol (SPa). All of them are assumed to be made of aluminum only. The curves for FCS and SPa were performed separately. Tests for achieving Z at these curves were carried out based on the standard operational profile (see Appendix A). All fatigue design curves showed behavior of the minimum required section modulus influenced by different parameters. Curves include point of actual section modulus for already built aluminum vessel, FCS 3307 ($Z_{actual}=0.18m^3$). Vessels larger 40 meters are made of hybrid material, which means steel hull and aluminum superstructure and thus separate curve for them was created.

To summarize, the fatigue design curves were performed of two types:

- Fatigue curves with variable operational profile and constant service conditions;
- Fatigue curves with variable engine power.

Based on the results achieved in the sensitivity study, for the first type of the curves several mostly influenced variable parameters have been selected as multi-axes for the fatigue design curves; one of these axes was the length of the vessel. Current curves cover the total sailing period from 45000h (for FCS)/40000h (for SPa) till 125000h for both types. All curves contain lines with achieved Z for 1m limiting wave height (in order to understand the lower wave influence) and for limiting wave height specified in the standard requirement (2.5m for FCS and 3.5m for SPa). These curves were designed for two operational areas with different wave behavior, DNV-3 and the Gulf of Mexico. Curves for FCS are represented in the figures below and for SPa in Appendix B.

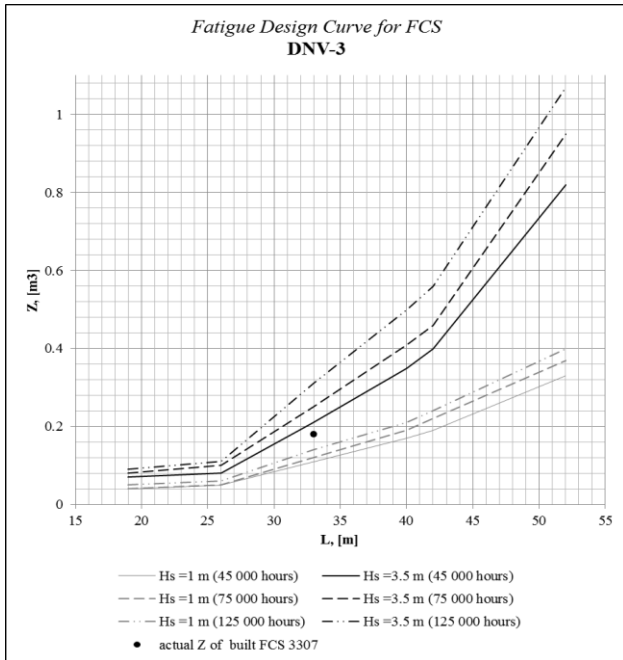


Fig.8: Fatigue design curve for FCS at DNV-3 with variable operational profile and constant service conditions

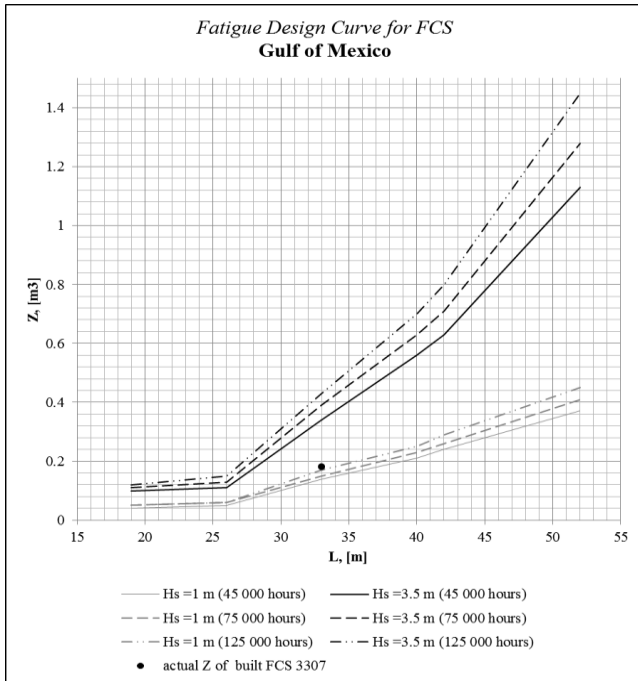


Fig.9: Fatigue design curve for FCS at Gulf of Mexico with variable operational profile and constant service conditions

The results showed a dramatic increase of minimum required section modulus with the growth of the vessel length. In addition, curves showed large difference in Z with actual and minimum required parameters for aluminum vessel FCS 3307, namely 0.07m^3 . In order to figure out if the same trend follows for hybrid vessels (FCS 4008 and FCS 5209) one curve at DNV-3 operating area was created, see Fig.10.

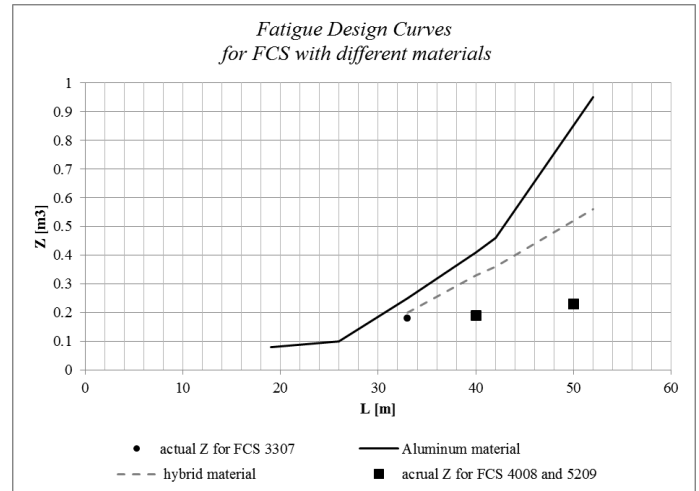


Fig.10: Fatigue design curve with aluminum and hybrid construction materials

Since suspicions were confirmed, the accuracy of the fatigue life prediction was assessed.

Different uncertainties are associated with the fatigue life prediction of the structures [10], [11]. The uncertainty regarding the load calculation greatly depends on available vessel data, weight distribution, calculation procedure, distribution of waves and hydrodynamic coefficients [12]. With respect to the weight distribution, used version of the Seaway Octopus in current study gives absolutely the same results when weight is distributed evenly and unevenly along the length of vessel. This finding in the program should be taken into consideration and the large distance in curves between actual and required Z can be the result of inaccurate calculation of the transfer function (bending moments). In order to figure out the validity of the calculated bending moments as compared with the actual ones, special measuring instruments (strain gauges) should be installed on the vessels, data should constantly be observed and the strains should be recorded measuring the structure response.

Moreover, the fatigue lifetime is very sensitive to distribution of waves [12]. During the study of Alufastship program, a major assumption referring to the wave distribution was identified. Since most fatigue damage is caused by the forward incoming waves between -45 to $+45$ degrees for high speed crafts (see Fig. 11), a factor 0.5 is used to take into account the wave distribution in Alufastship which considers reduction in number of cycles by 50 %.

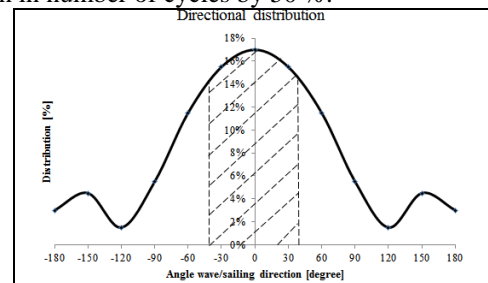


Fig.11: Directional distribution based on DNV report 97-0152

This assumption can lead to some uncertainty of fatigue lifetime calculation and thus, additional tests should be conducted.

In addition, there are several uncertain points with respect to stress calculation which depend on the structural response, FAT class and calculation of the stress concentration factor. The SCF in this study was estimated as 1.15 due to the butt welds corresponding to FAT class 6 (Germanischer Lloyd). However, such category can be very conservative. In order to accurately determine SCF, the finite element analysis should be carried out rather than assume or use parametric equations which were established several years ago [12].

Above curves were established based on the standard operational profile where only wave height and required lifetime were variable. However, more powerful engines which give new higher speeds for each vessel can be set. Thus, another fatigue curve was created based on the standard operational profile ($H_s=2.5m$, 75000 hours, DNV-3) where engines are the only variables. All previous tests were carried out with a minimum engine (power) set on the vessel. Thus, alternate engines were selected, with maximum engine power in order to show the whole range of Z allowable for the specified length of the vessel based on the total power range. Unfortunately, two smallest vessels (FCS 1905 and 2610) do not have choice in different engines. The results are plotted in the figure below.

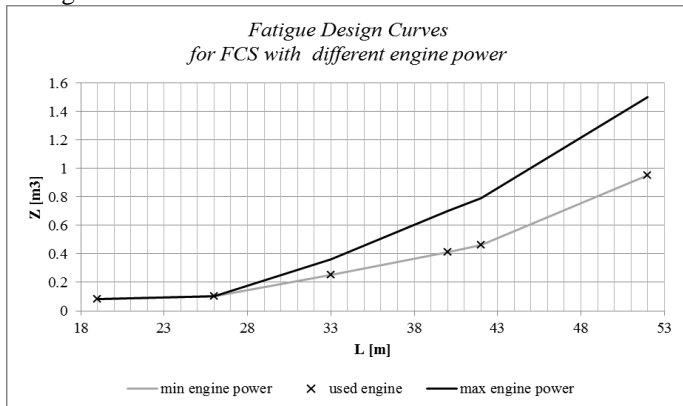


Fig.12: Fatigue design curve for FCS at DNV-3 with different engine power

In current figure, the grey line represents the minimum required section modulus of each vessel on which the smallest and least powerful engine has been set. Crosses (x) on this line represent Z received in the previous tests. The black line shows the minimum required section modulus of each vessel on which the largest and most powerful engine has been set. As it was mentioned above, points (cycles) on the curve are actual section moduli for built vessels.

The test shows that the range of increase Z is from 31% to 42%, but in chaotic order and is not a constant value. Comparing increased moduli with corresponding increased speeds, it was revealed that each vessel received a unique percentage of increased speed on average. Moreover, the results show nonlinear dependency between increased speeds

and Z, for example, the increased speed by 20% for FCS 3307 led to increased Z by 31% (11% of difference), while the increased speed by 34% for FCS 4207 led to increased Z by 42% (7% of difference).

Table 2 Comparison of increased vessel speed and achieved Z in %

FCS	1905	2610	3307	4008	4207	5209
Analyzed frame	6	10	14	16	20	20
Increased Z in %	0%	0%	31%	41%	42%	37%
Increased Vs in % to corresponded engine power	0%	0%	20%	34%	34%	25%

Therefore, it may be concluded that each set engine had a unique influence on speeds and finally on Z. Thus, estimated range of Z for particular length of vessels is unique and is valid only for the specified vessels and their conditions. In order to understand the influence of speed on acquired bending moments (forces) and finally on Z, additional observation was conducted.

As a test vessel, FCS 3307 was investigated. The test was conducted for all frames, two speeds, namely 8 and 26 knots; and 2 wave frequencies corresponded to largest bending moment at each speed. Unfortunately, the program provides a natural frequency of ship only in heave and pitch motions. So, this value is out of consideration in current analysis. The results have been plotted in the figure below.

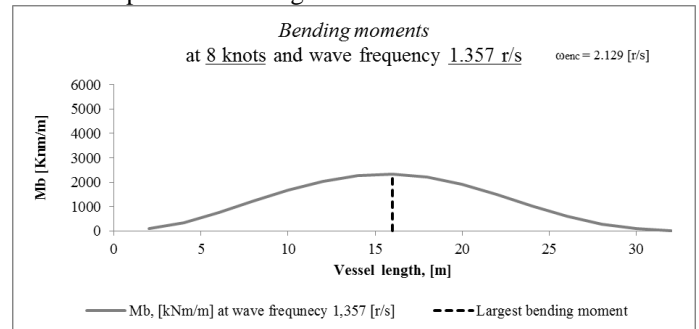


Fig.13: Bending moments along the vessel length at 8 knots

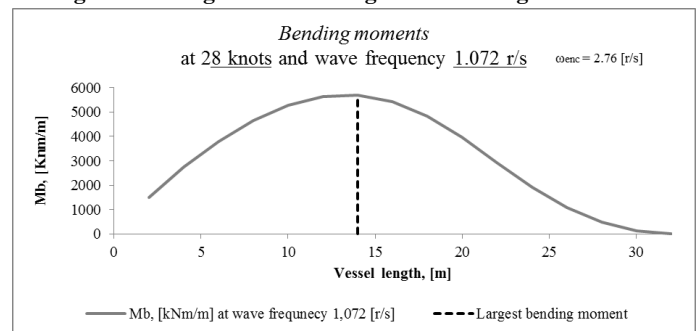


Fig.14: Bending moments along the vessel length at 28 knots

Figures above show the behavior of bending moments (first mode of vibrations). Since the largest bending moment at 8 knots was achieved for frame 16 and corresponds to wave frequency $\omega=1.357$ [r/s], it was assumed as constant in the upper diagram. As the largest bending moment at 28 knots was achieved for frame 14 and corresponds to wave frequency

$\omega=1.072$ [r/s], that frequency was assumed as constant in the lower diagram. In addition, the program calculated the encounter frequency by equation (6) for corresponding speed and wave frequency. The results in the upper right corner of the diagrams show that with increased speed, the encounter frequency also increased.

The frequency of encounter in head seas can be found as follows:

$$\omega_e = \omega + \frac{\omega^2 \cdot V_s}{g} \quad (6)$$

where ω – wave frequency;
 V_s – the vessel speed.

Overall, while considering behavior of bending moments through the whole length of the vessel, it is seen that increased speed shifts the maximum bending moment toward the stern and largest bending moment is at the lower wave frequency. However, due to limited resources and information, the reasons for such event should be investigated in future work.

CONCLUSION

The fatigue design assessment produced the following outcome. Firstly, the sensitivity analysis of the fatigue design tool was conducted in order to indicate which parameters have the most significant impact on the fatigue lifetime and which vessel details are mostly prone to the fatigue failure. Secondly, fatigue design curves for the range of vessels designed in Damen were developed in order to help engineers at the design stage to make a proper selection regarding the main particulars of the vessel for a specific operational profile or for an individual customer's requirement

To summarize, the findings during the study are as follows:

- Mostly prone to fatigue failure are the details located at the frames with the transition from the hull to the superstructure and with the calculated largest hull girder bending moment.
- It is speed that influences mostly the fatigue lifetime while less important parameters are: time spent at the top speed, time spent at the average speed, an intended service period and the operating area.
- Seemingly modest area like N-Arabian Sea can be more dangerous for fatigue lifetime of vessel, than North Sea, due to manually limitation of wave heights, dominating wave length and wave period.
- Large difference in Z with actual and minimum required for both aluminum and hybrid vessels are caused by uncertainty associated with load and stress calculations.
- Each set engine had a unique influence on speeds and finally on Z.
- Increased speed shifted the largest bending moment toward stern and at lower wave frequency.

To summarize, several uncertainties in the study should be further investigated, such as a calculated response of the vessel

and output sensitivity to weight distribution in Seaway Octopus software. In addition, the way of wave distribution in Alufastship should be checked and if necessary improved. Moreover, the SCF should be determined by FEM analysis. Finally, the behavior of largest bending moments at low wave frequencies with increased speed should be investigated in the future work.

NOMENCLATURE

DNV	Det Norske Veritas;
FAT	Stress level of the S-N curve at 2 million stress cycles;
FCS	Fast Crew Suppliers;
FEM	Finite Element Method;
PFA	Preliminary fatigue analysis;
RAO	Response Amplitude Operator;
SCF	Stress Concentration Factor;
SPa	Stan Patrol;
S-N	Stress range - Number of stress cycles until failure (S-N curve).

REFERENCES

1. Capanoglu, C.C., *fatigue Technology Assessment and Strategies For Fatigue Avoidance in Marine Structures*. 1993: Washington DC. p. 412.
2. Allday, B., *Aluminium alloys - design for fatigue*. Ship & Boat International, 1993: p. 25-39.
3. Lyngstad, O.A., *Fatigue of High Speed Craft - In Service Experience* 2002. p. 306 - 328.
4. Hall, T., D.F. Violette, and H. Chung, *Fatigue Design Assessment of Aluminium Fast Craft, in AUSMARINE - CONFERENCE '98*, A. Jeffs, Editor. 1998, Baird Publications: Fremantle; Australia. p. 125-136.
5. DNV, *Fatigue Assessment of Ship Structures* 2010, Det Norske Veritas: Høvik, Norway. p. 108.
6. Fines, S., *Loads on Ocean Structures*, ed. A.Almer-Næss. 1985, Oslo: Tapir. 50.
7. Roylance, D., *Fatigue*. 2001, Massachusetts Institute of Technology: Cambridge MA. p. 9.
8. Berge, S., *Basic Fatigue properties of Welded Joints*, ed. A.Almer-Næss. 1985, Trondheim: Tapir. 76.
9. Veritas, D.N., *Rules for the design, construction and inspection of offshore structures, 1977 / Det Norske Veritas*. 1977, Oslo: Det Norske Veritas. 1-67.
10. Wirsching, P.H., *Probability - Based Fatigue Design Criteria for Offshore Structures*. 1983, University of Arizona: Tucson.
11. Gran, S., *Fatigue and Crack Failure Prediction Methods in Marine Structures*. 1980, Det Norske Veritas.
12. Lotsberg, I., A.Almer-Næss, and A.S. Veritec, *Fatigue Life Calculations*, ed. A.Almer-Næss. 1985, Trondheim: Tapir. 53.

**APPENDIX A
STANDARD OPERATIONAL PROFILE**

Type of vessel	Fast Crew Supplier	Stan Patrol
Weight distribution	50% of loading conditions	
Speed	According to the engine power. 3 speeds	
Service conditions	100% MCR – 50% of time 50% MCR – 20% of time 10% MCR – 30% of time	100% MCR – 5% of time 25% MCR – 75% of time Idle engine speed – 20% of time
Wave height constraint (H_s , [m])	2.5	3.5
WSD	DNV-3	
Intended service period	15 years	20 years
Sailing hours per year	5000h/y	2000 h/y

**APPENDIX B
FATIGUE DESIGN CURVES FOR STAN PATROLS**

